On Heads and Tails

Foundations seminar

Raul Vicente, 11th March 2025

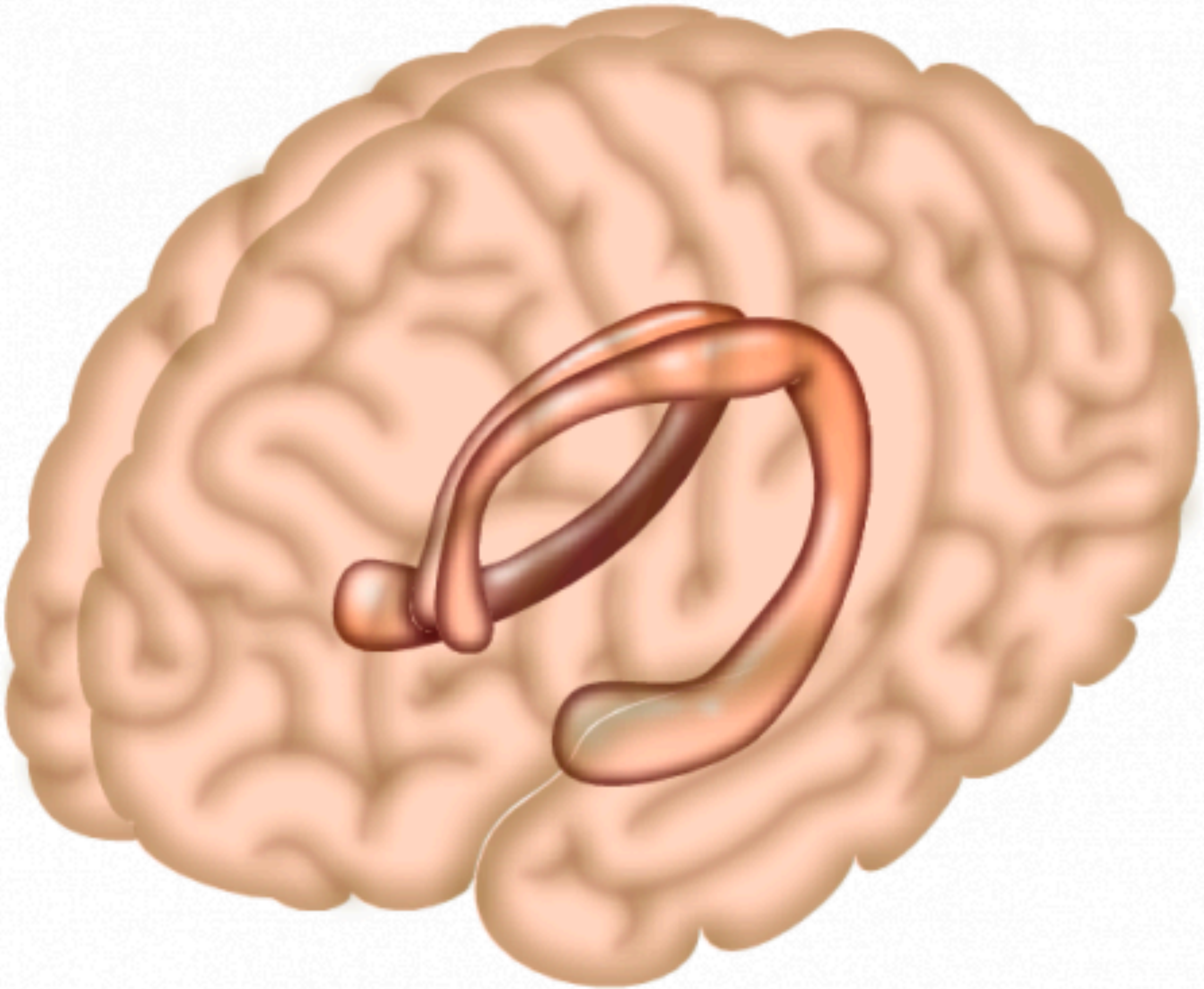

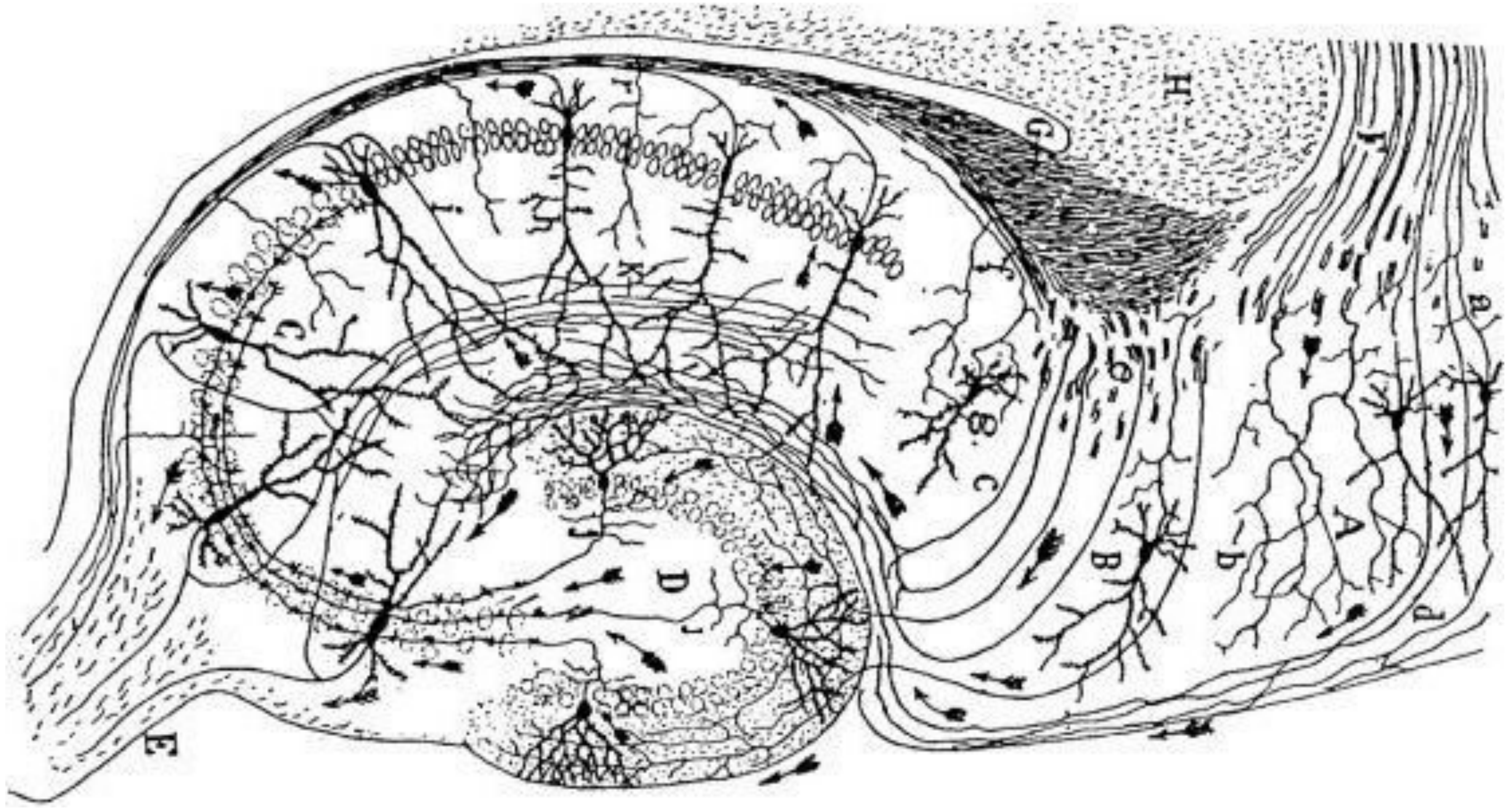

Place cells

In 1971, researchers John O'Keefe and John Dostrovsky worked with rats to discover place cells. Located in the hippocampus region of the brain, different place cells are acitvated only at specific locations. They tell us where we are.

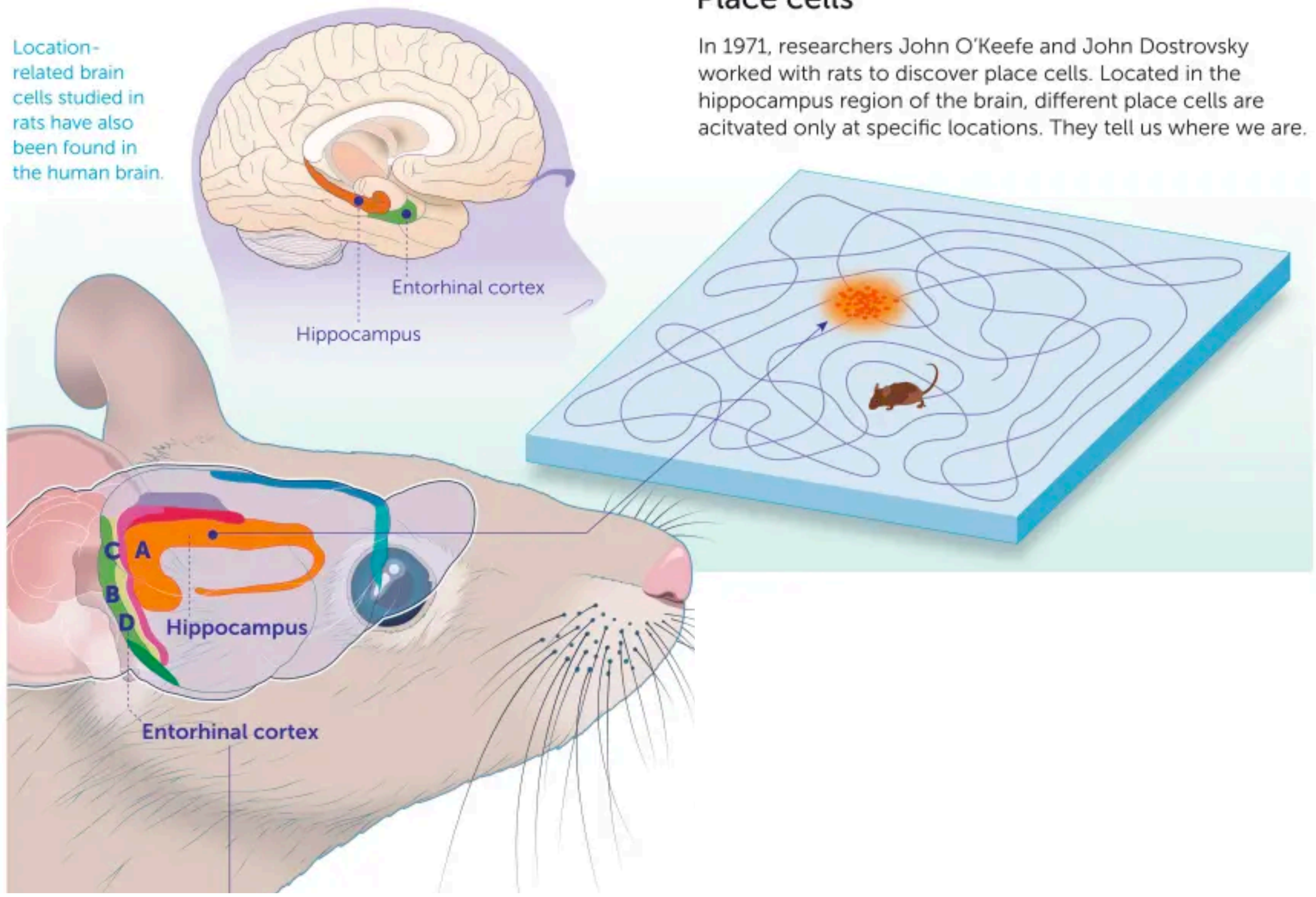

Place cells

In 1971, researchers John O'Keefe and John Dostrovsky worked with rats to discover place cells. Located in the hippocampus region of the brain, different place cells are acitvated only at specific locations. They tell us where we are.

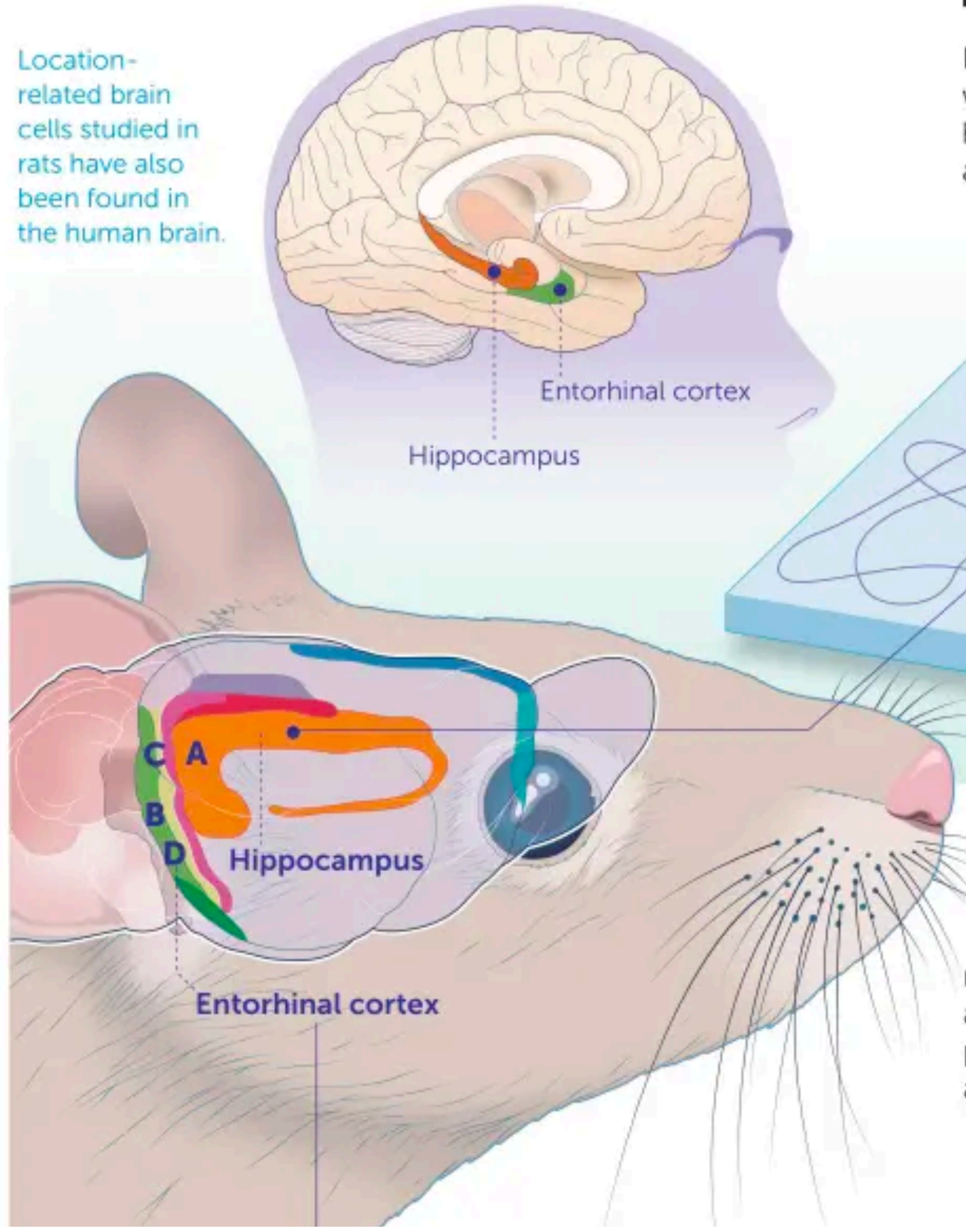

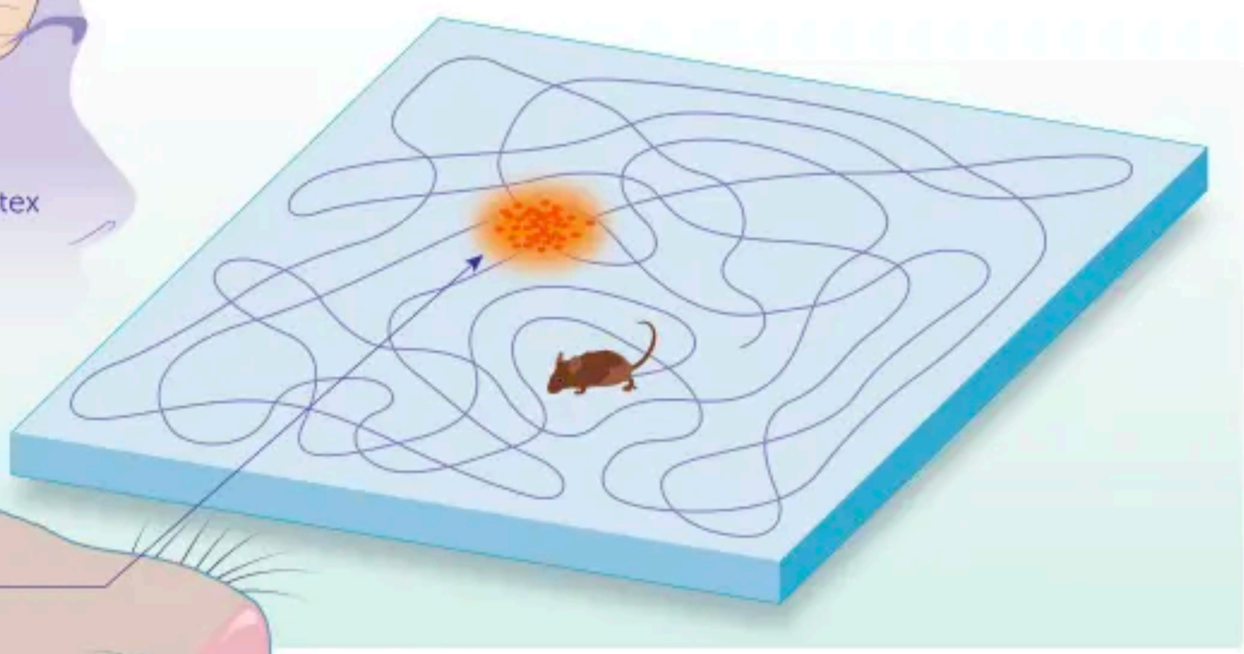

To navigate successfully in the environment, you need to know your starting position, walking direction, and speed. In addition to **place cells (A)**, other cell types have a unique role in navigation. **Speed cells (B)** increase their activity when an animal moves faster, helping it calculate the distance it passes when it moves. **Head direction cells (C)** inform the animal in which direction it is heading.

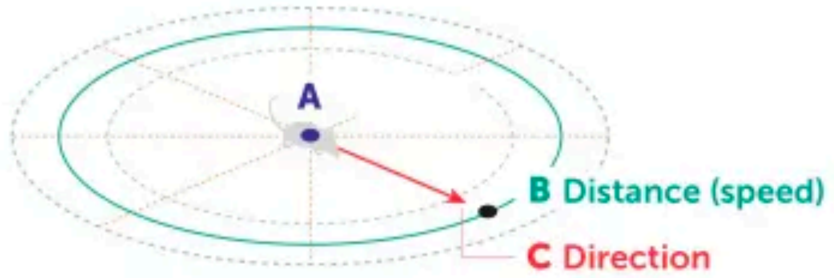

Place cells

In 1971, researchers John O'Keefe and John Dostrovsky worked with rats to discover place cells. Located in the hippocampus region of the brain, different place cells are acitvated only at specific locations. They tell us where we are.

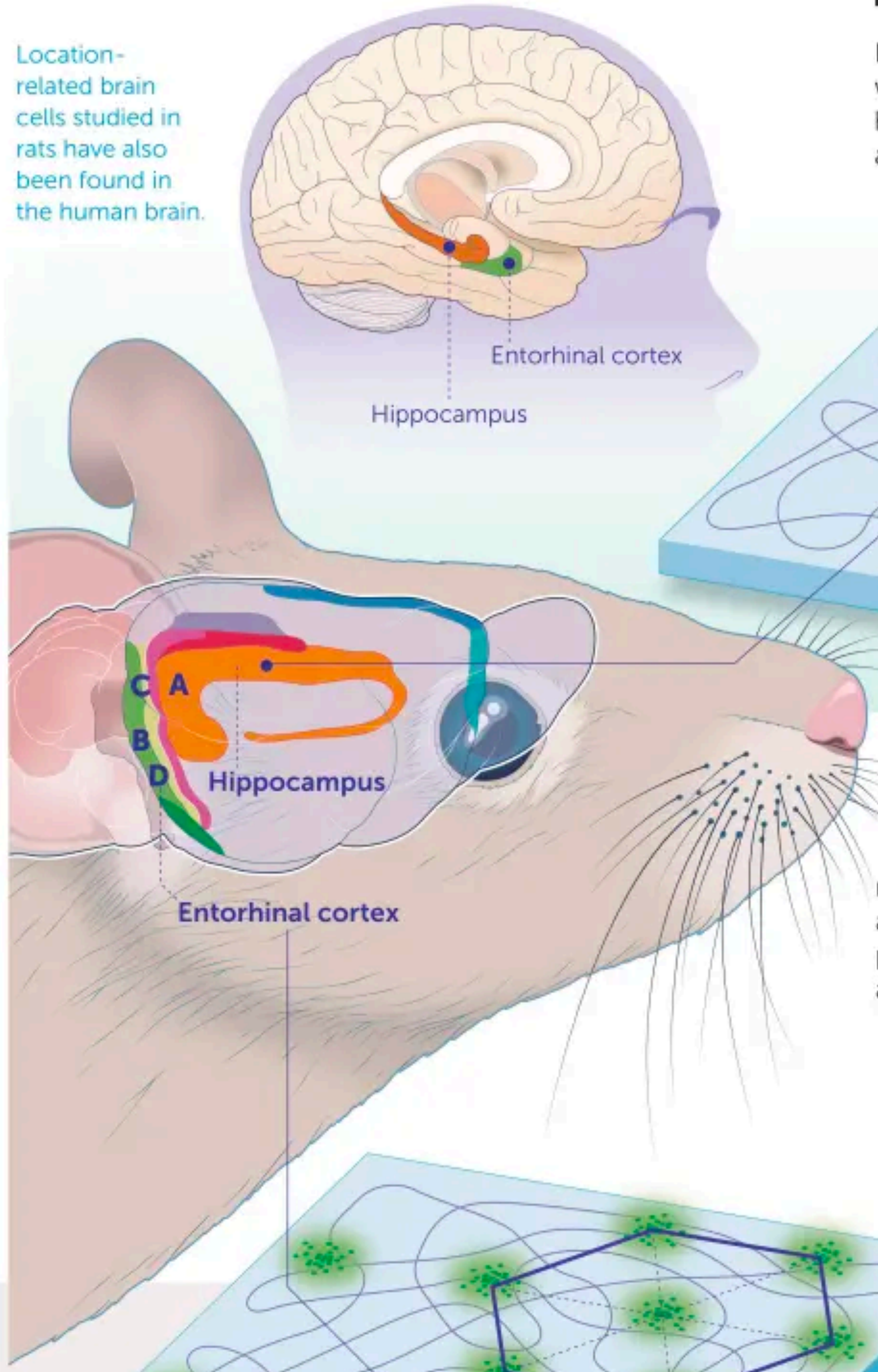

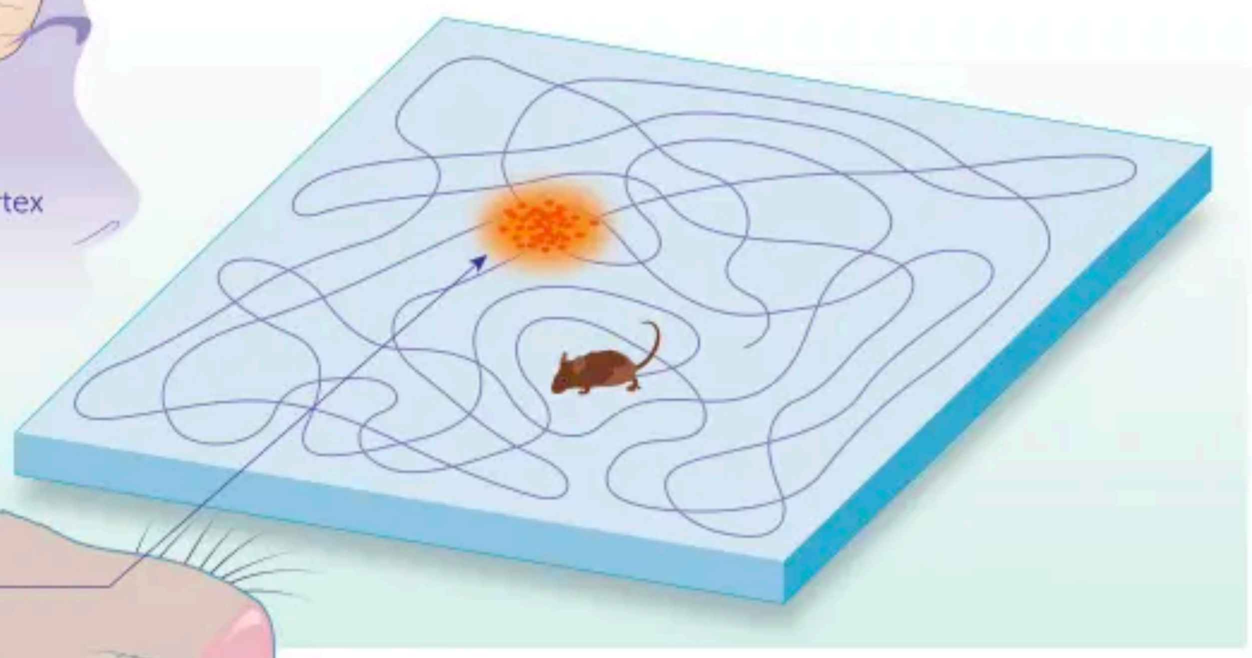

To navigate successfully in the environment, you need to know your starting position, walking direction, and speed. In addition to **place cells (A)**, other cell types have a unique role in navigation. **Speed cells (B)** increase their activity when an animal moves faster, helping it calculate the distance it passes when it moves. **Head direction cells (C)** inform the animal in which direction it is heading.

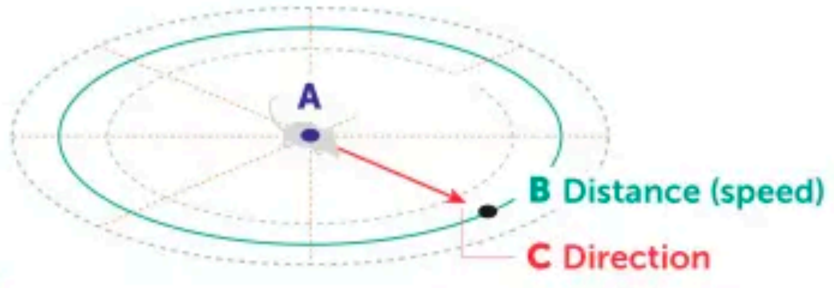

Grid cells

In 2005 May-Britt and Edvard Moser discovered **grid cells**, located in the entorhinal cortex **(D)**. Unlike place cells, active at only one location, each grid cell becomes active in multiple locations in an environment, which are evenly spaced in a repeating hexagonal pattern. This creates a system of coordinates with a metric, similar to the latitude-longitude grid we use in maps.

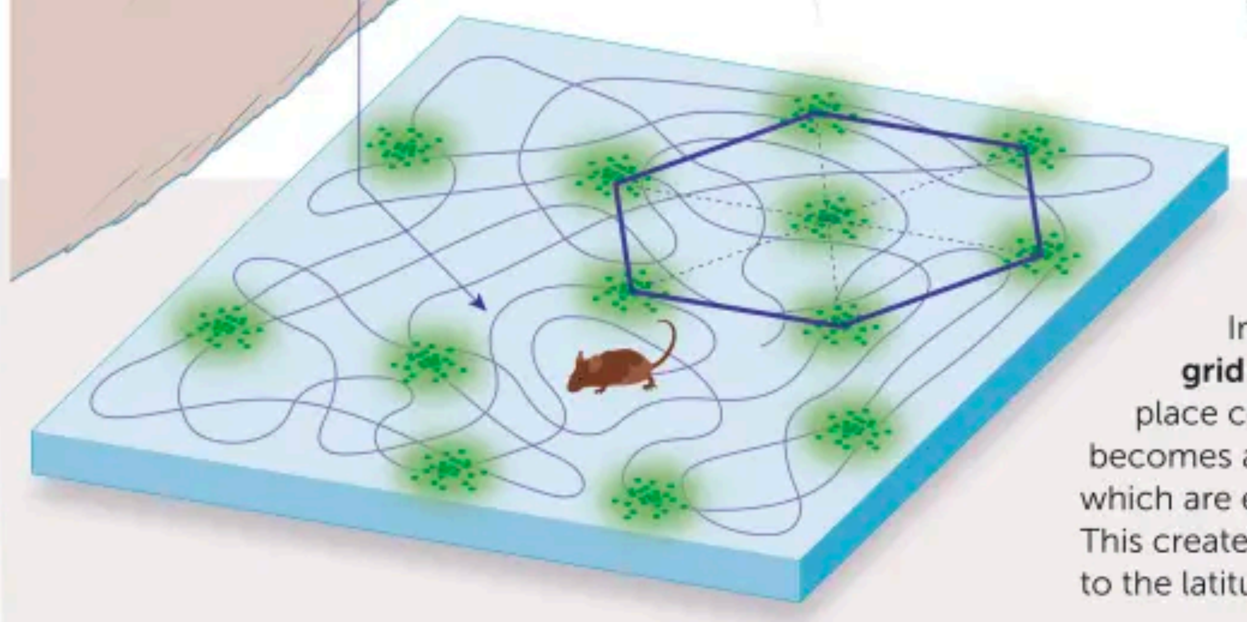

Place cells

In 1971, researchers John O'Keefe and John Dostrovsky worked with rats to discover place cells. Located in the hippocampus region of the brain, different place cells are acitvated only at specific locations. They tell us where we are.

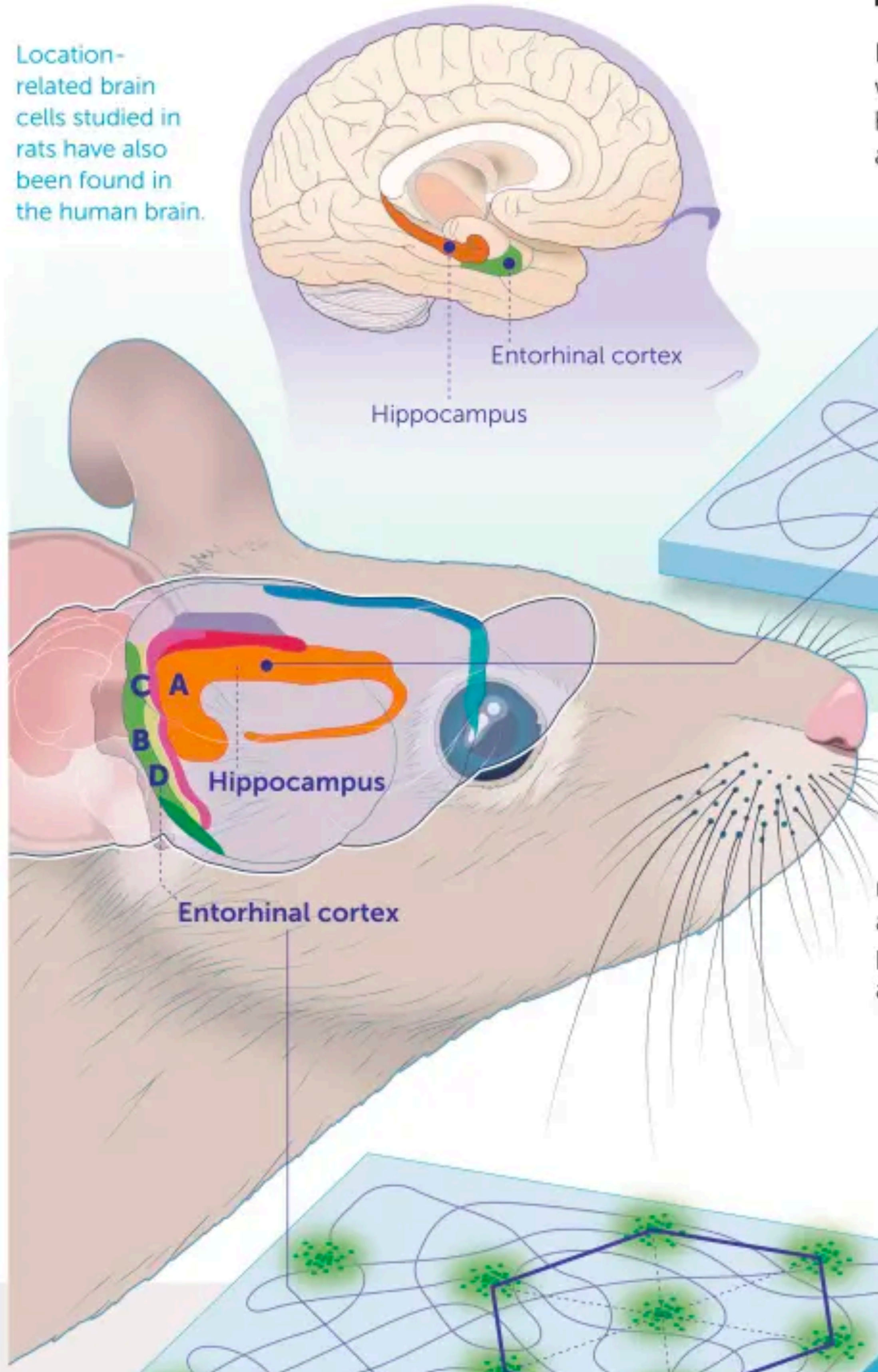

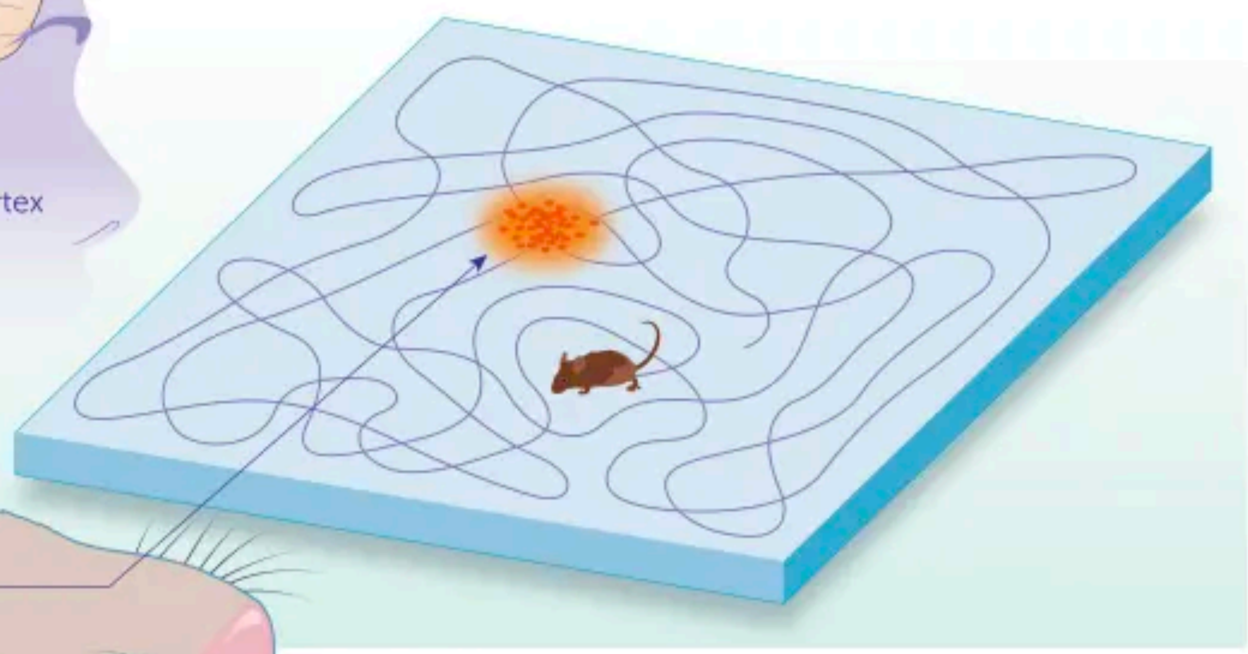

To navigate successfully in the environment, you need to know your starting position, walking direction, and speed. In addition to **place cells (A)**, other cell types have a unique role in navigation. **Speed cells (B)** increase their activity when an animal moves faster, helping it calculate the distance it passes when it moves. **Head direction cells (C)** inform the animal in which direction it is heading.

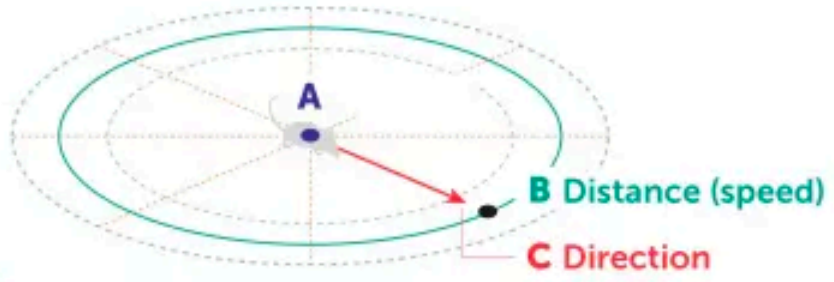

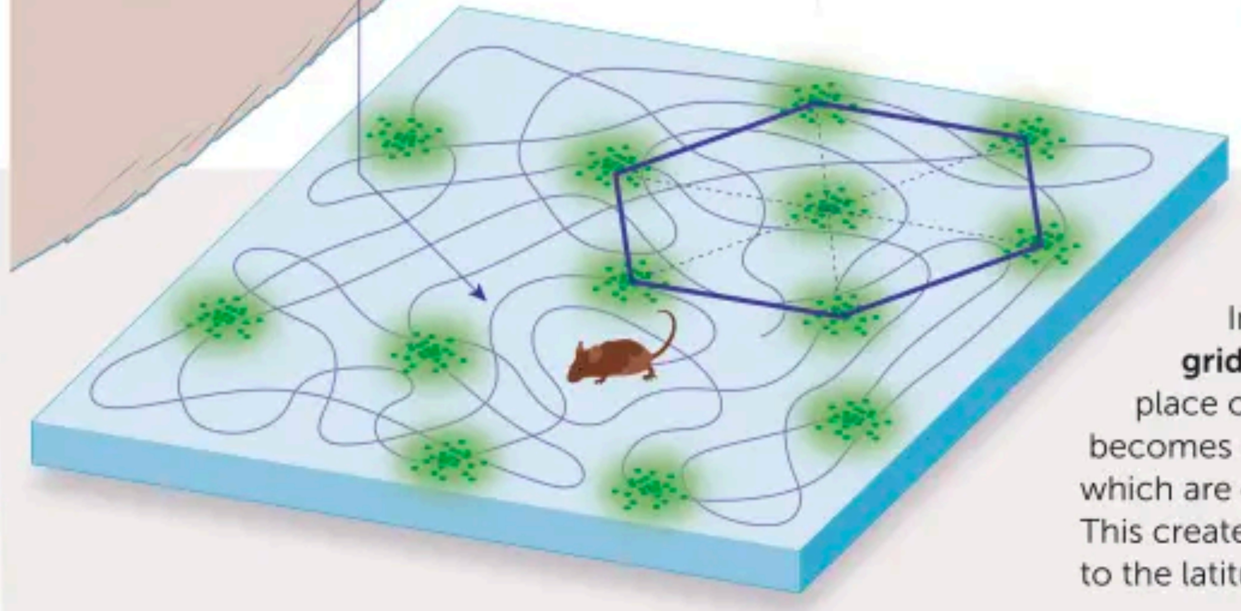

Grid cells

In 2005 May-Britt and Edvard Moser discovered **grid cells**, located in the entorhinal cortex **(D)**. Unlike place cells, active at only one location, each grid cell becomes active in multiple locations in an environment, which are evenly spaced in a repeating hexagonal pattern. This creates a system of coordinates with a metric, similar to the latitude-longitude grid we use in maps.

Grid cells help determine location ...

Different grid cells produce different hexagonal patterns at different scales and shifted with respect to the grids of other cells. Using the overlapping grids of several cells, location can be uniquely identified by coincident firing of multiple grid cells.

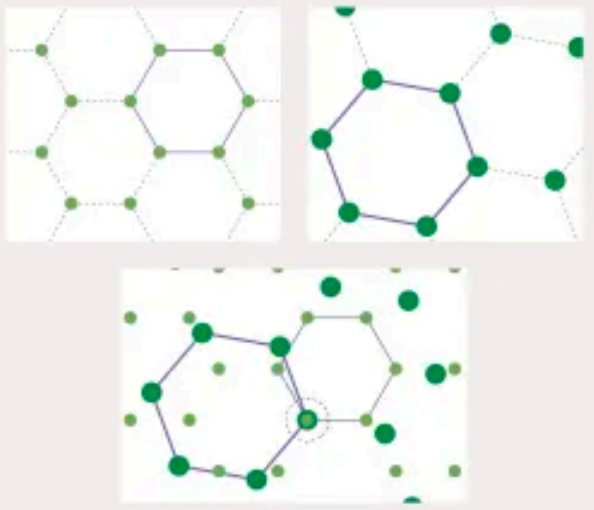

... similarly to GPS systems

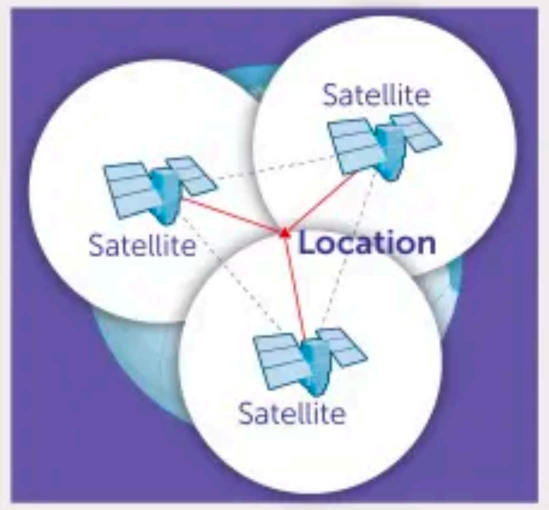

In a similar way, in GPS systems the distance measuring of one satelite alone can't pinpoint a location, but the overlap of at last three satelites is used to pinpoint the exact location of a receiver.

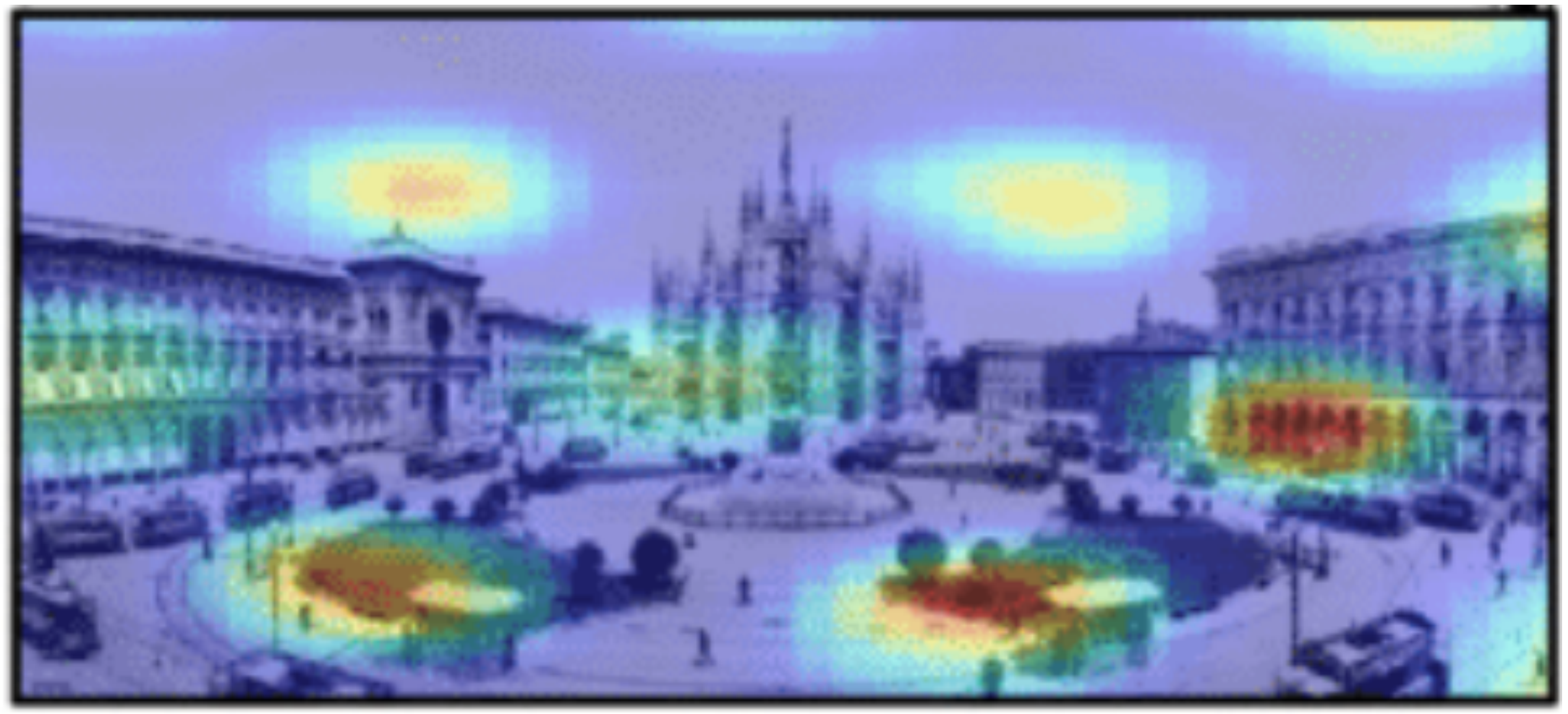

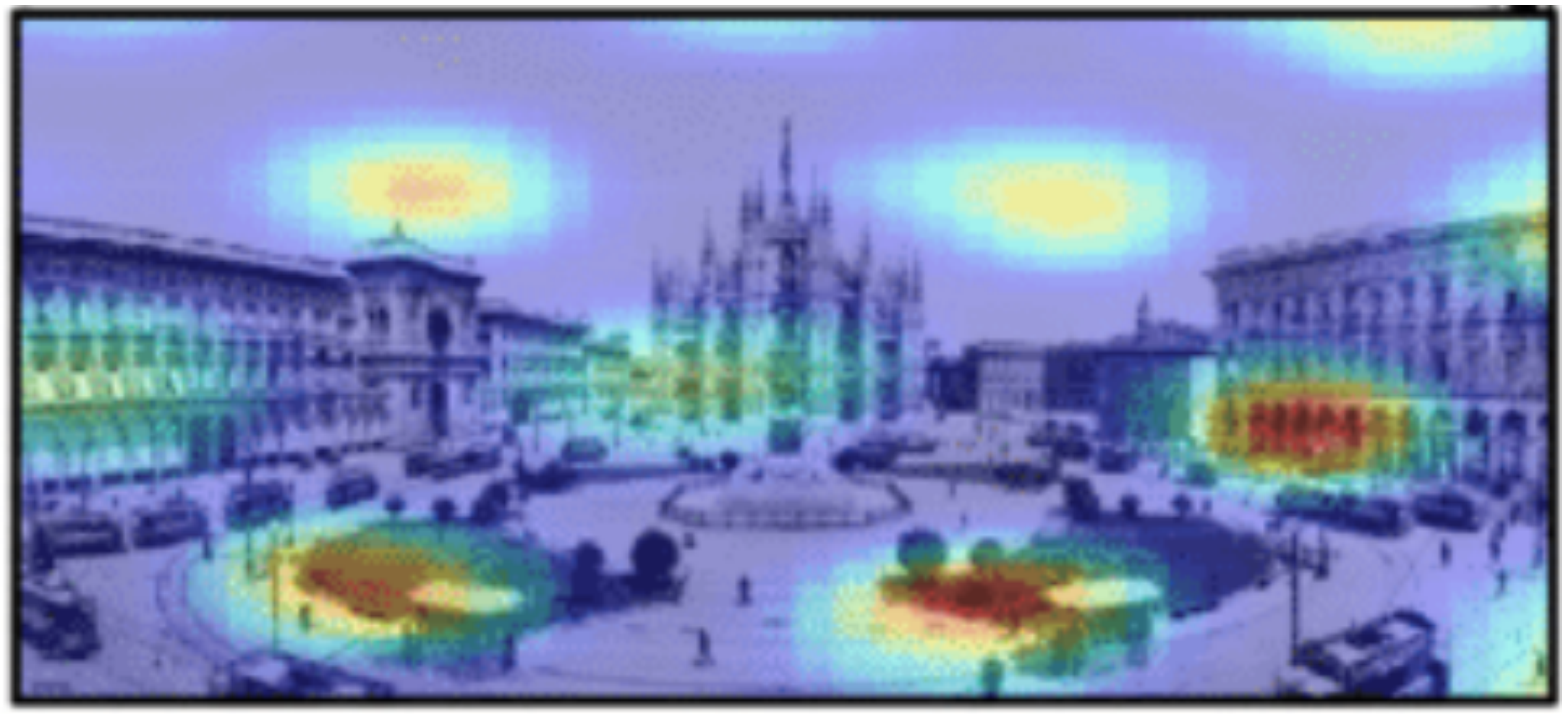

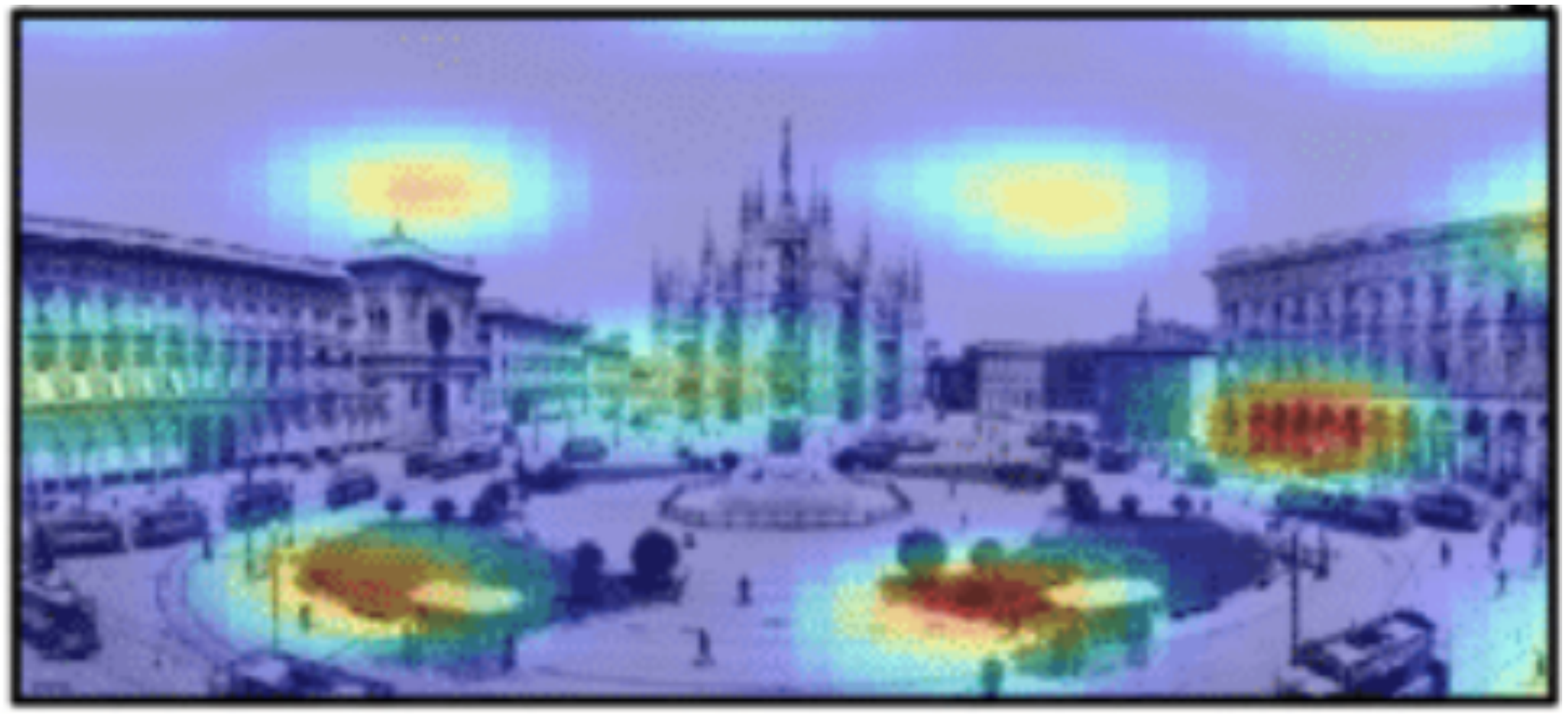

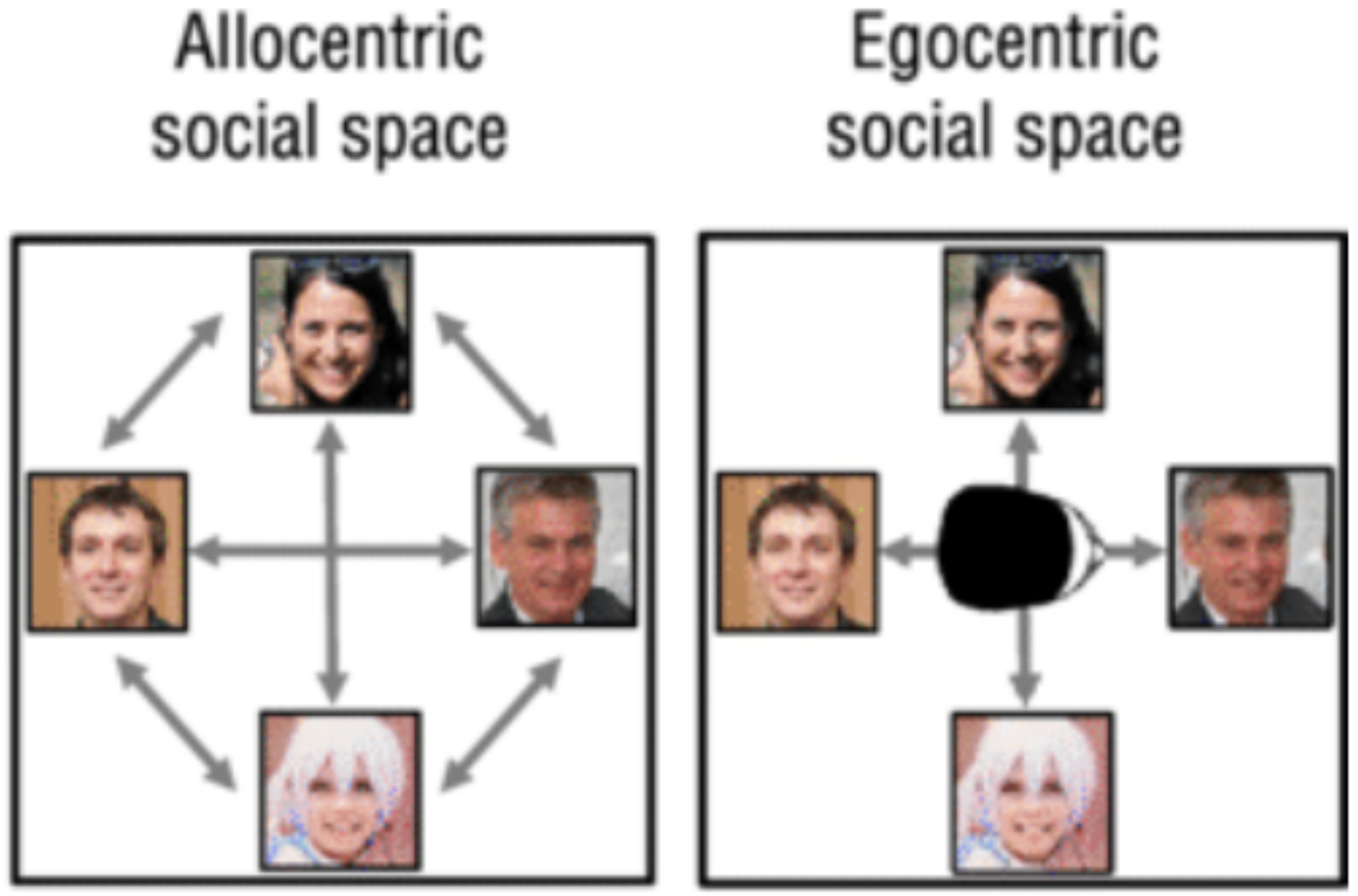
Allocentric
social space
Egocentric
social space

Artificial neural networks

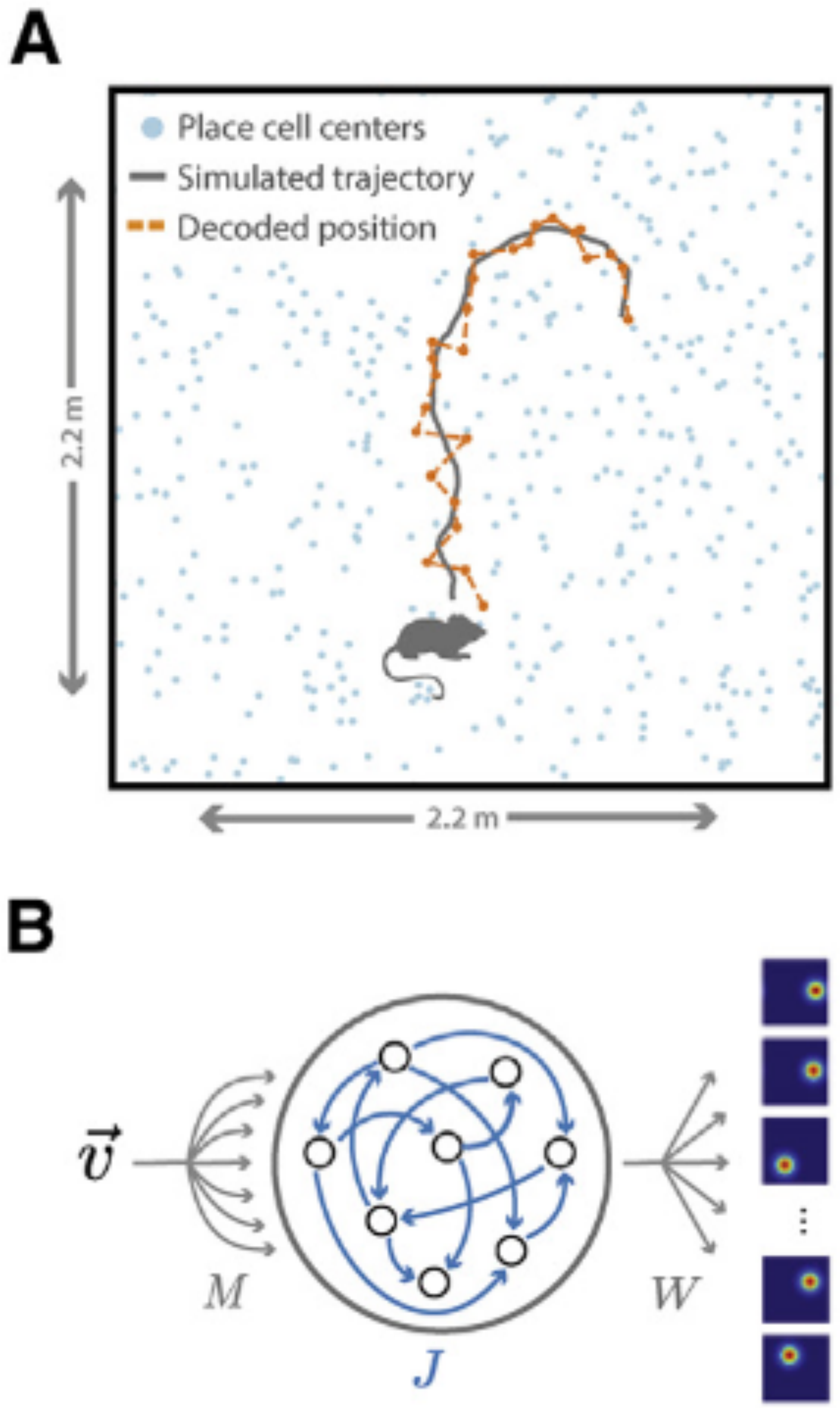

Sorscher et al 2023, Neuron

Artificial neural networks

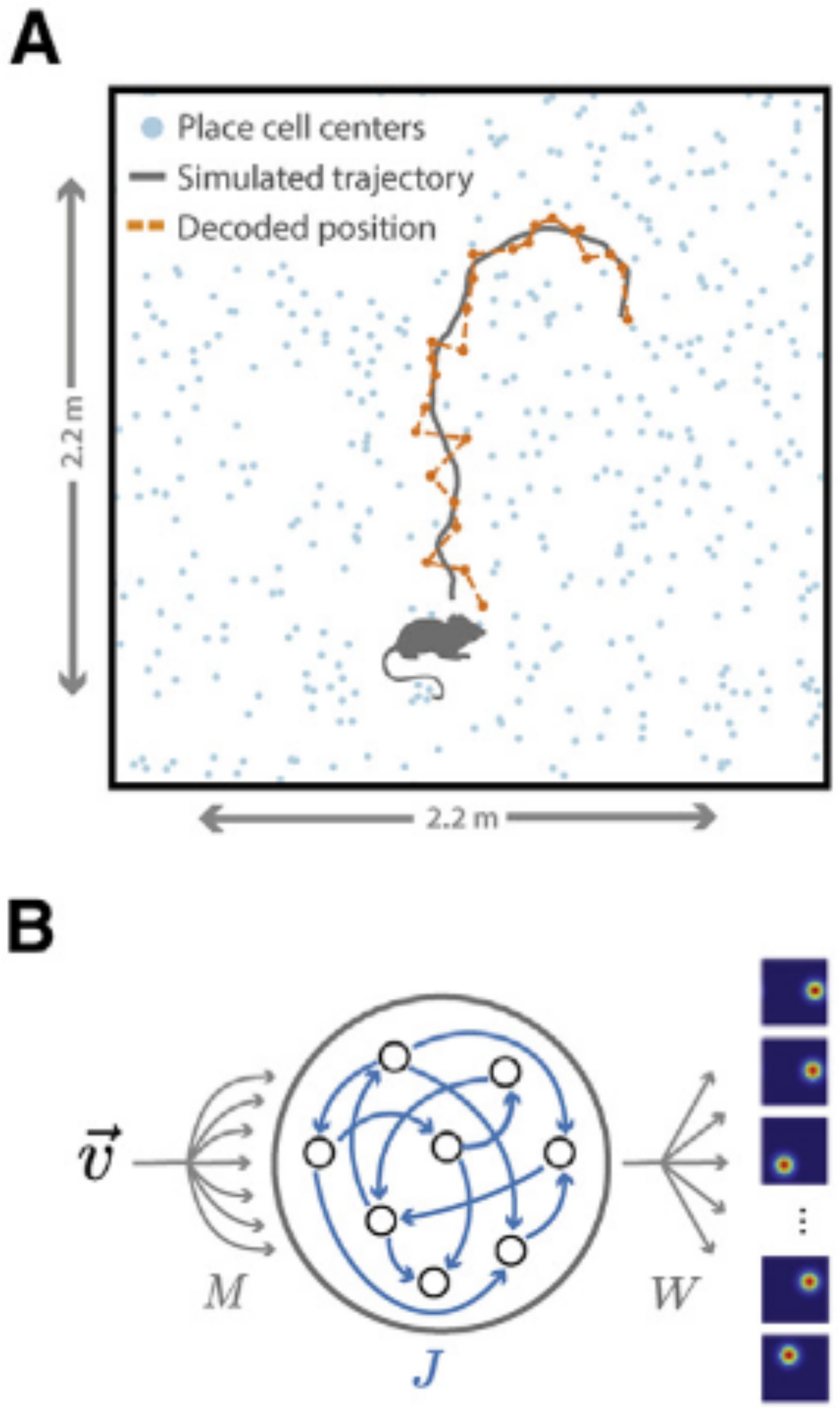

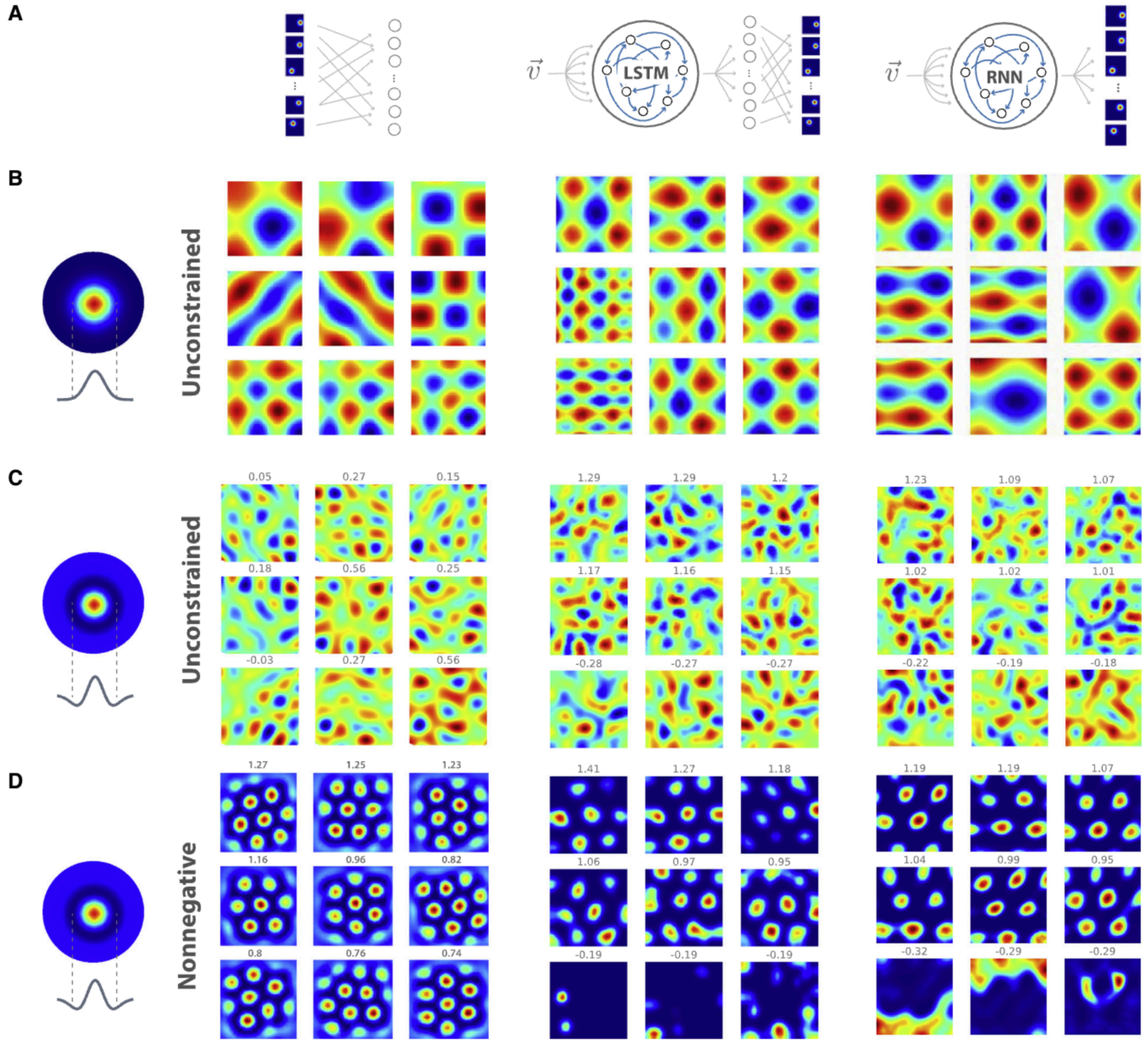

Sorscher et al 2023, Neuron

The 2014 Nobel Prize in Physiology or Medicine

John O'Keefe
Born 1939, USA
University College London

May-Britt Moser
Born 1963, Norway
Norwegian University of Science and Technology, Trondheim

Edvard I. Moser
Born 1962, Norway
Norwegian University of Science and Technology, Trondheim

1. Phase

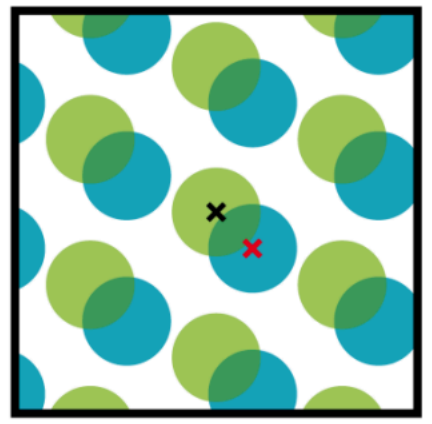

2. Scale

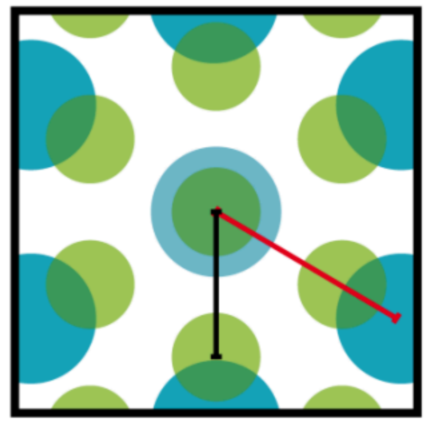

3. Orientation

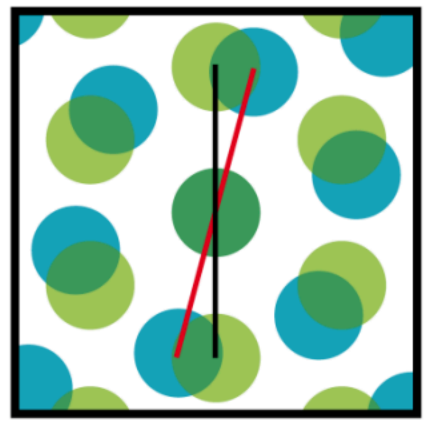

1. Phase

2. Scale

3. Orientation

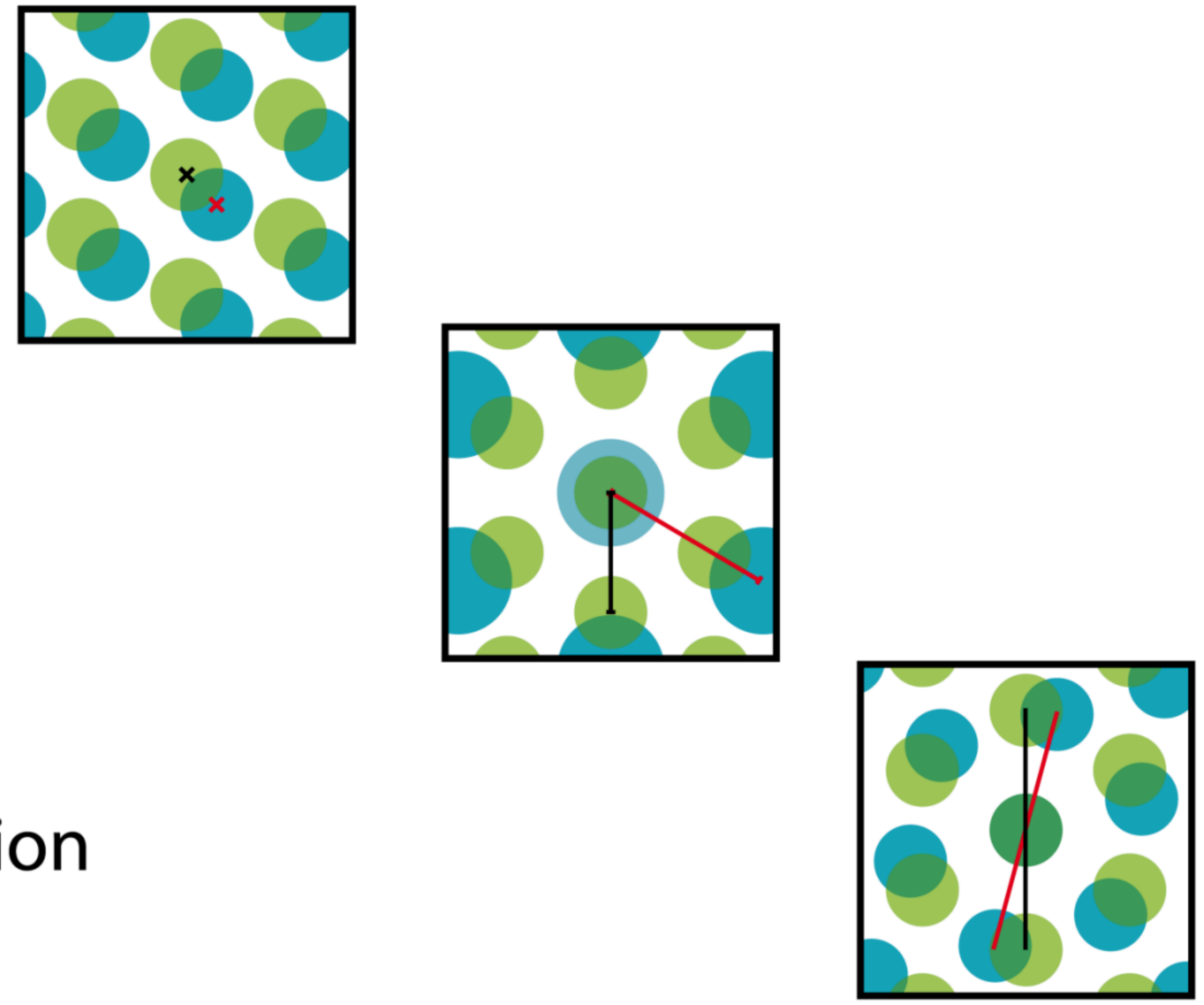

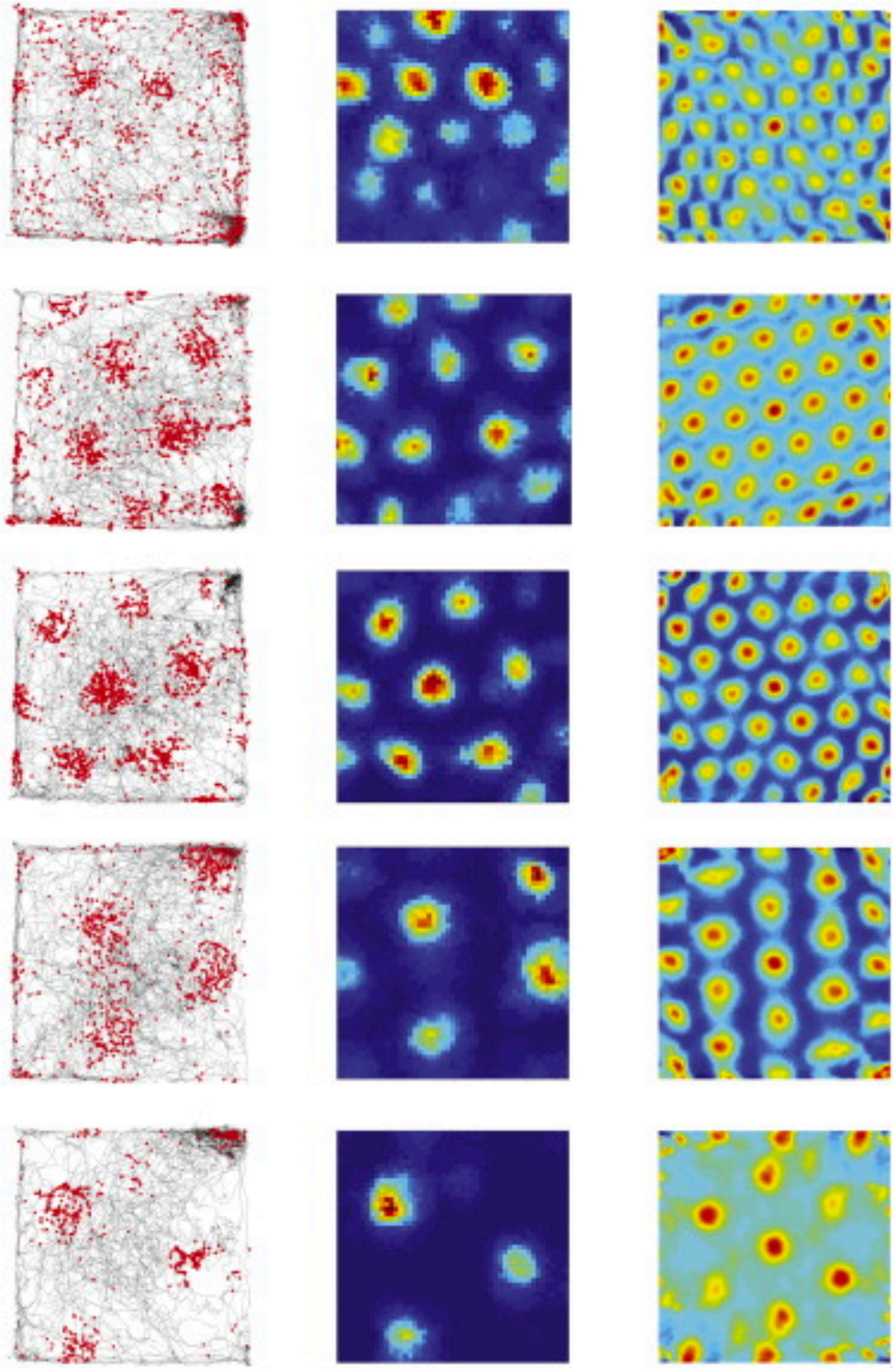

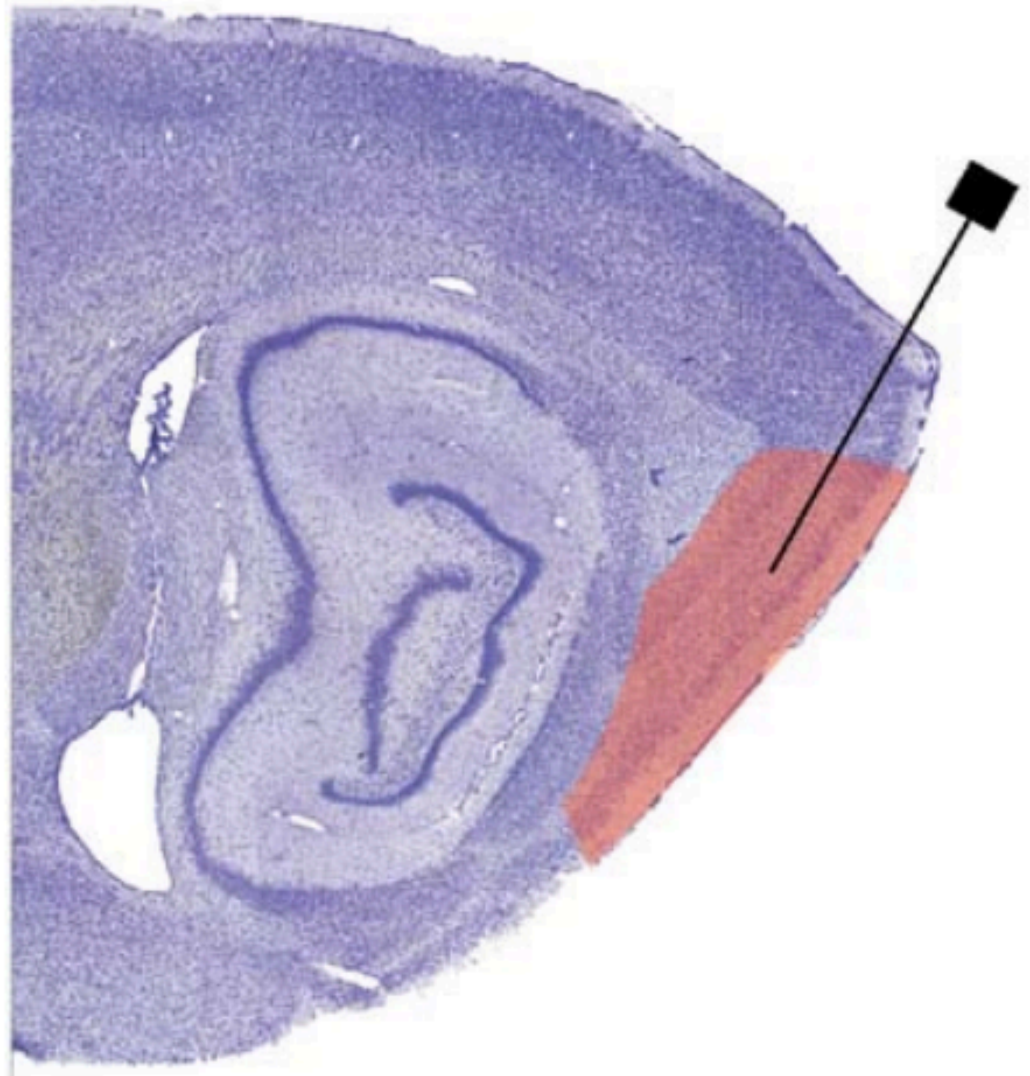

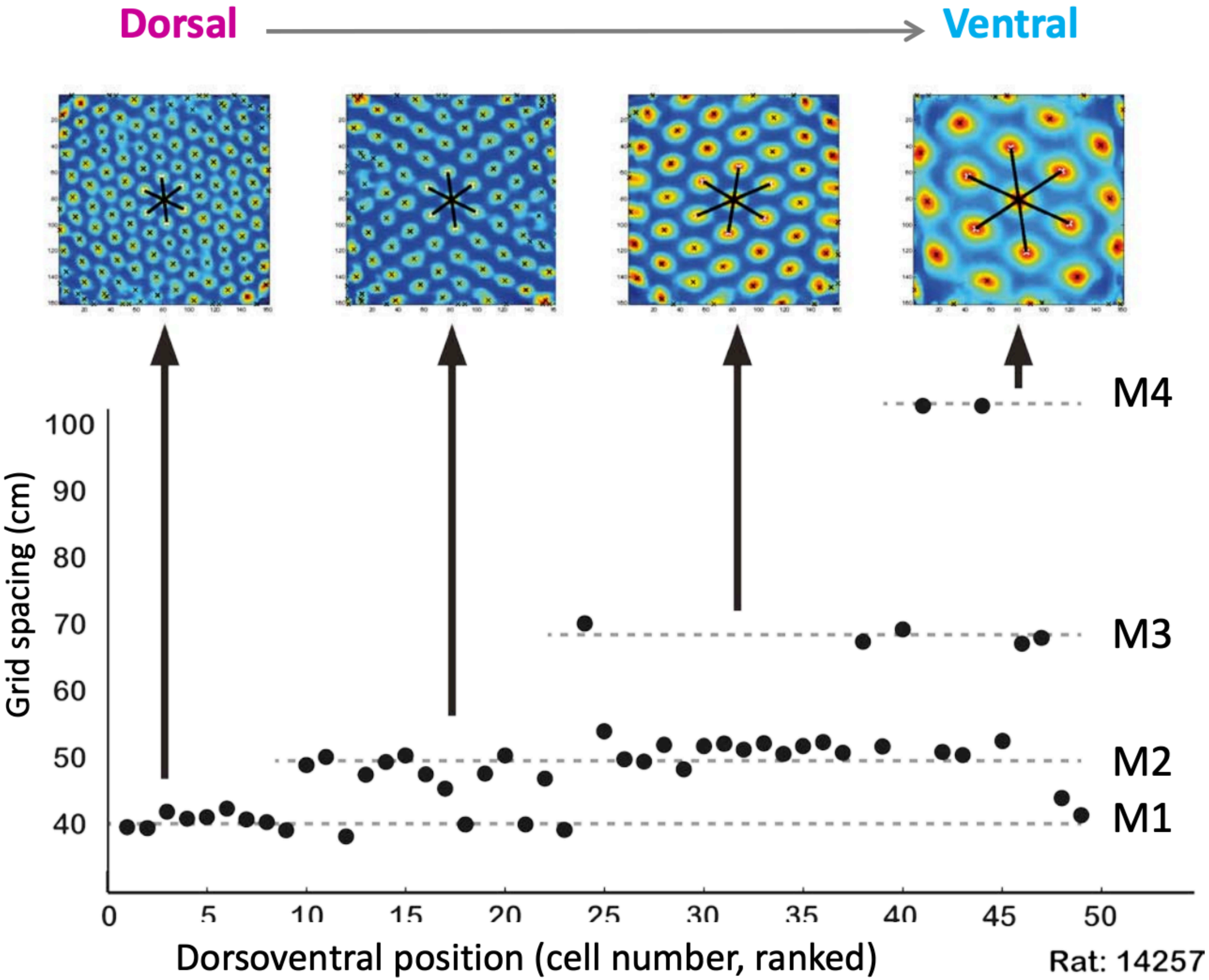

Tor & Hanne Stensola

Trygve Solstad
Kristian Frøland

Stensola et al. *Nature*, 492, 72-78 (2012)

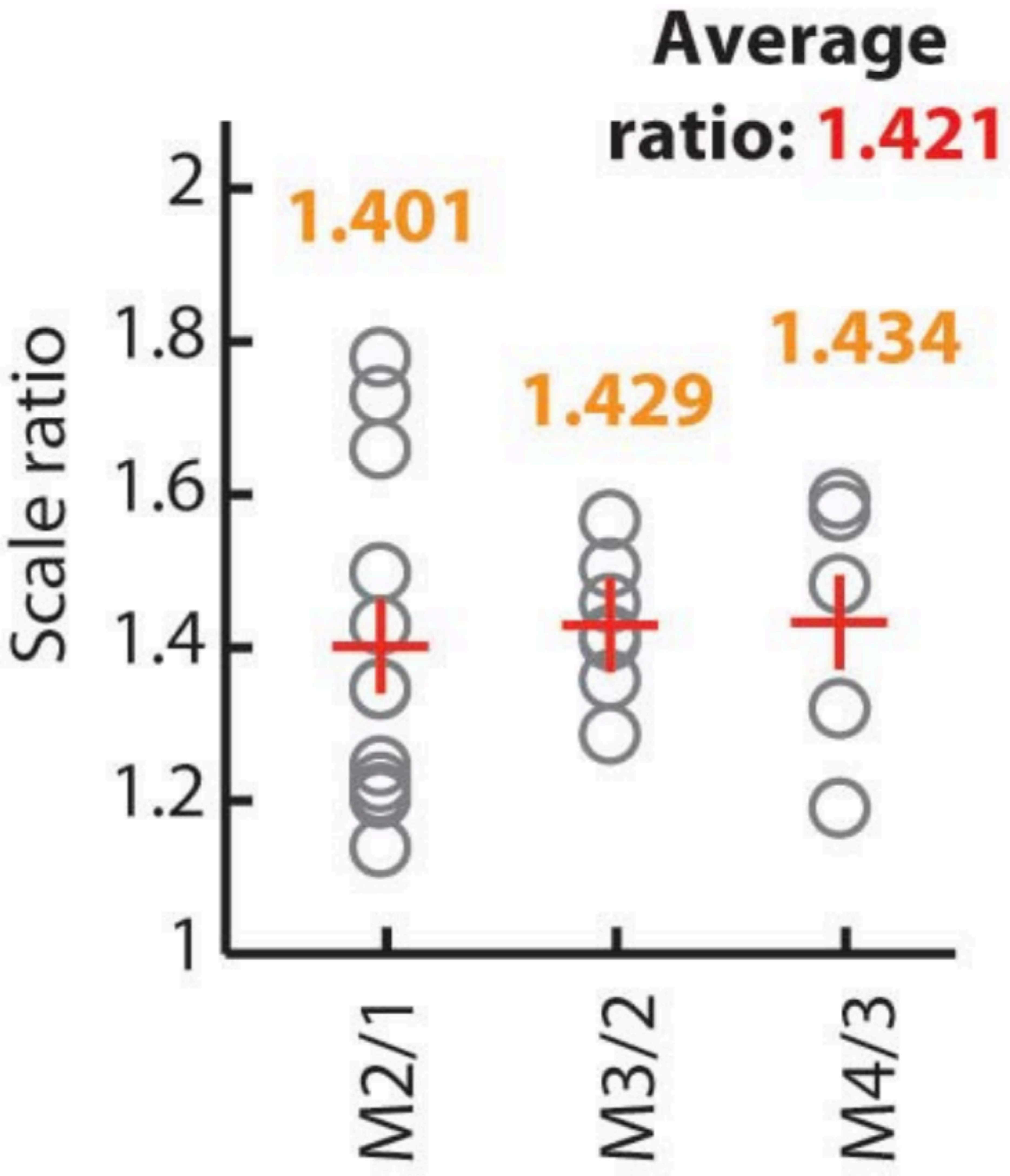

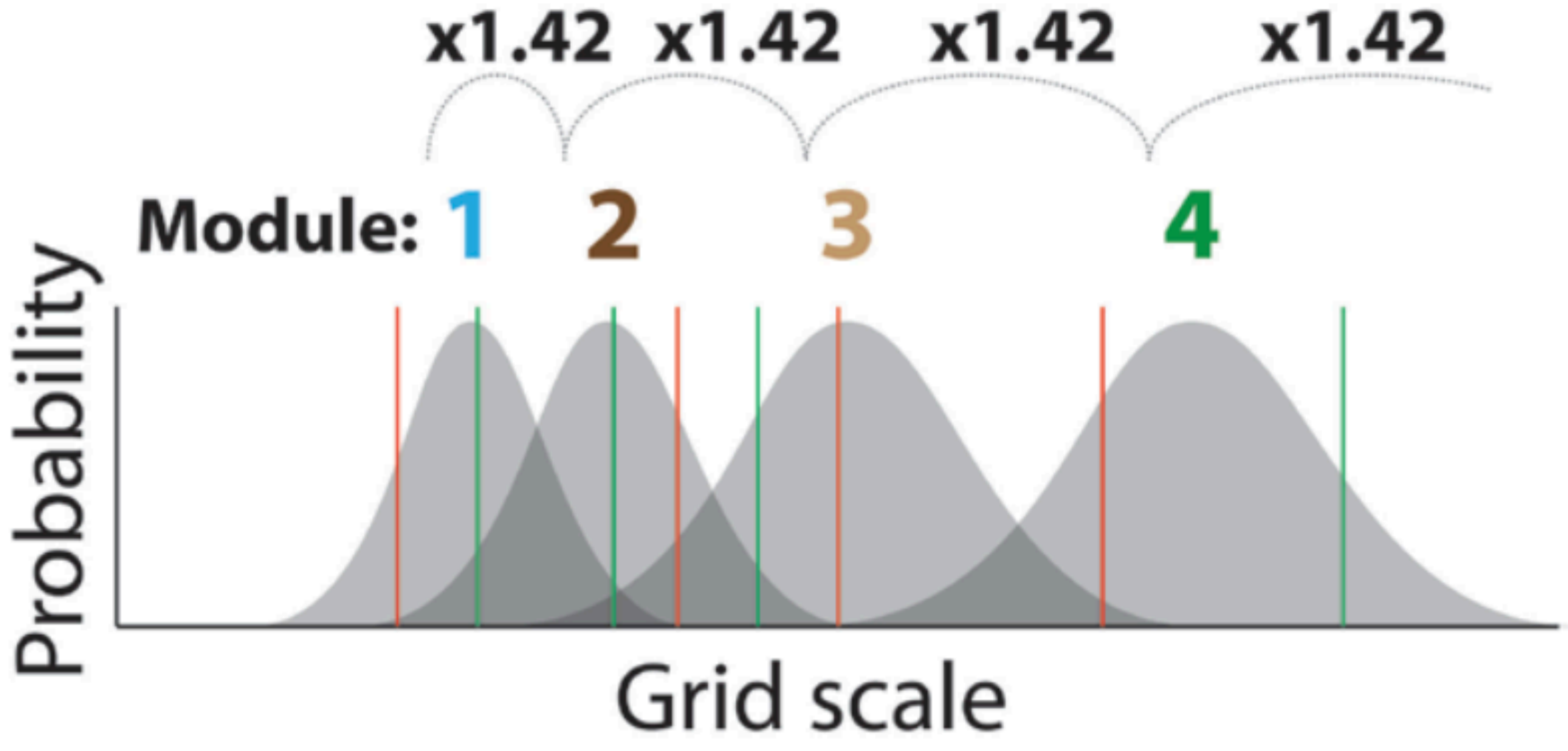

Although the set point is different for different animals, modules scale up, on average, by a factor of ~1.42 (sqrt 2).

Stensola et al. *Nature*, 492, 72-78 (2012)

How do these neurons activate on a hexagonal pattern
and
what is their functional role?

Classical theory

Path integration

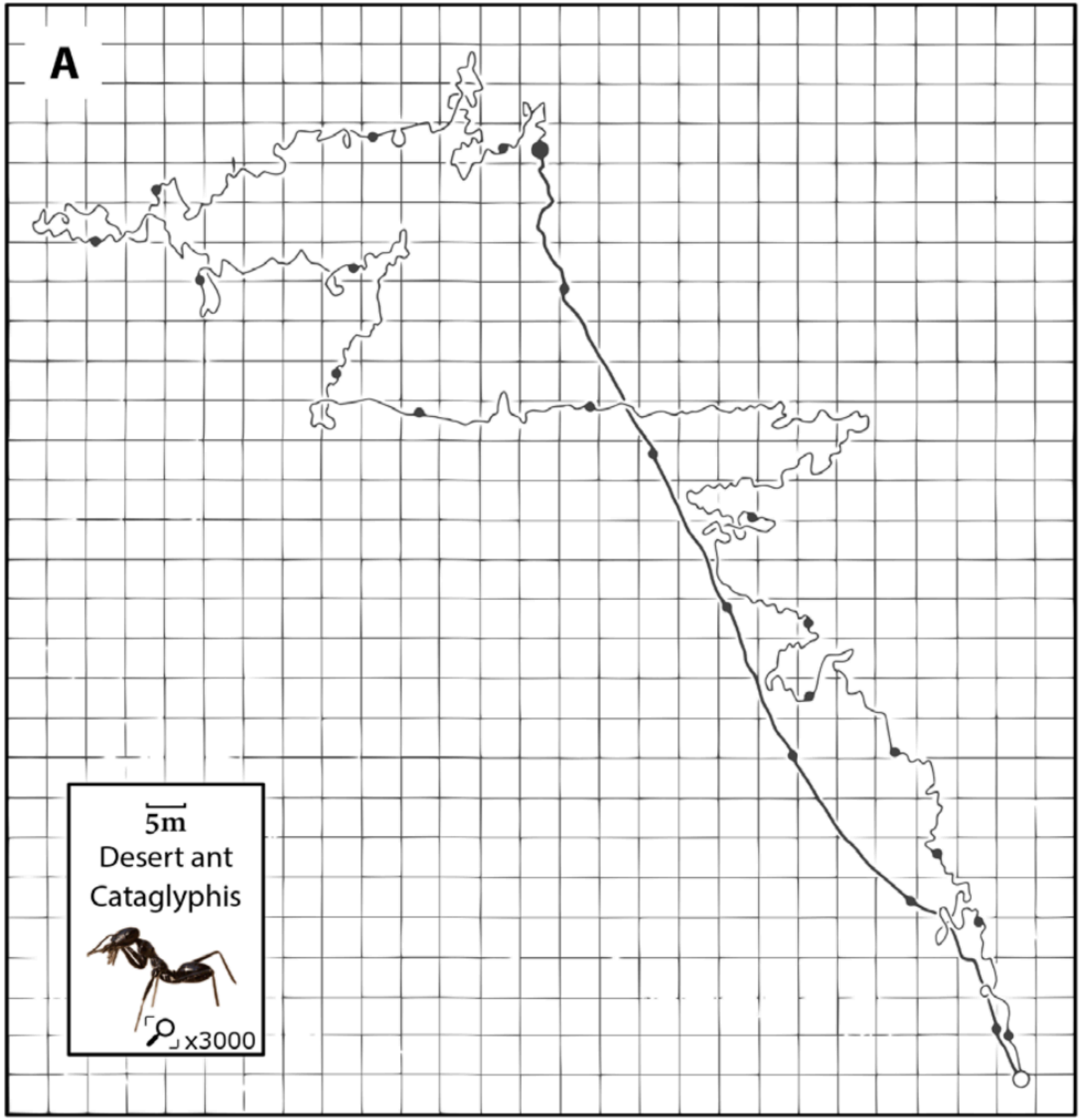

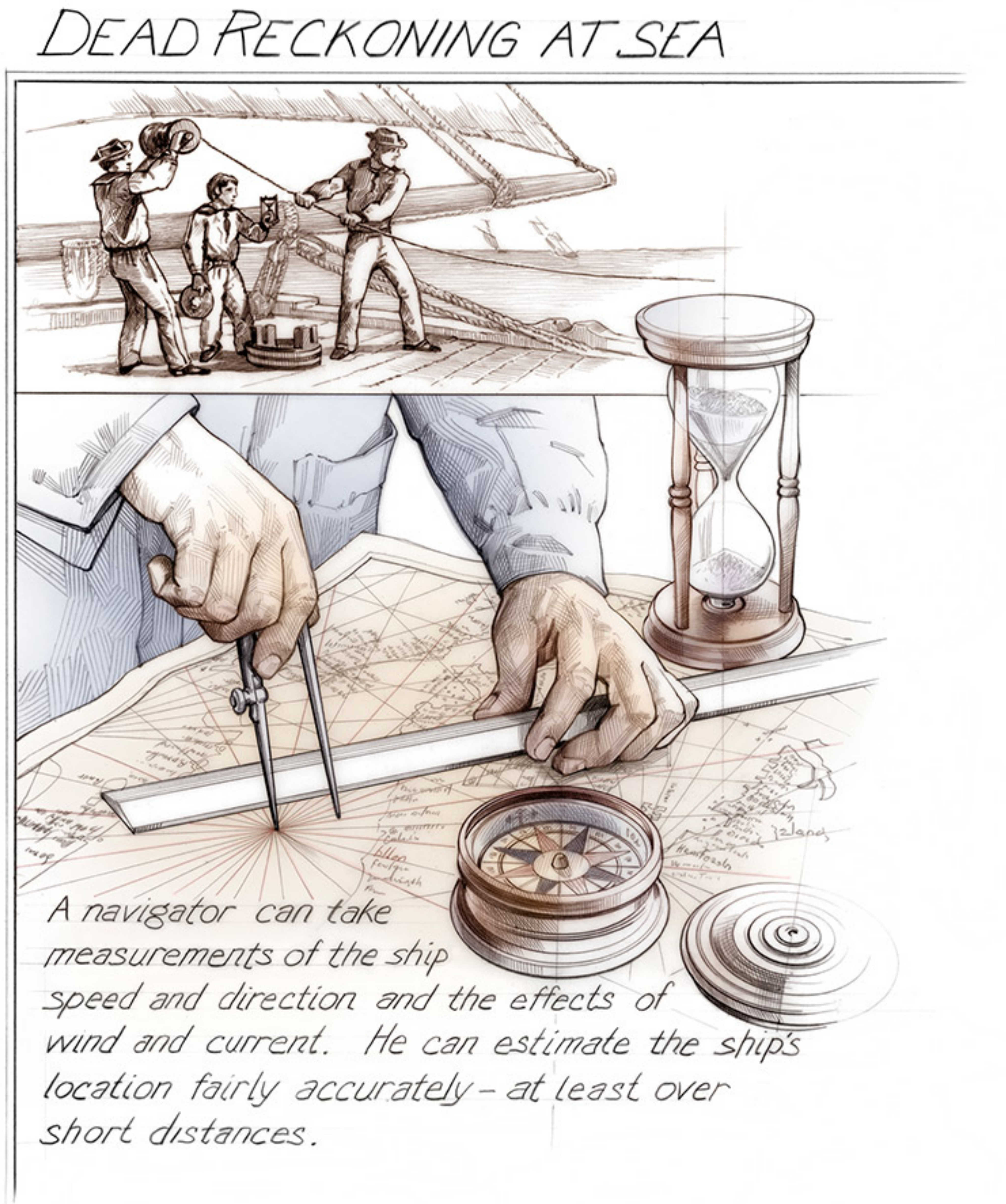
DEAD RECKONING AT SEA
A navigator can take measurements of the ship speed and direction and the effects of wind and current. He can estimate the ship's location fairly accurately - at least over short distances.

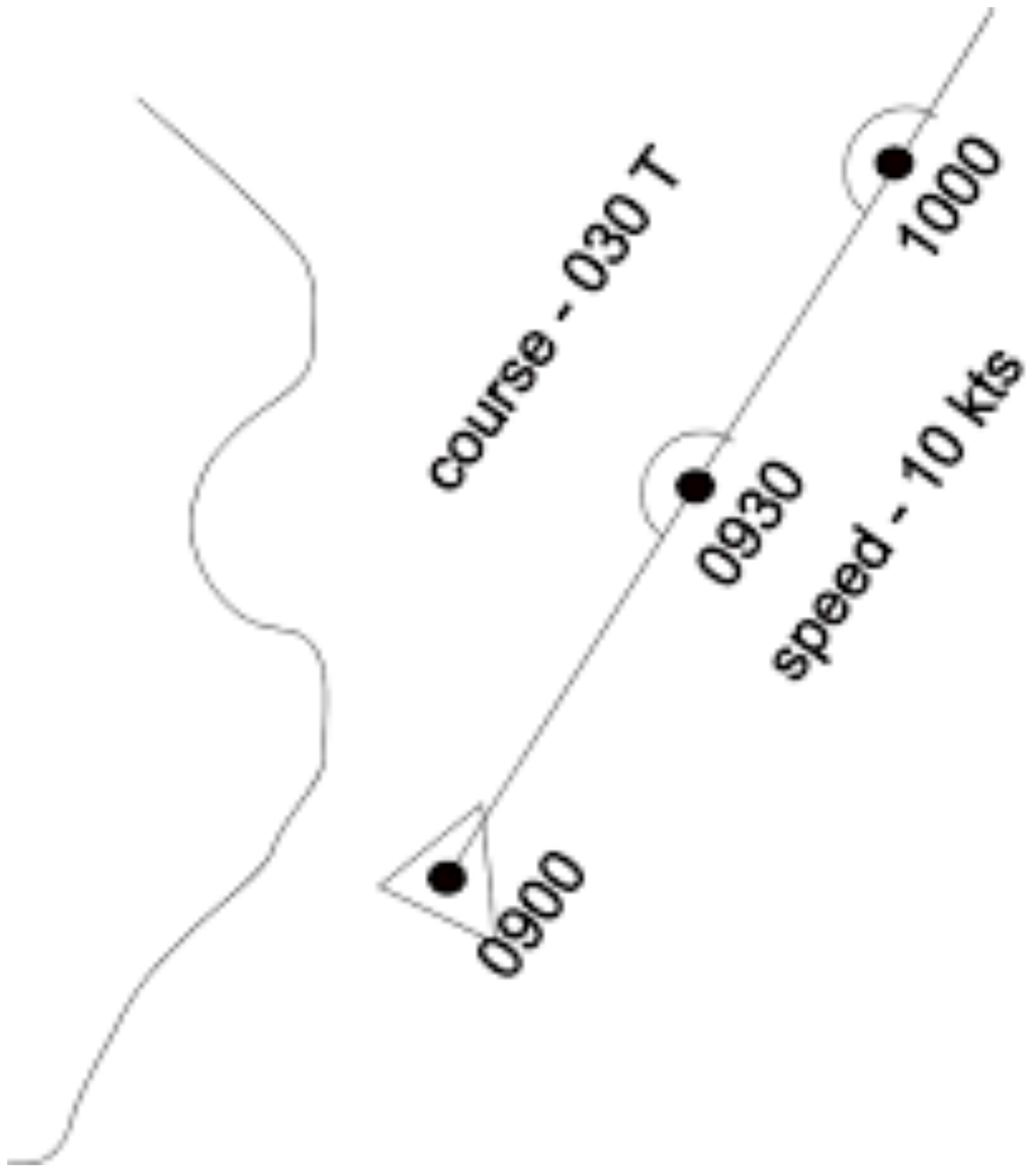
course - 030 T
speed - 10 kts
0900
0930
1000

Classical theory of grid cells

- Toroidal connectivity of neurons

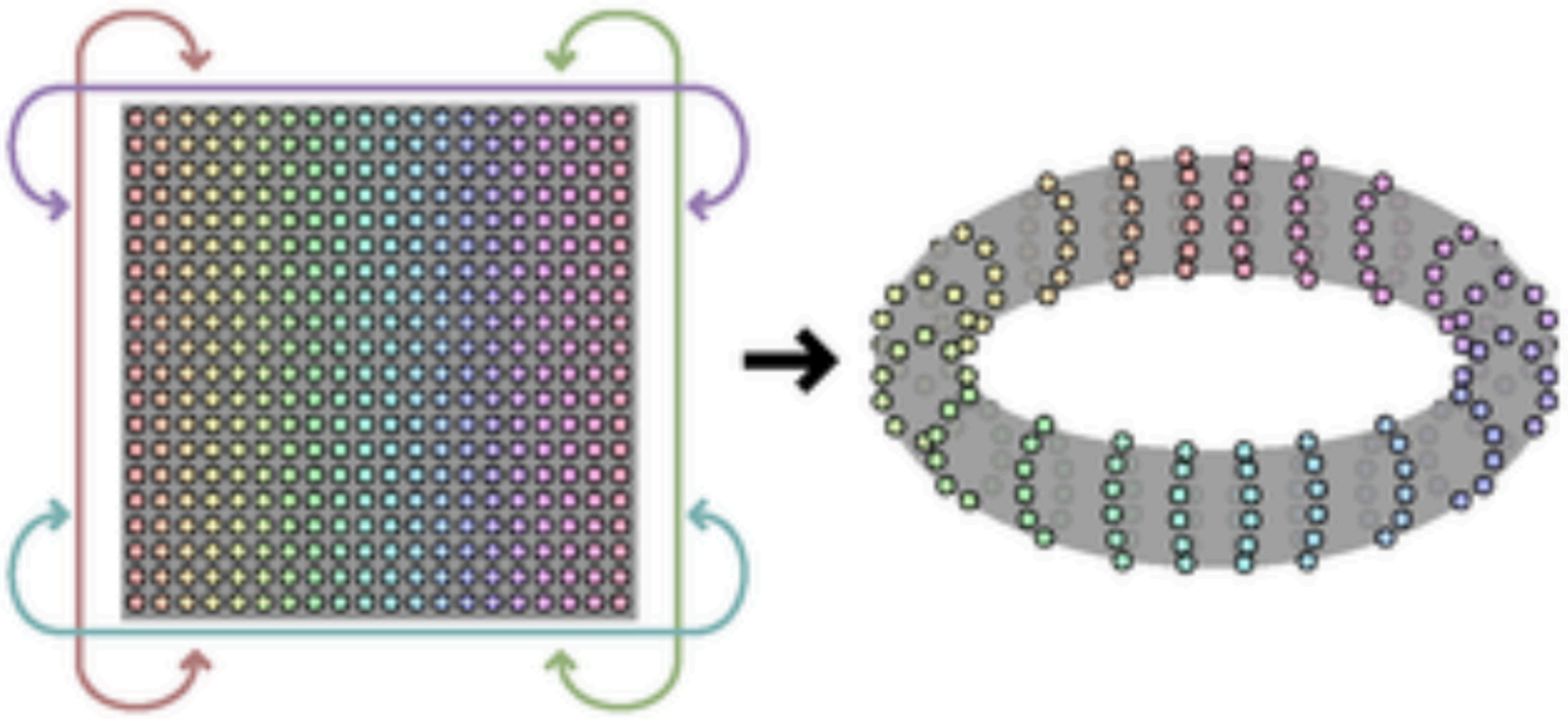

Neuronal space

Classical theory of grid cells

- Toroidal connectivity of neurons
- Bump of activity updated by ideothetic (velocity) cues

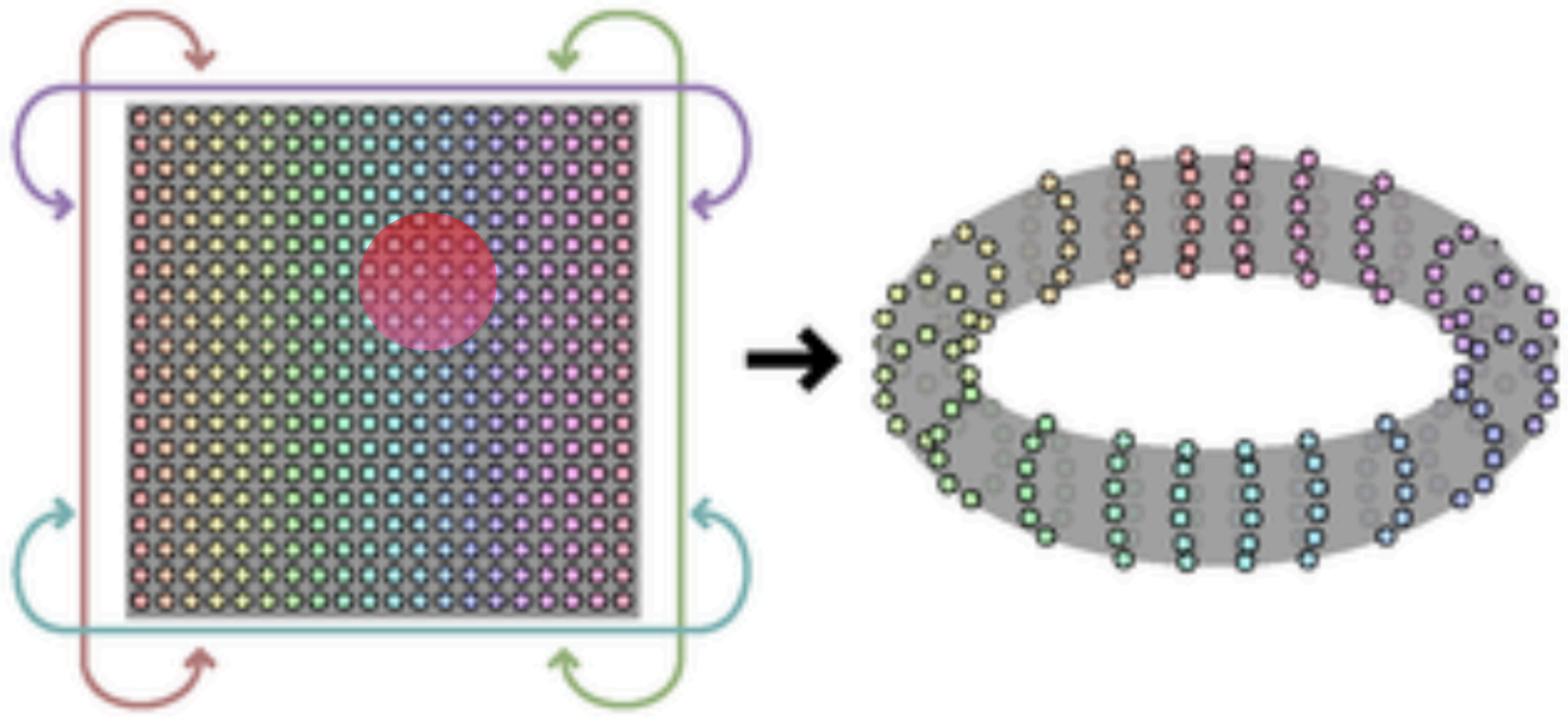

Neuronal space

Classical theory of grid cells

- Toroidal connectivity of neurons
- Bump of activity updated by ideothetic (velocity) cues

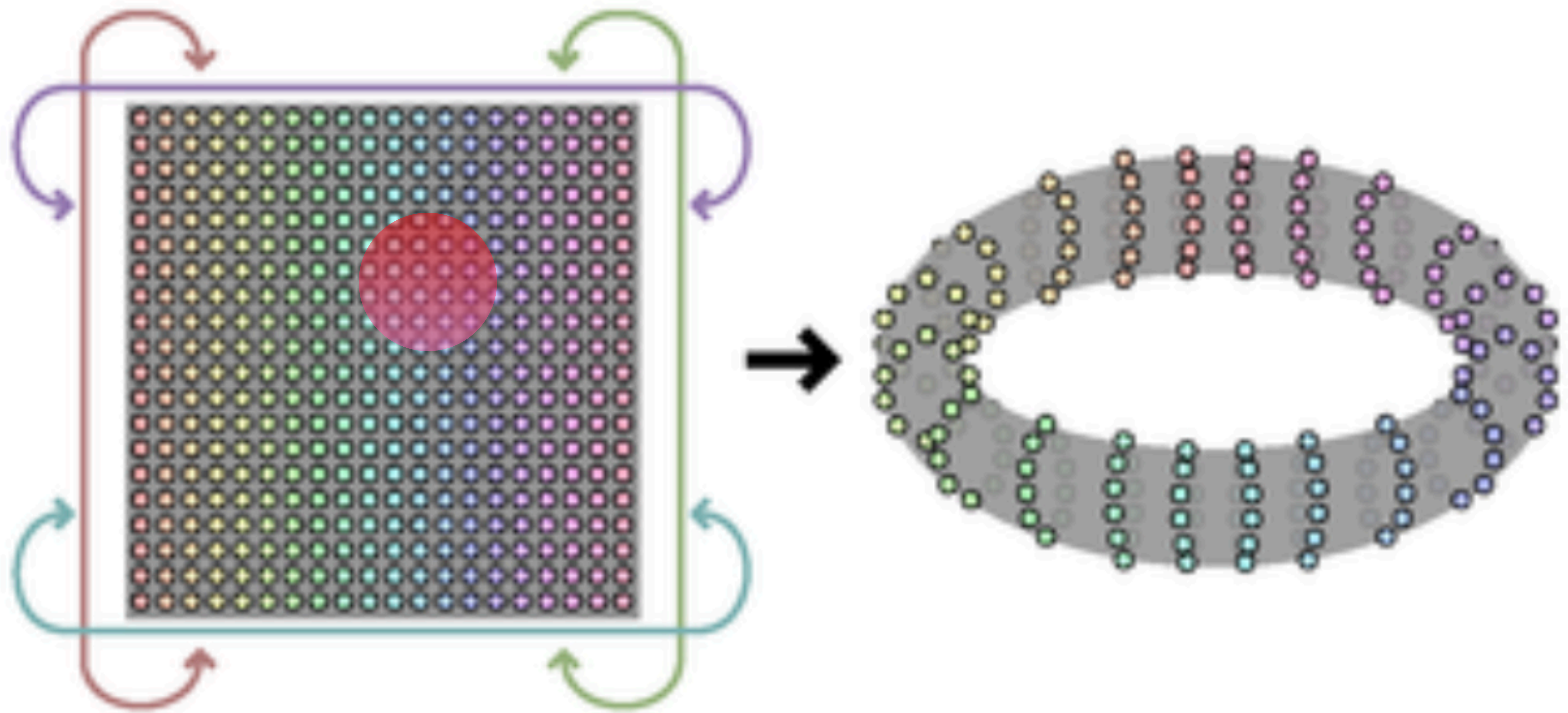

Neuronal space

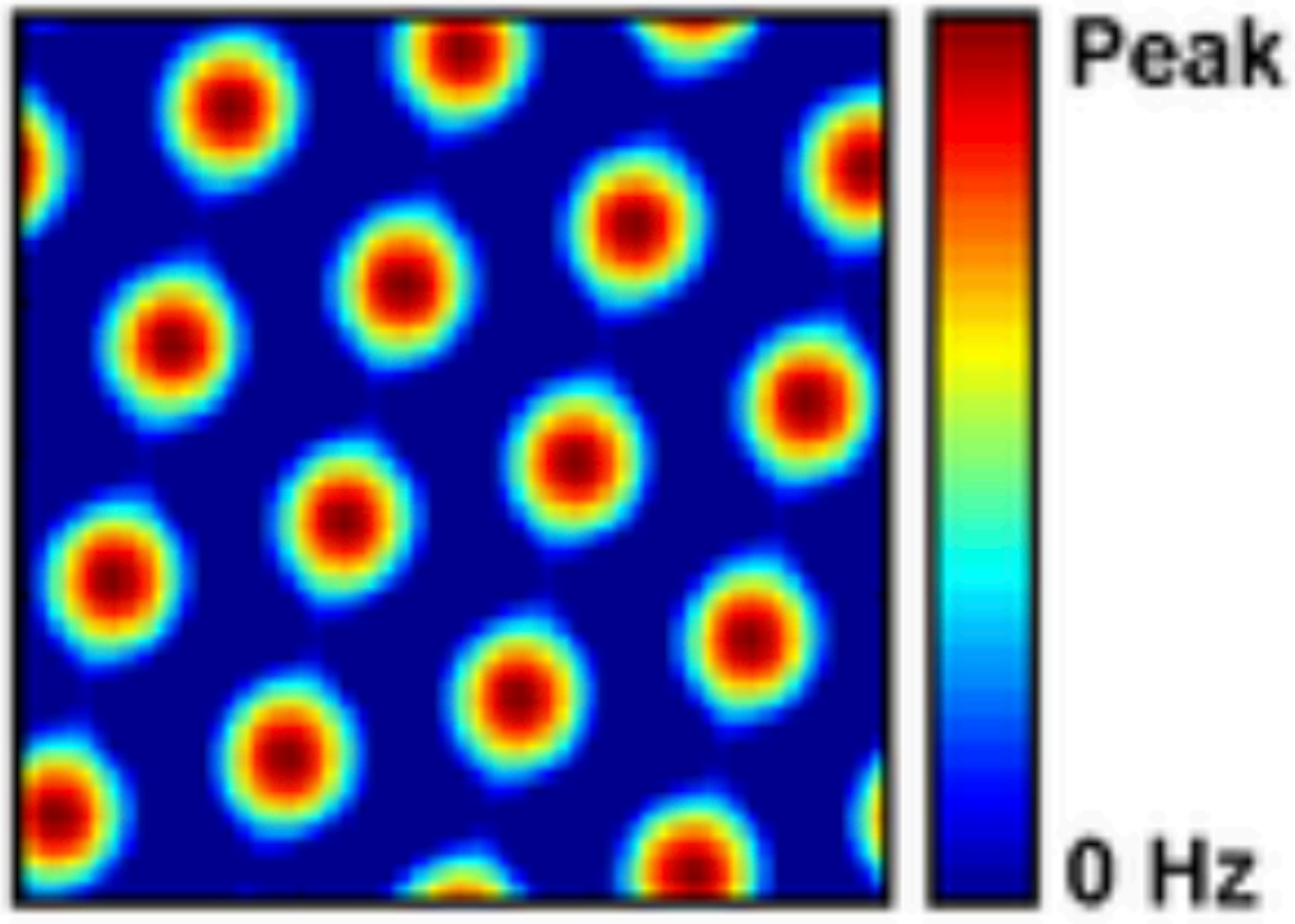

Physical space

Classical theory of grid cells

- Toroidal connectivity of neurons
- Bump of activity updated by ideothetic (velocity) cues

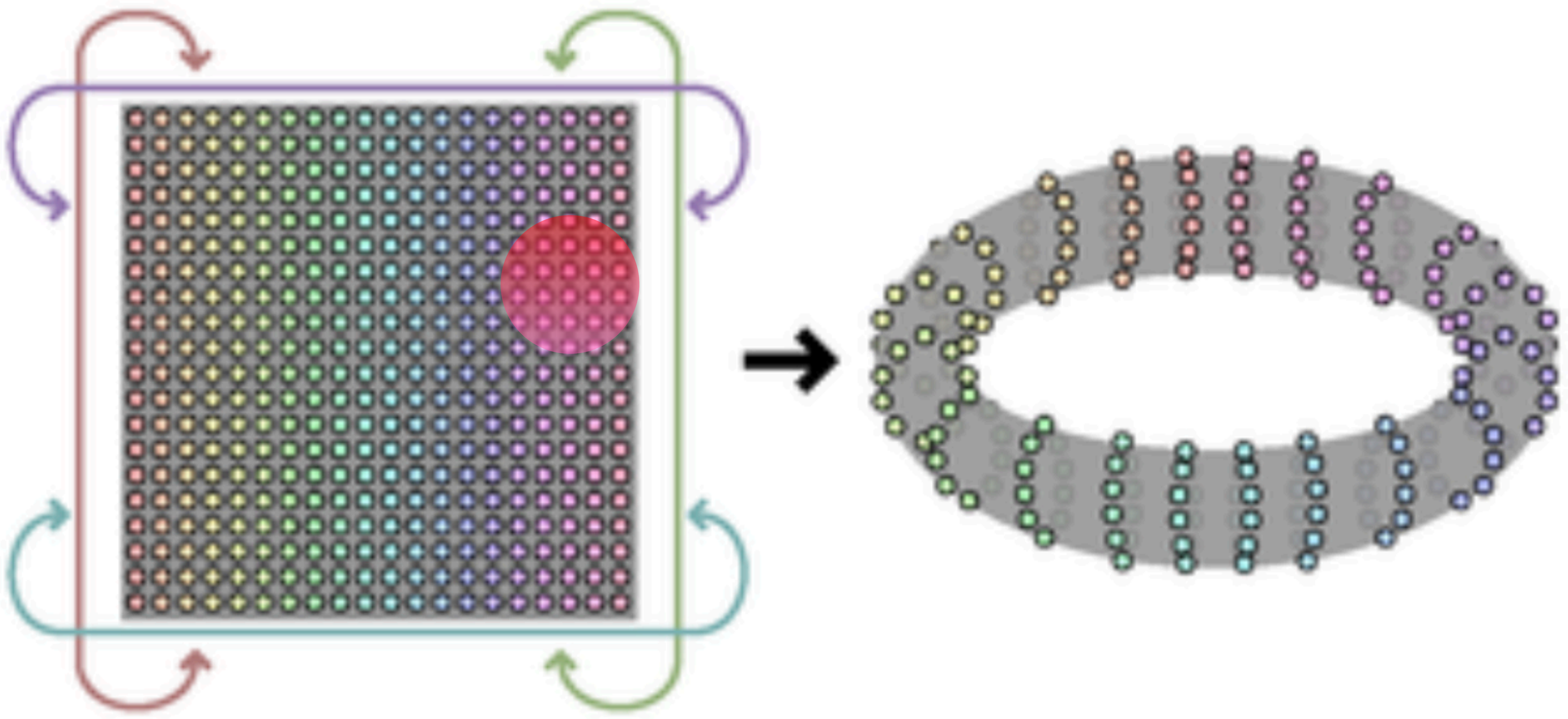

Neuronal space

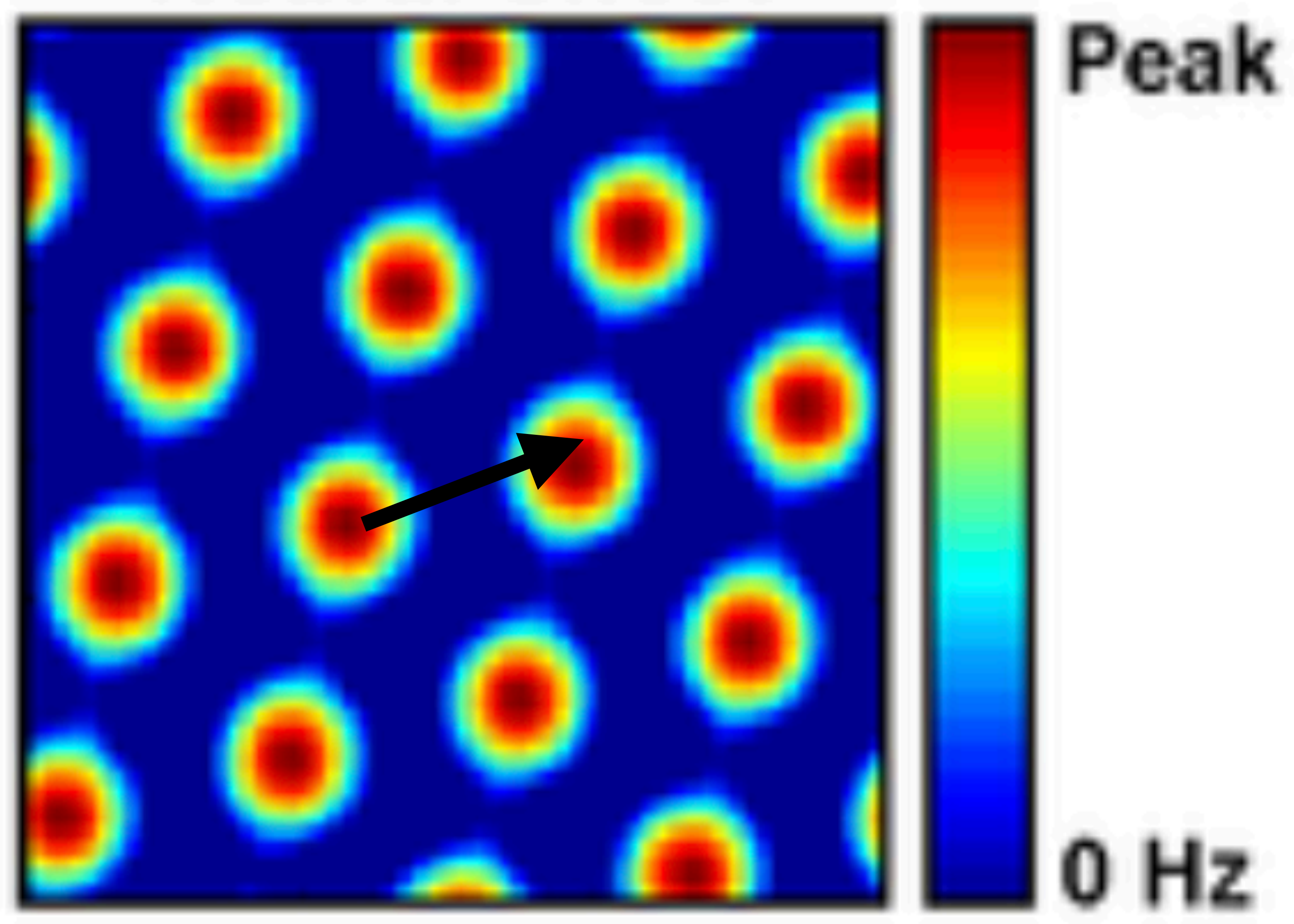

Physical space

Classical theory of grid cells

- Toroidal connectivity of neurons
- Bump of activity updated by ideothetic (velocity) cues

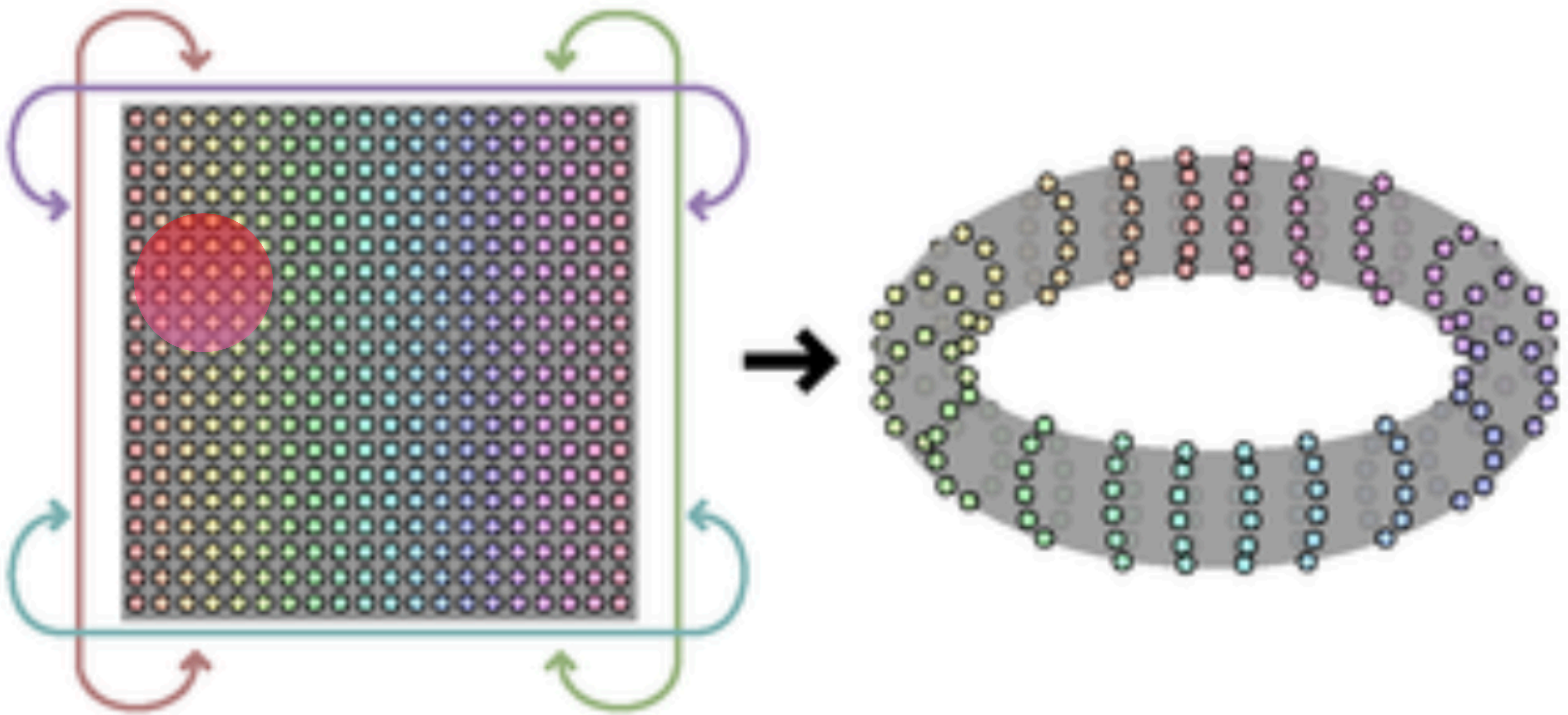

Neuronal space

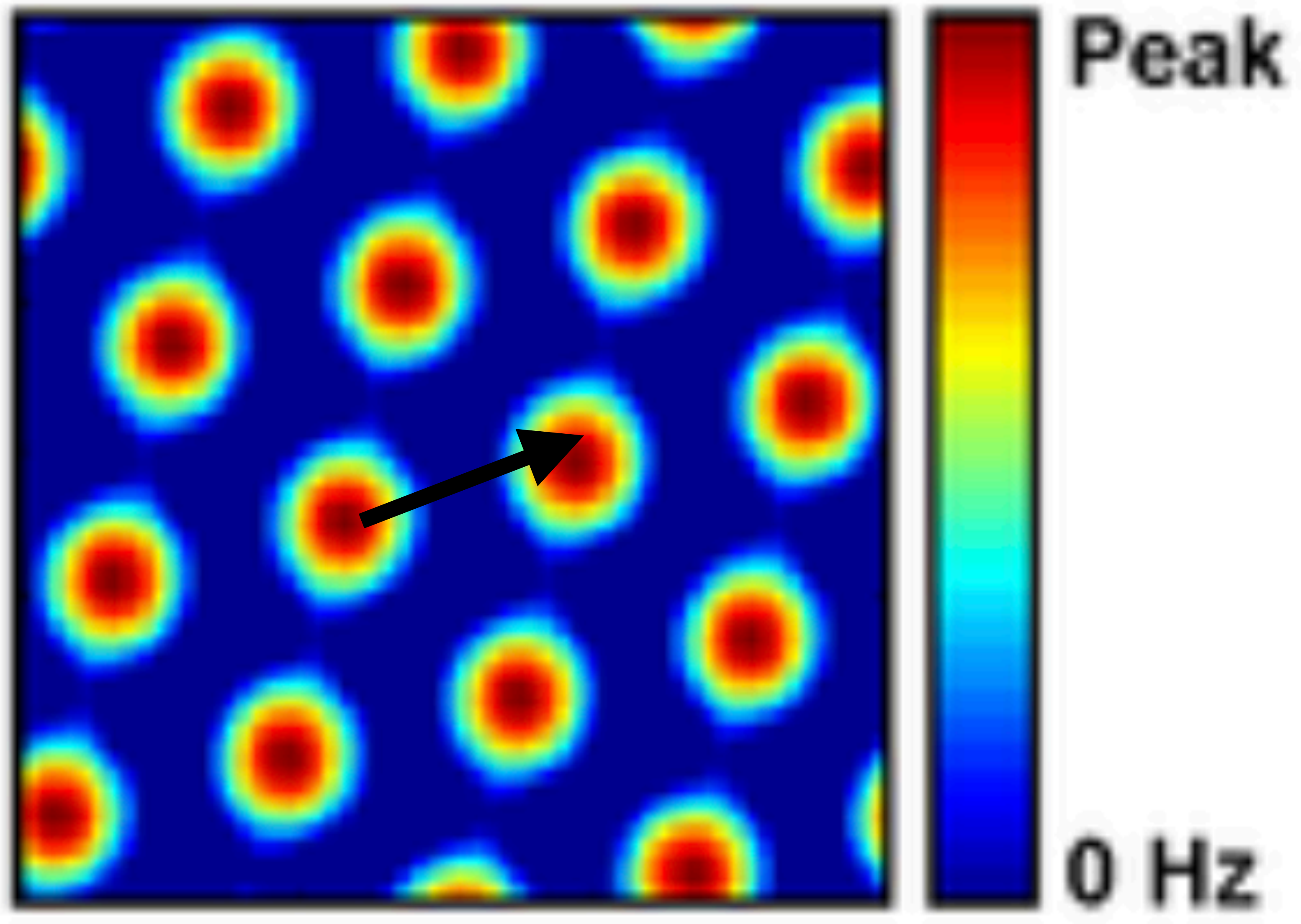

Physical space

Classical theory of grid cells

- Toroidal connectivity of neurons
- Bump of activity updated by ideothetic (velocity) cues

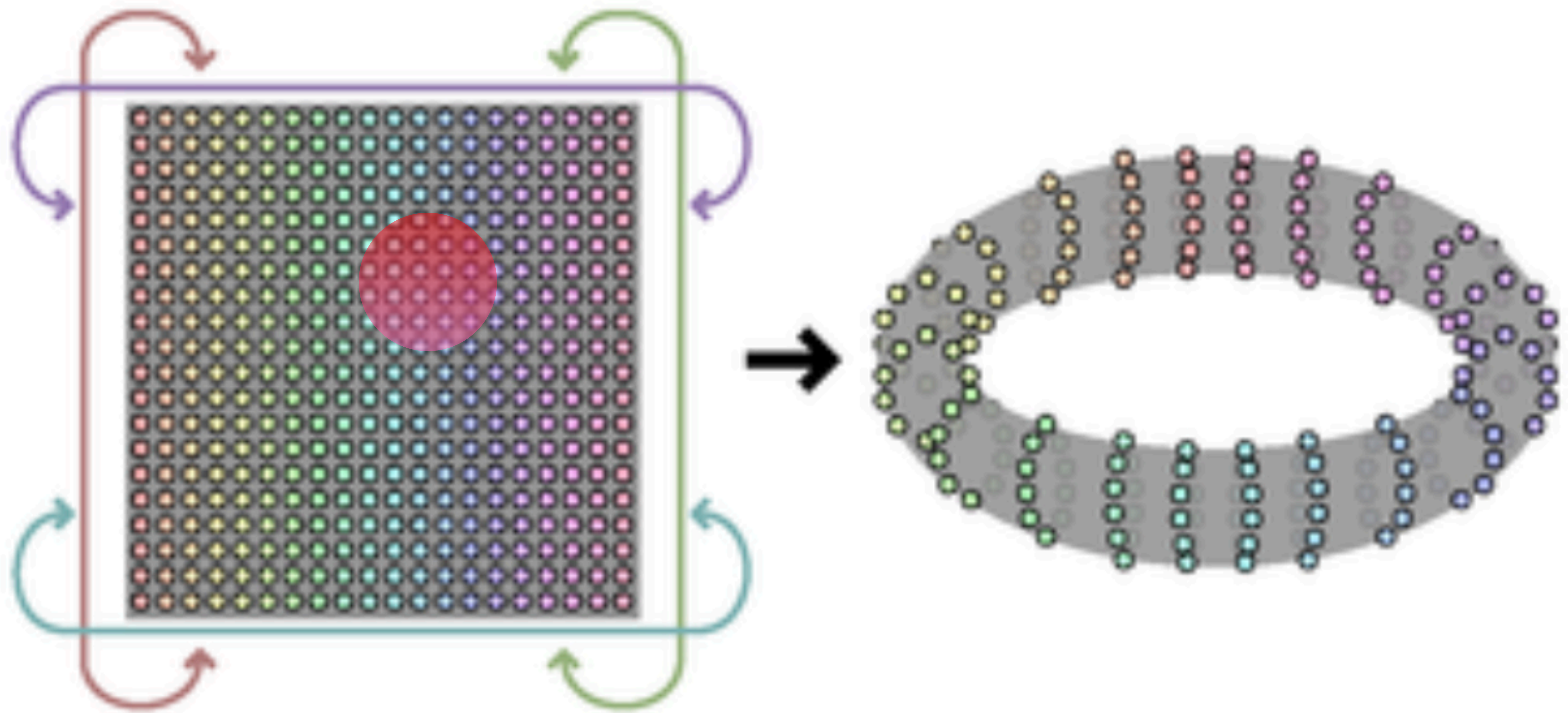

Neuronal space

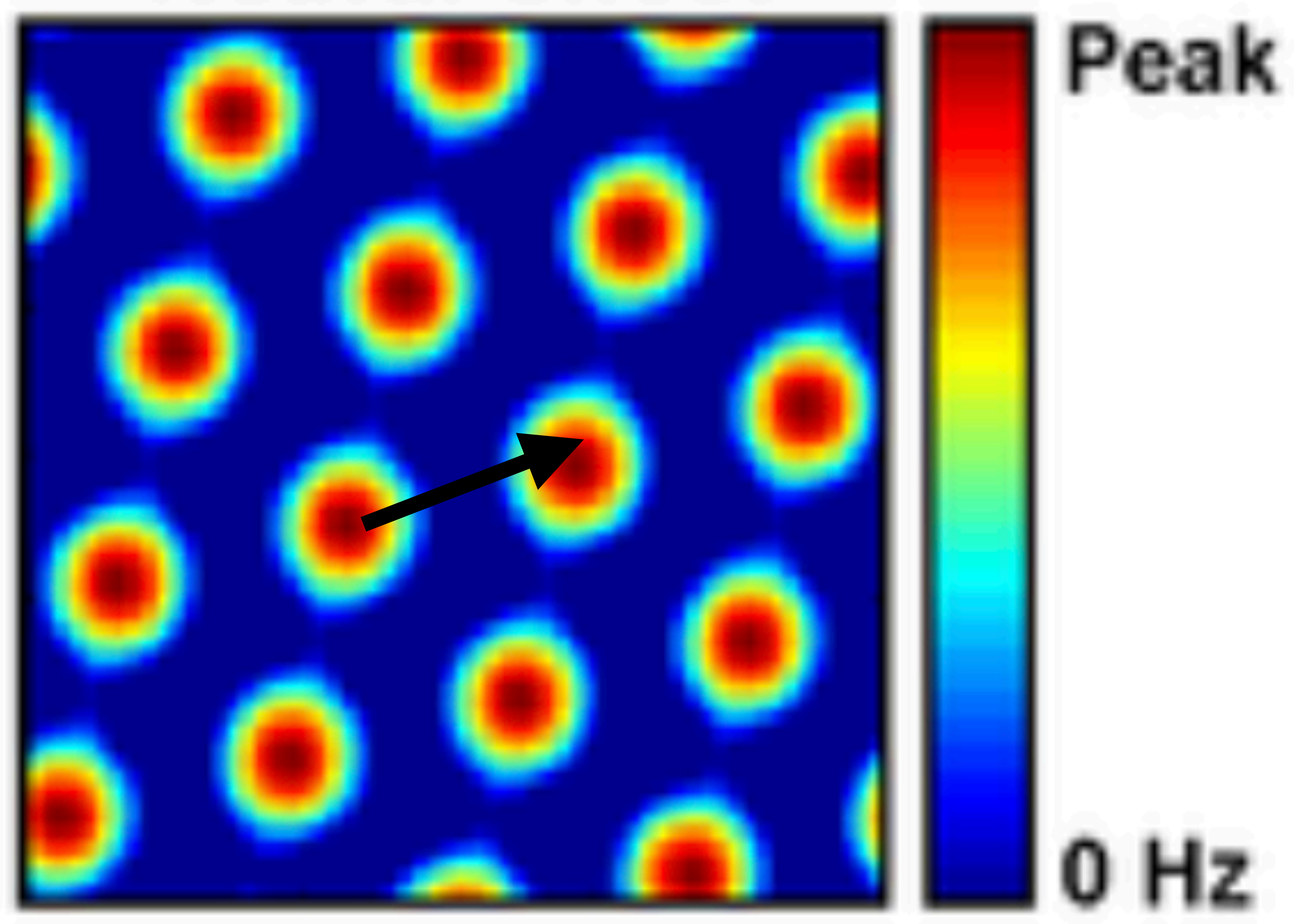

Physical space

Classical theory of grid cells

- Toroidal connectivity of neurons
- Bump of activity updated by ideothetic (velocity) cues
- Kantian view of spatial sense (innate, “must be found in us prior any perception of an object”)

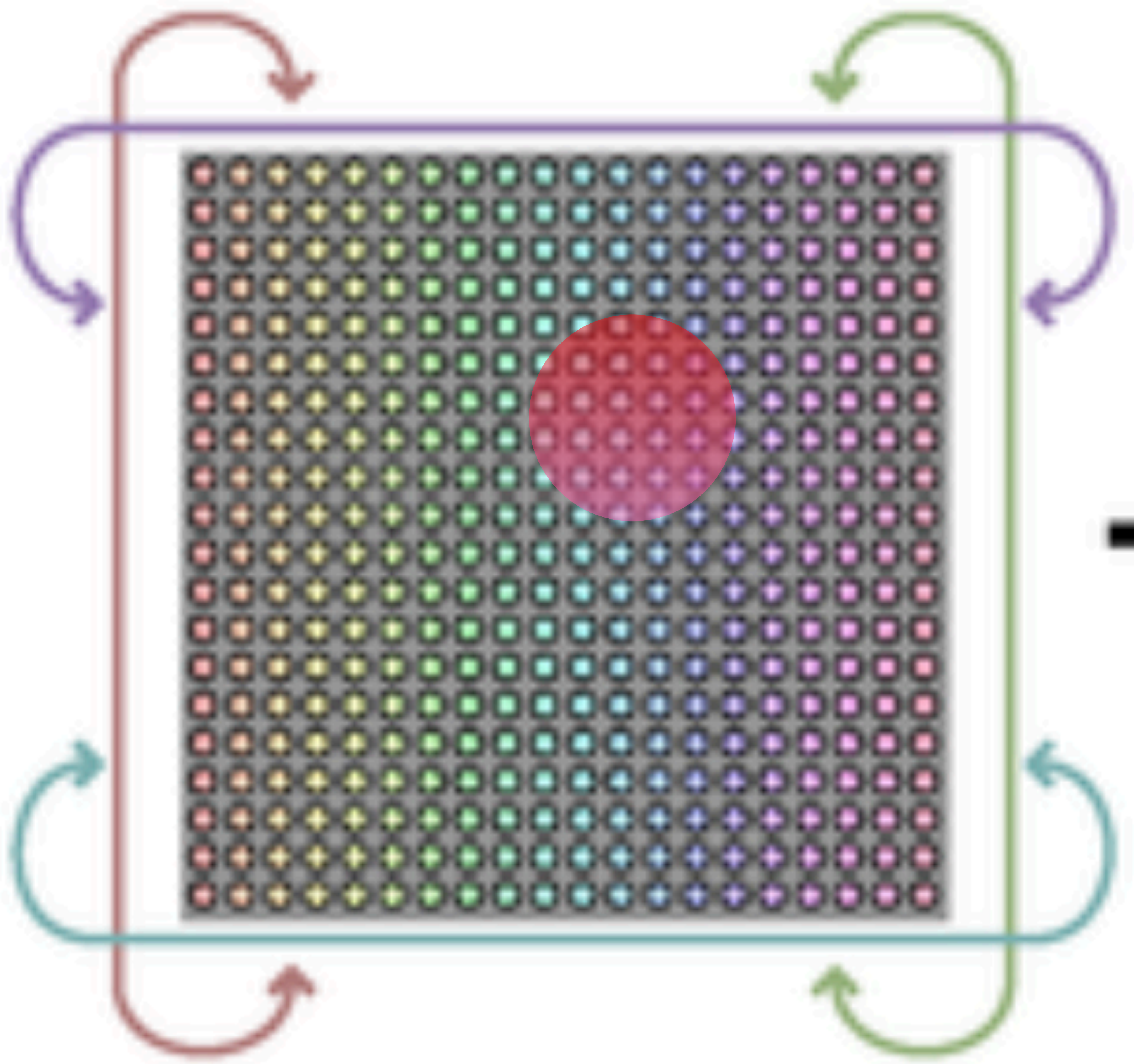

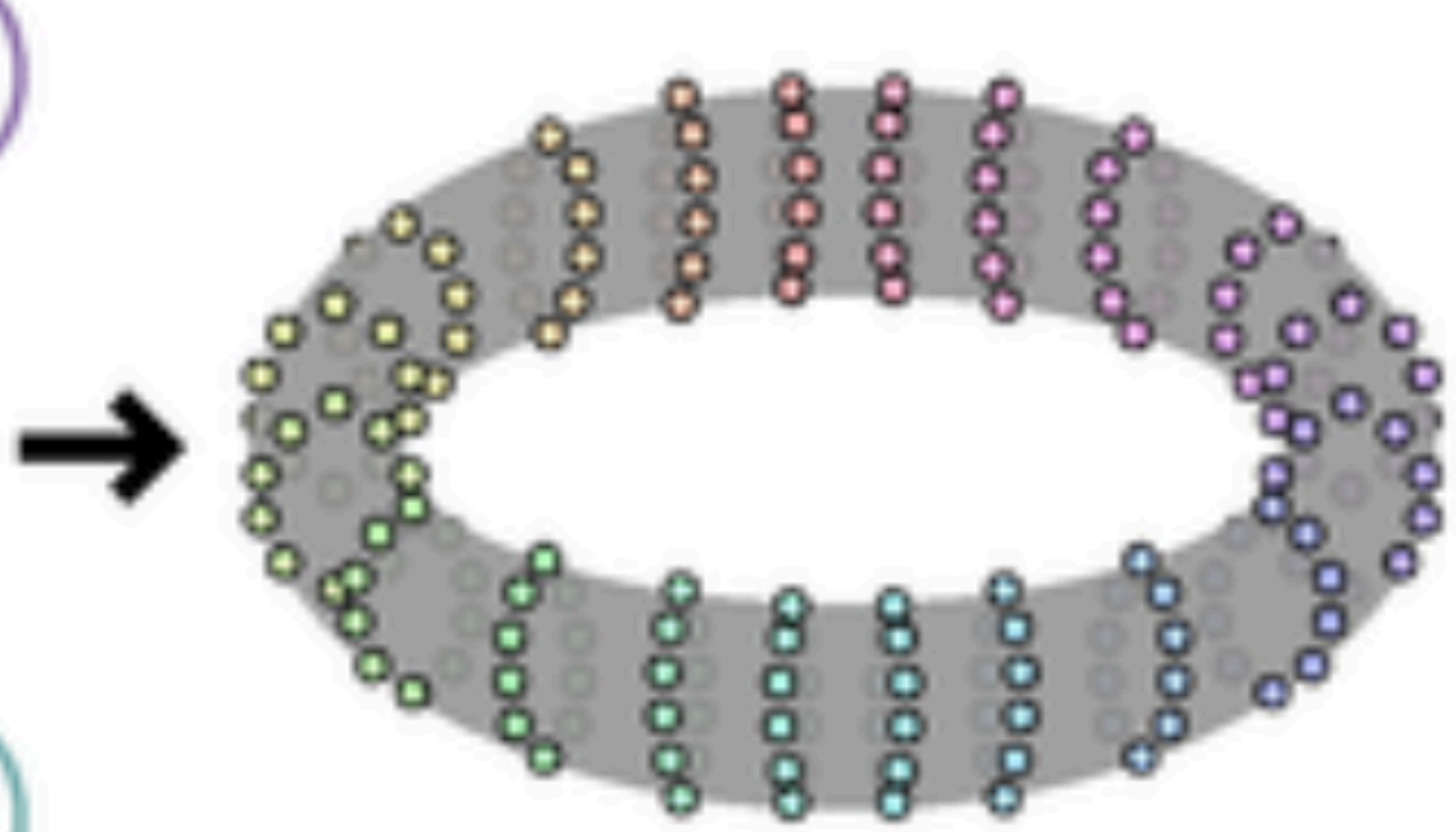

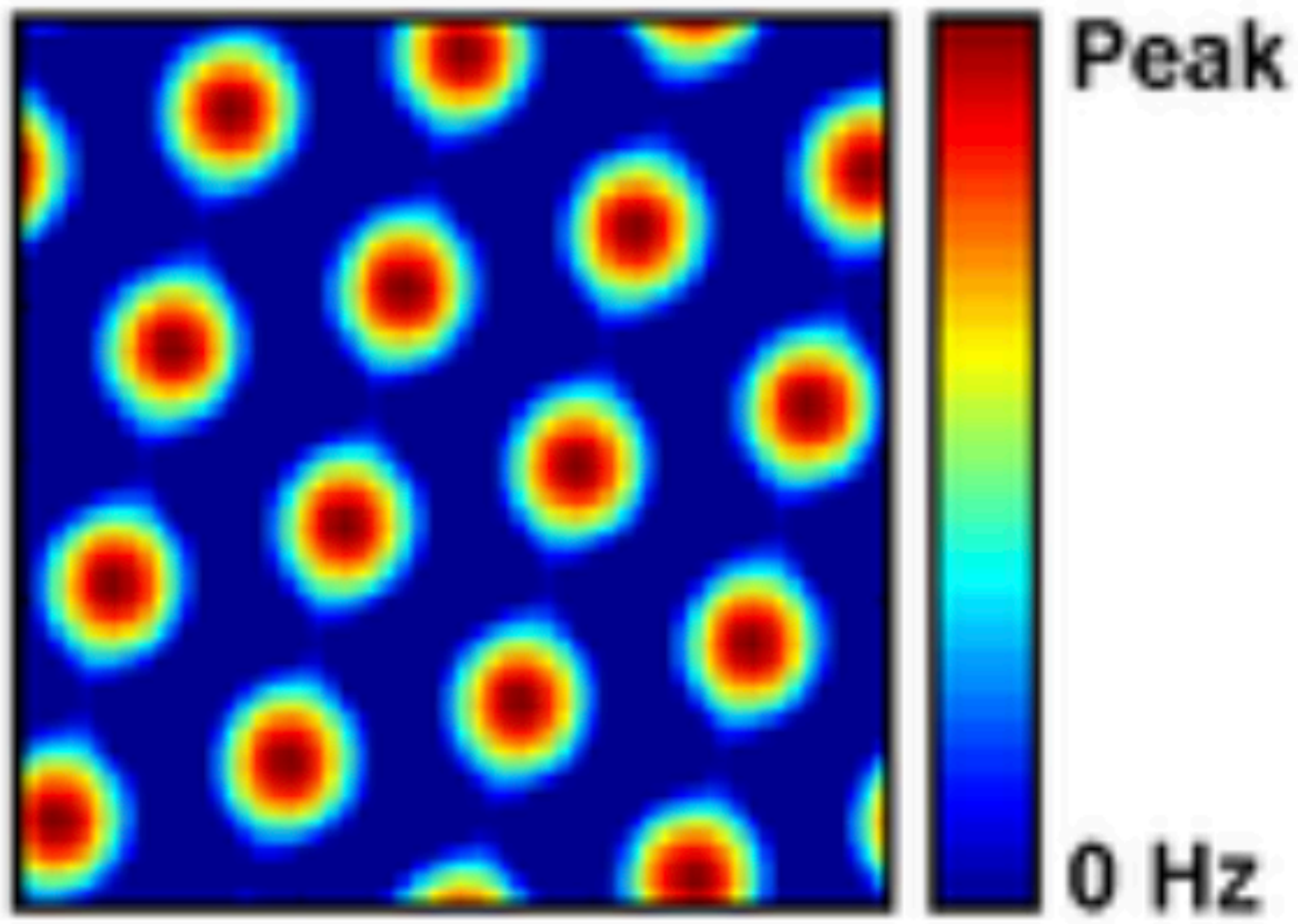

Neuronal space

Physical space

Difficulties for the classical theory: effects of the environment shape

Environment effects

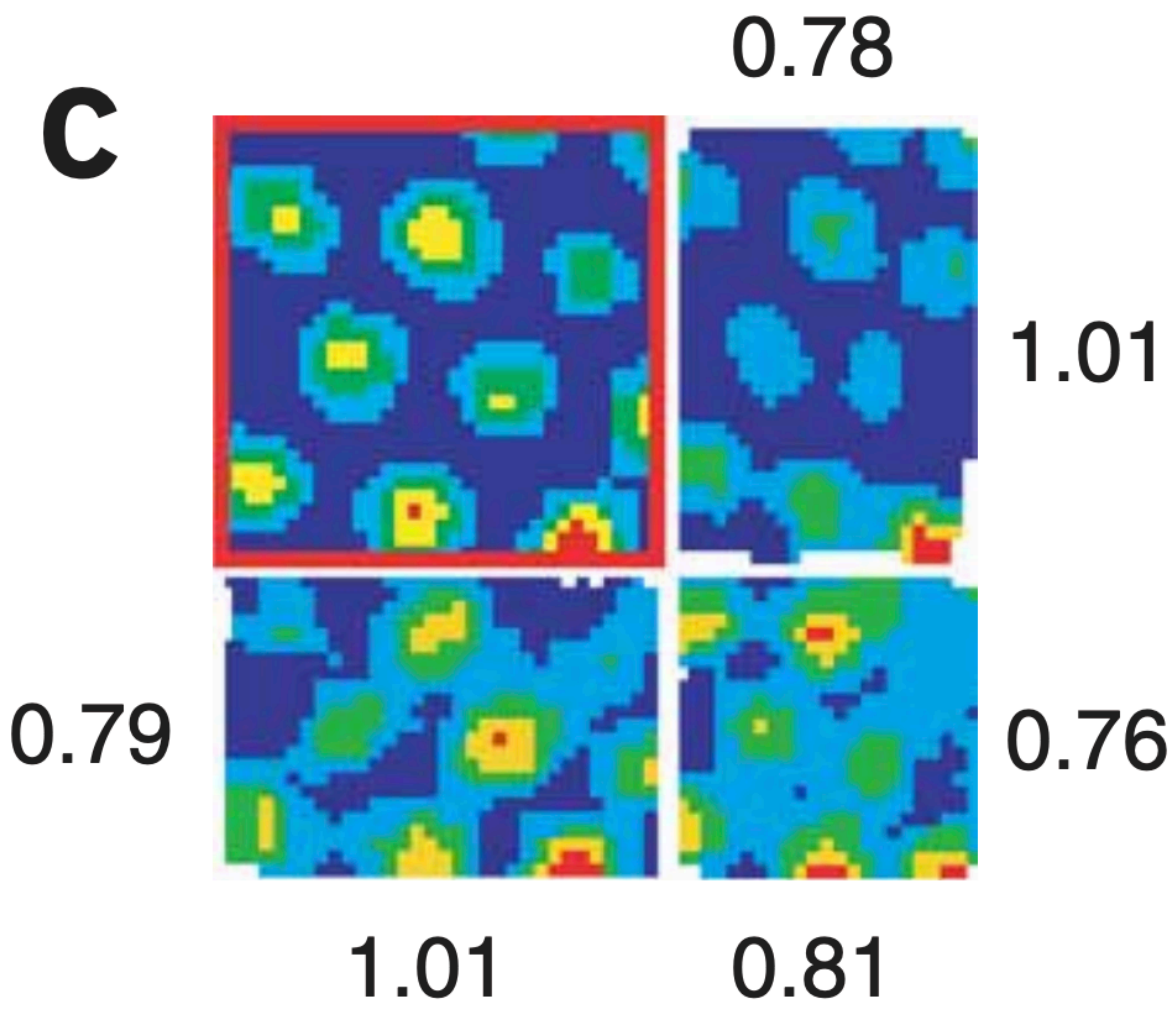

- Size

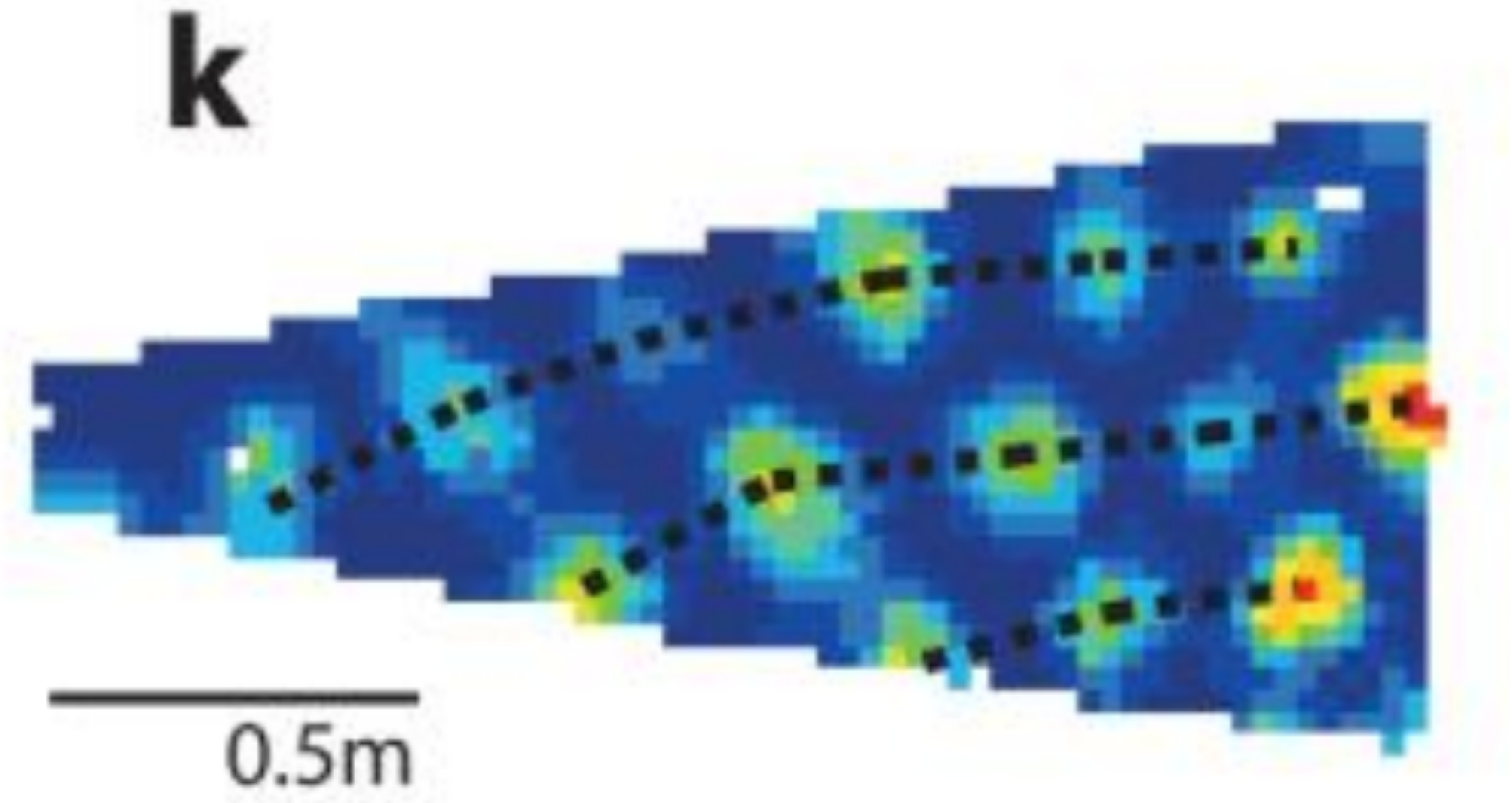

- Shape

A different type of theory

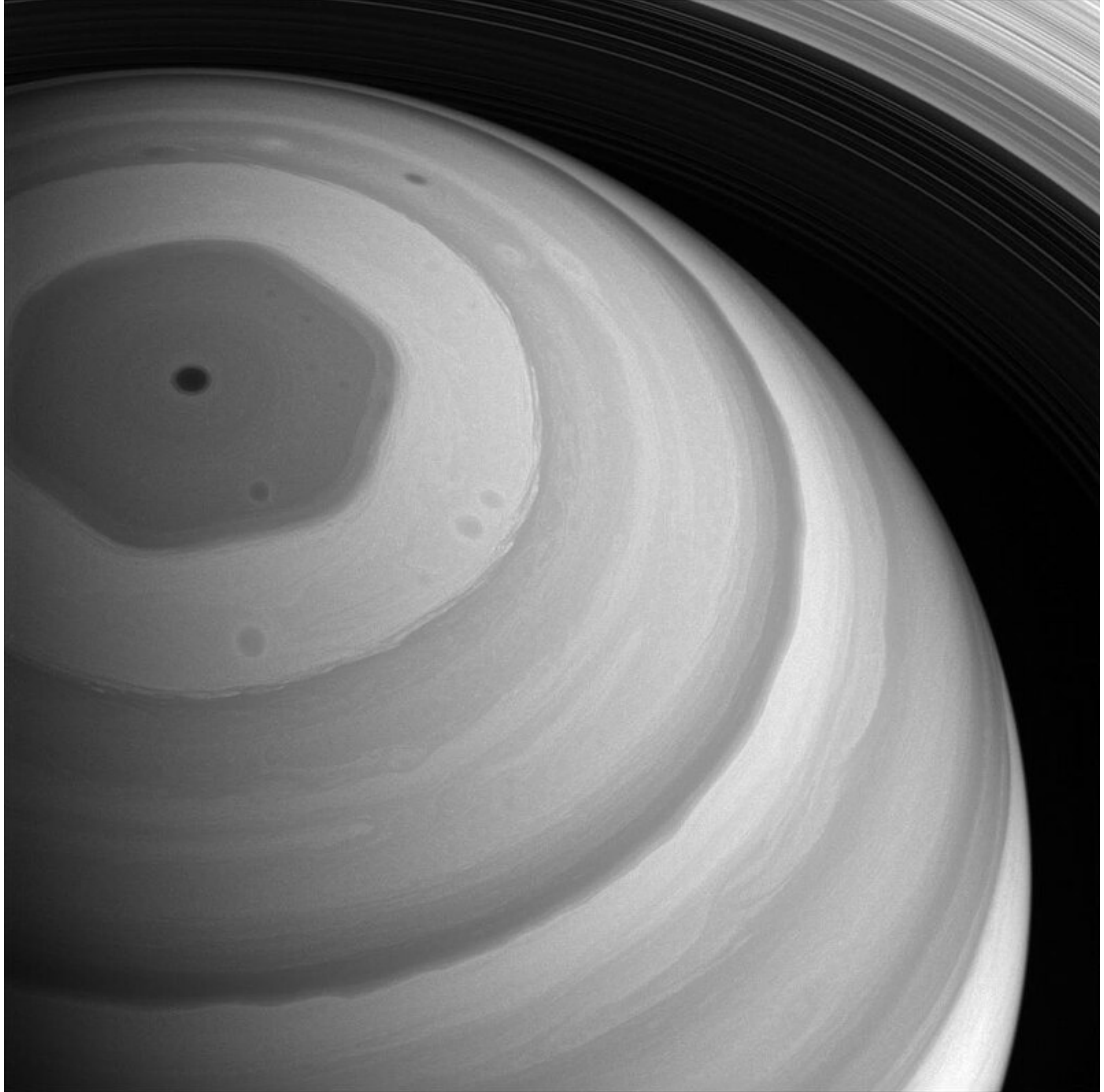

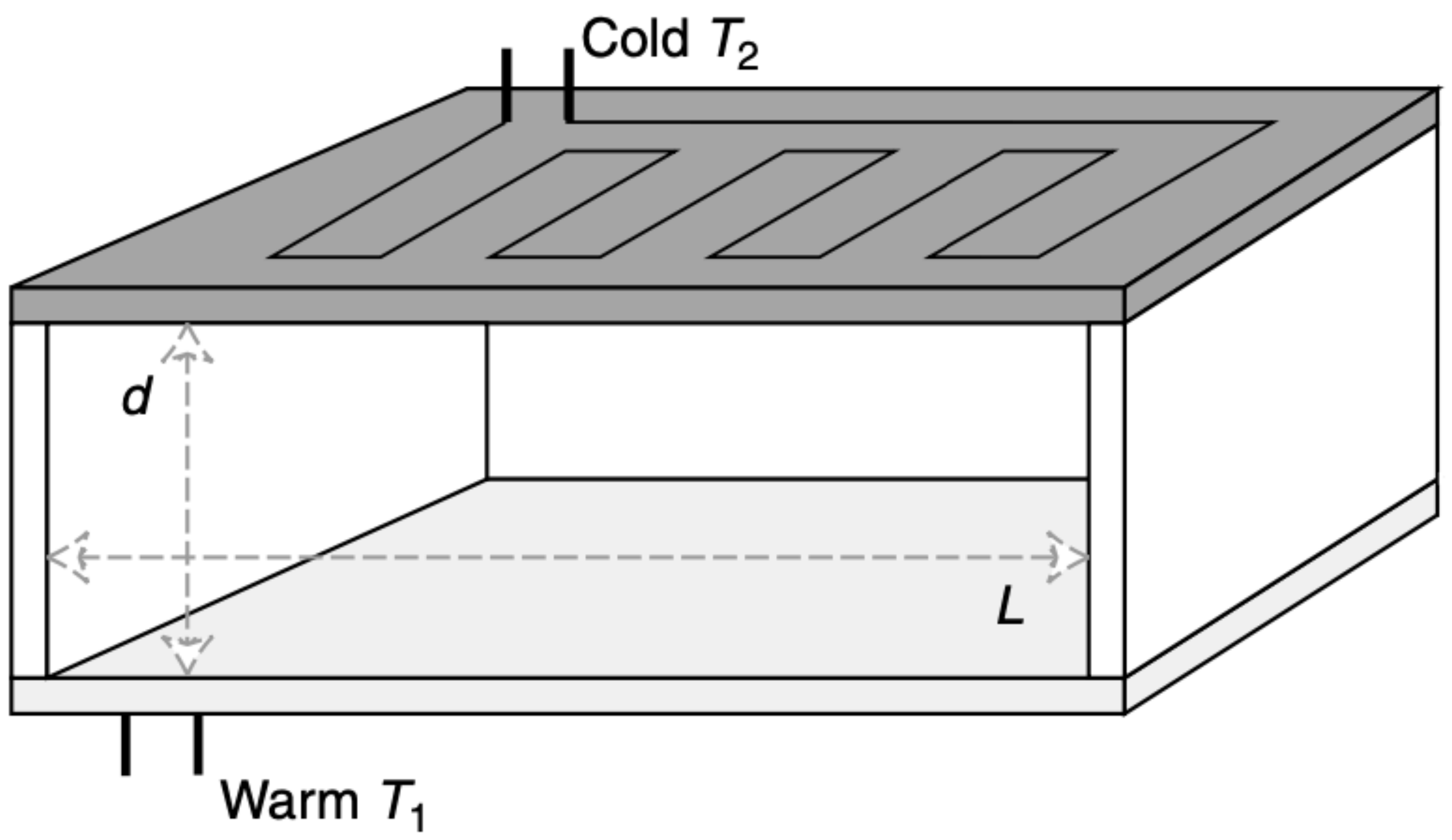

Cold T_2
d
L
Warm T_1

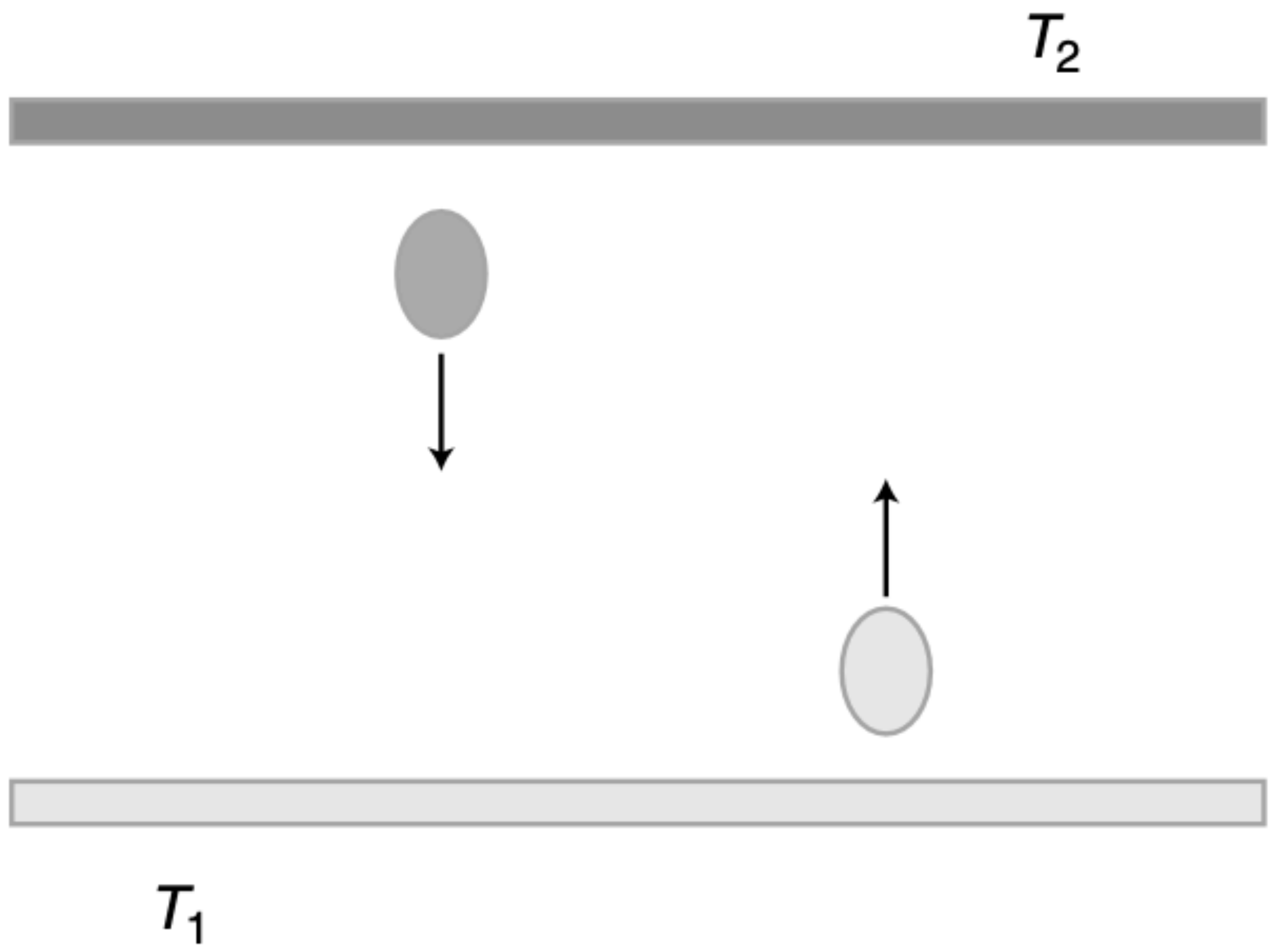

T_2
T_1

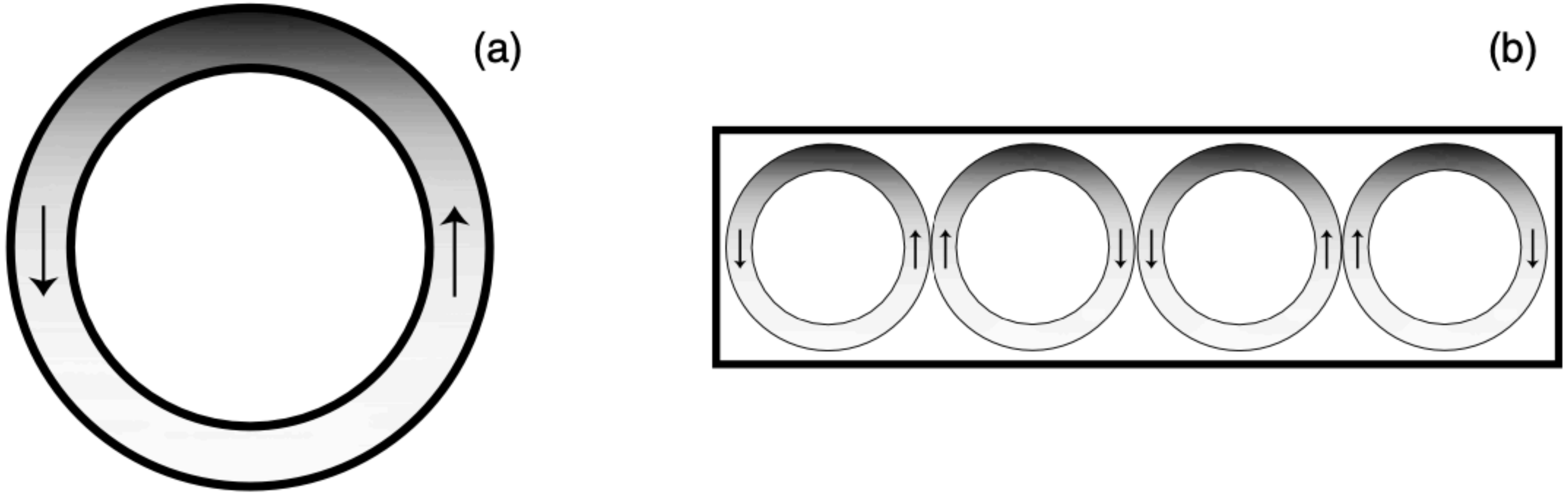

(a)
(b)

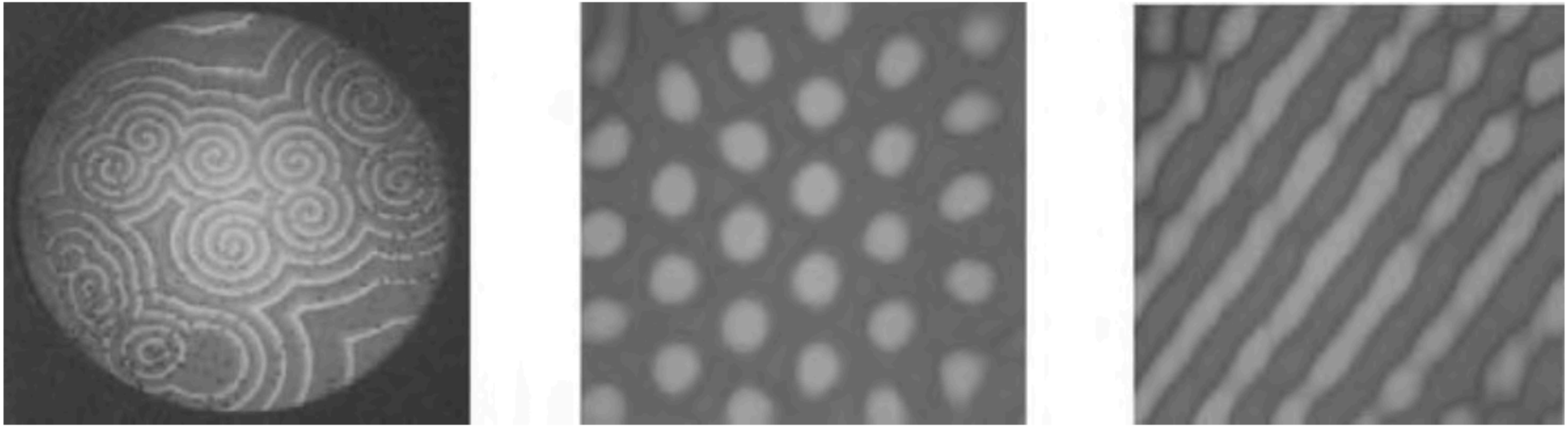

Pattern formation


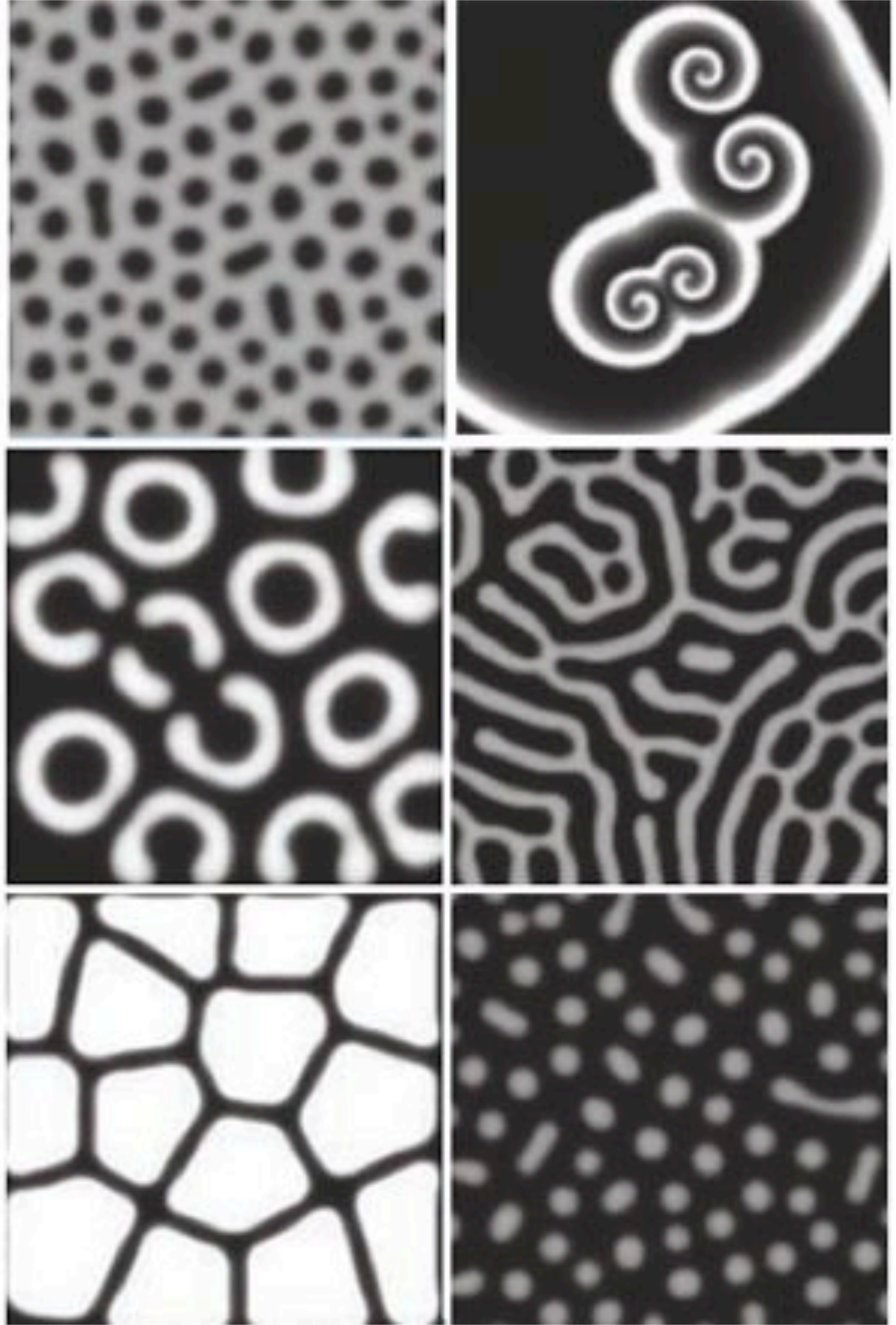

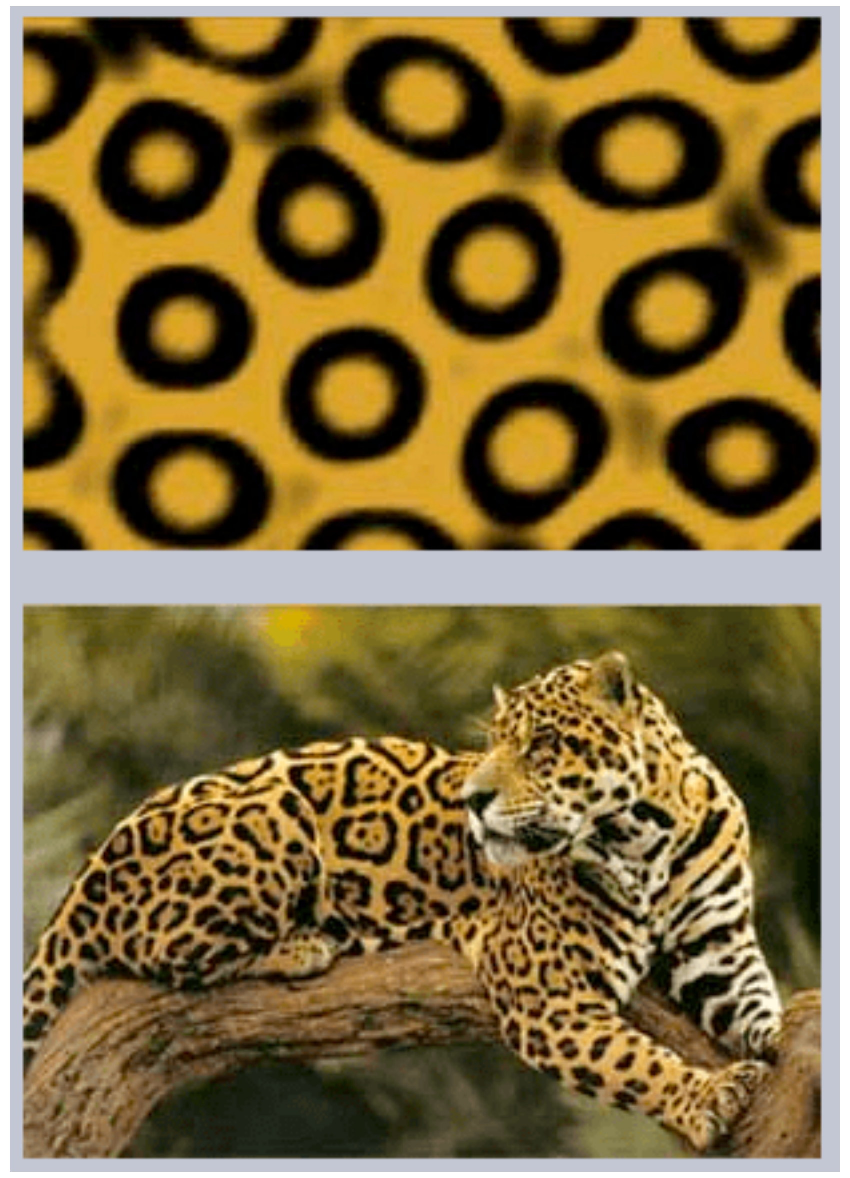

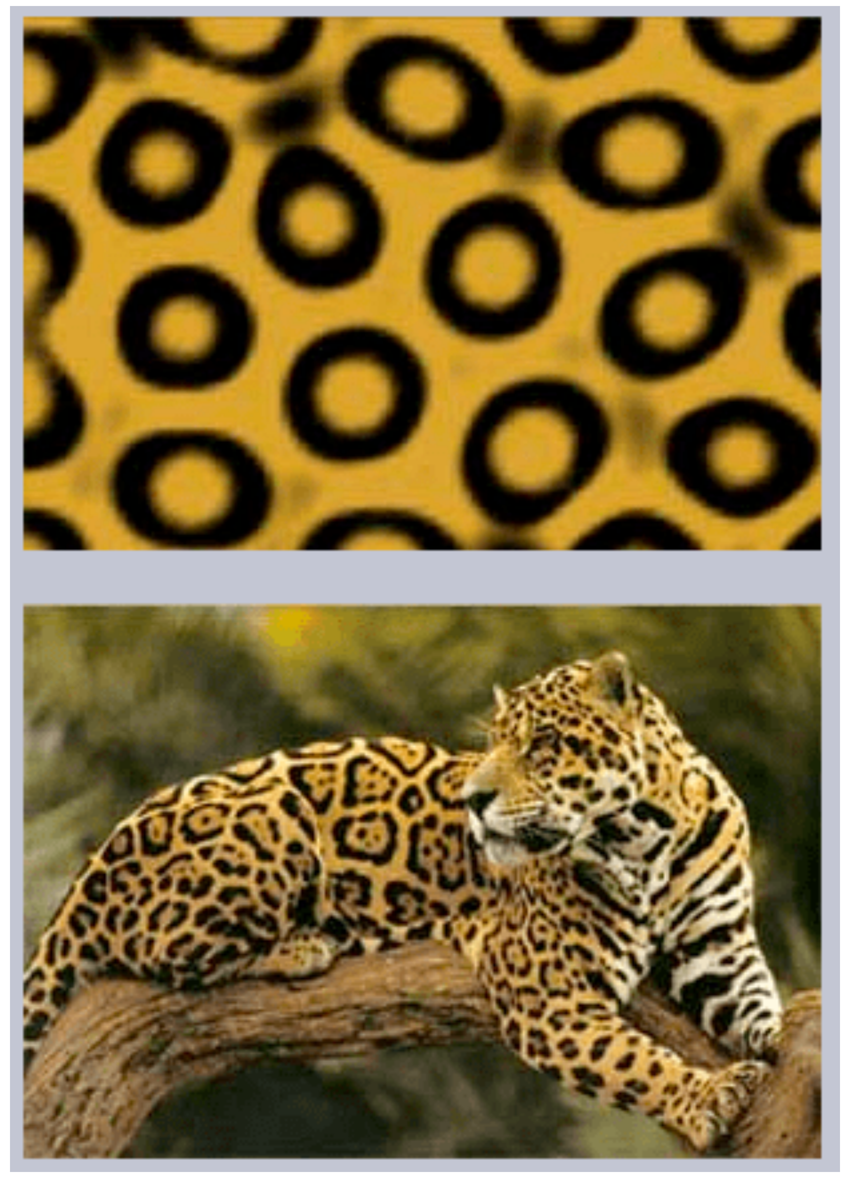

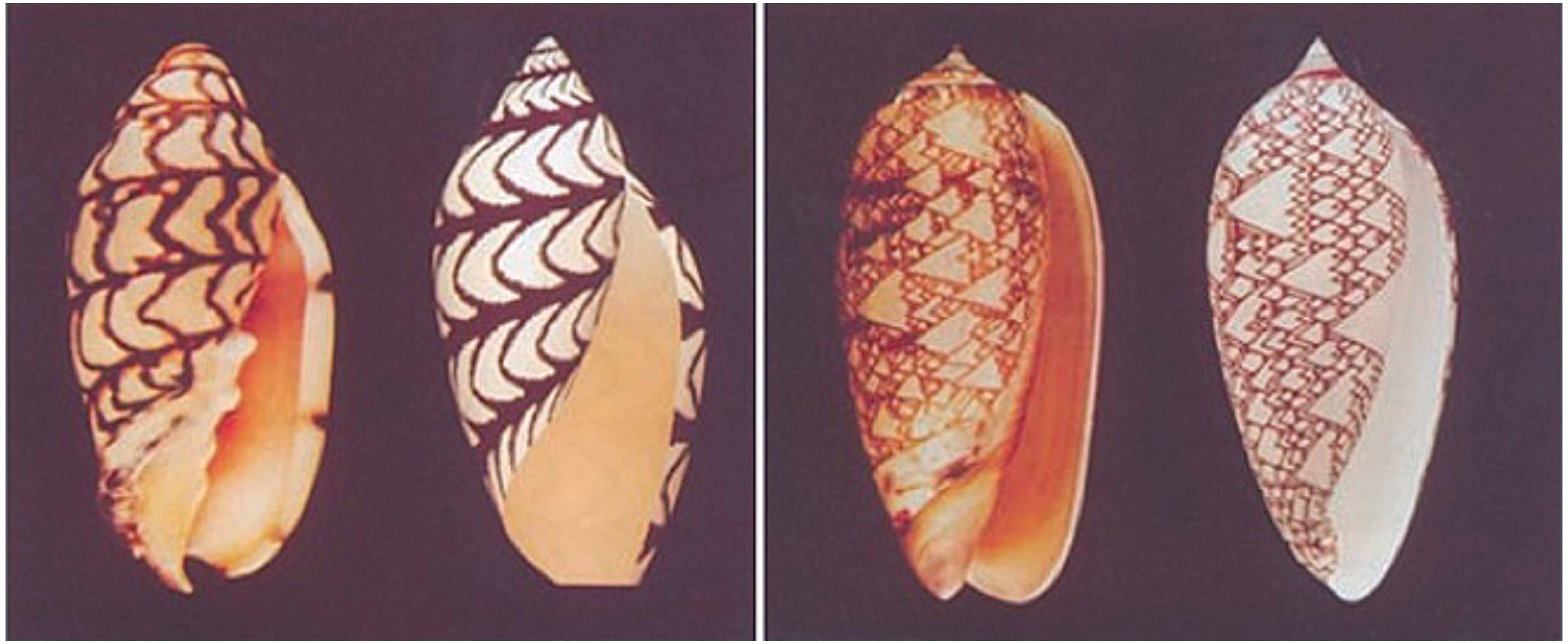

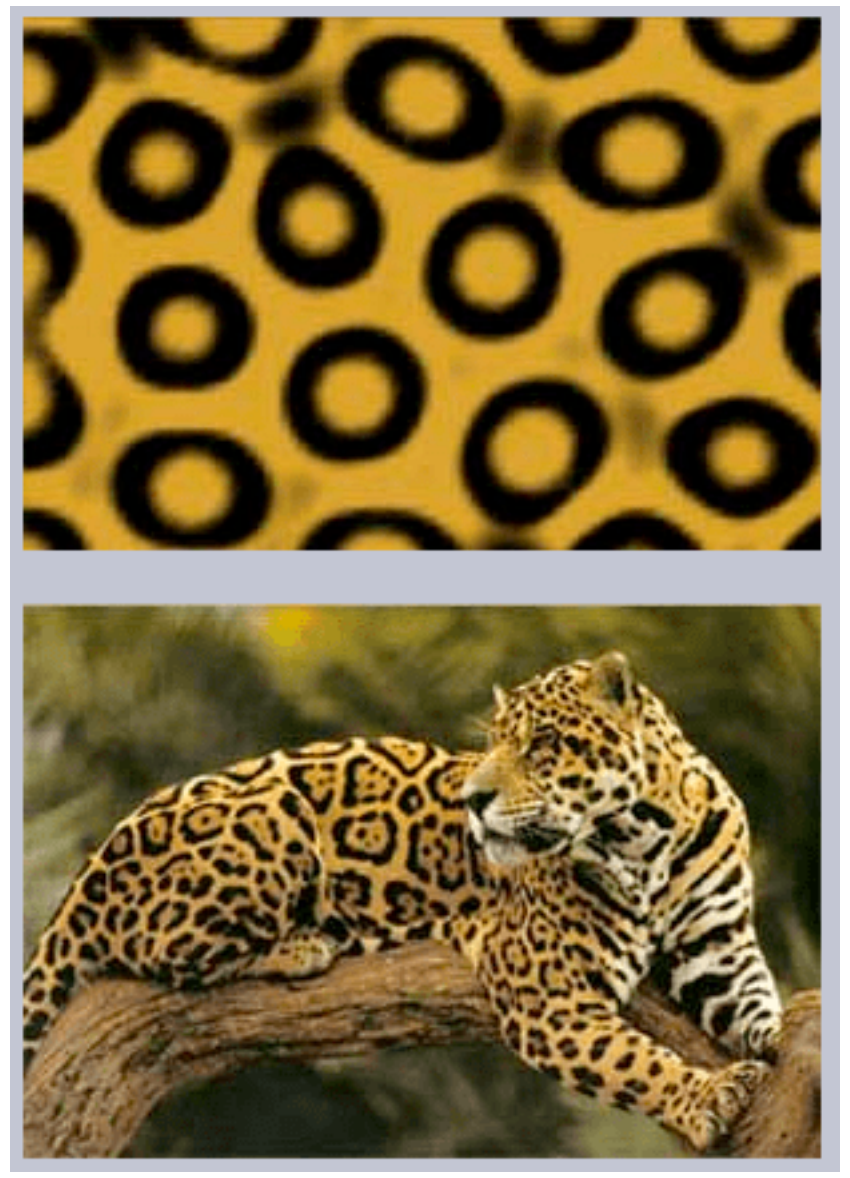

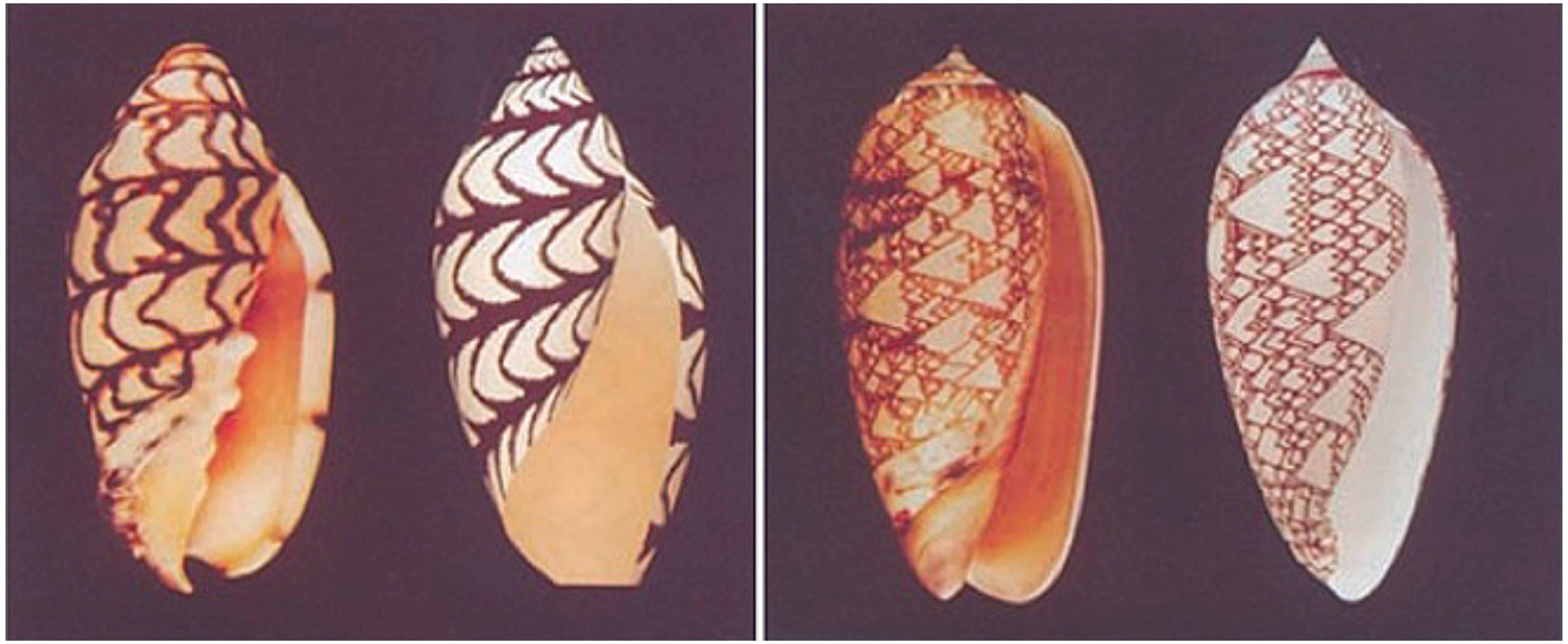

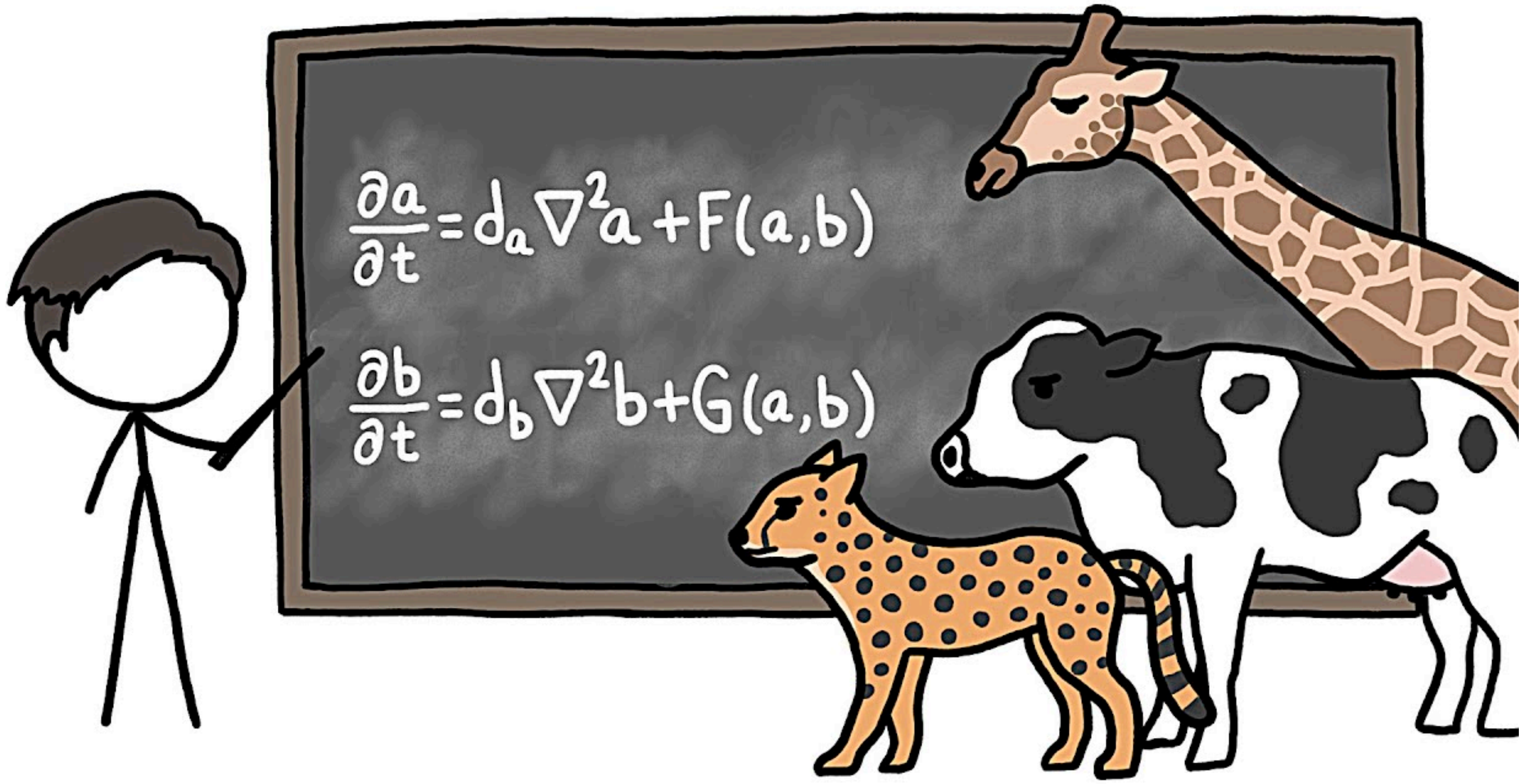

$\frac{\partial a}{\partial t} = d_a \nabla^2 a + F(a,b)$
$\frac{\partial b}{\partial t} = d_b \nabla^2 b + G(a,b)$

Analysis: Linearisation + Stability

Analysis: Linearisation + Stability

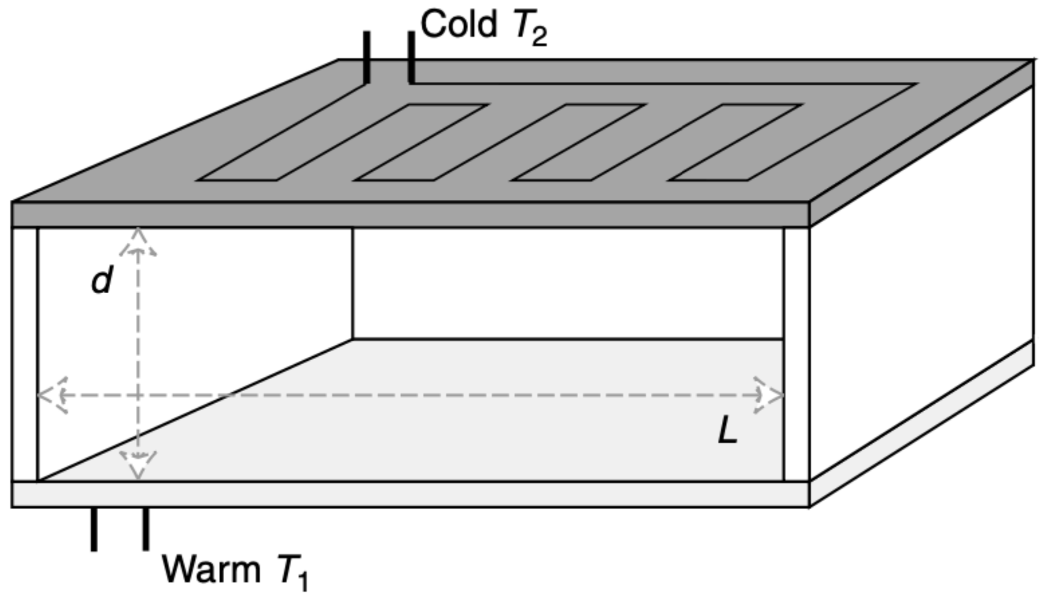

Swift-Hohenberg example:

$$\partial_t u(x,t) = (r-1)u - 2\partial_x^2 u - \partial_x^4 u - u^3.$$

Analysis: Linearisation + Stability

Swift-Hohenberg example:

$$\partial_t u(x,t) = (r-1)u - 2\partial_x^2 u - \partial_x^4 u - u^3.$$

$$u_{\mathrm{p}}(x,t) = u(x,t) - u_{\mathrm{b}},$$

Analysis: Linearisation + Stability

Swift-Hohenberg example:

$$\partial_t u(x,t) = (r-1)u - 2\partial_x^2 u - \partial_x^4 u - u^3.$$

$$u_{\mathrm{p}}(x,t) = u(x,t) - u_{\mathrm{b}},$$

$$\partial_t u_{\mathrm{p}} = \left(r - 1 - 2\partial_x^2 - \partial_x^4\right) u_{\mathrm{p}}.$$

Analysis: Linearisation + Stability

Swift-Hohenberg example:

$$\partial_t u(x,t) = (r-1)u - 2\partial_x^2 u - \partial_x^4 u - u^3.$$

$$u_{\mathrm{p}}(x,t) = u(x,t) - u_{\mathrm{b}},$$

$$\partial_t u_{\mathrm{p}} = \left(r - 1 - 2\partial_x^2 - \partial_x^4\right) u_{\mathrm{p}}.$$

$$u_{\mathrm{p}}(x,t) = Ae^{\sigma t} e^{iqx},$$

Analysis: Linearisation + Stability

Swift-Hohenberg example:

$$\partial_t u(x,t) = (r-1)u - 2\partial_x^2 u - \partial_x^4 u - u^3.$$

$$u_{\mathrm{p}}(x,t) = u(x,t) - u_{\mathrm{b}},$$

$$\partial_t u_{\mathrm{p}} = \left(r - 1 - 2\partial_x^2 - \partial_x^4\right) u_{\mathrm{p}}.$$

$$u_{\mathrm{p}}(x,t) = A e^{\sigma t} e^{iqx},$$

$$\sigma_q = r - (q^2-1)^2.$$

Analysis: Linearisation + Stability

Swift-Hohenberg example:

$$\partial_t u(x,t) = (r-1)u - 2\partial_x^2 u - \partial_x^4 u - u^3.$$

$$u_{\mathrm{p}}(x,t) = u(x,t) - u_{\mathrm{b}},$$

$$\partial_t u_{\mathrm{p}} = \left(r - 1 - 2\partial_x^2 - \partial_x^4\right) u_{\mathrm{p}}.$$

$$u_{\mathrm{p}}(x,t) = Ae^{\sigma t}e^{iqx},$$

$$\sigma_q = r - (q^2-1)^2.$$

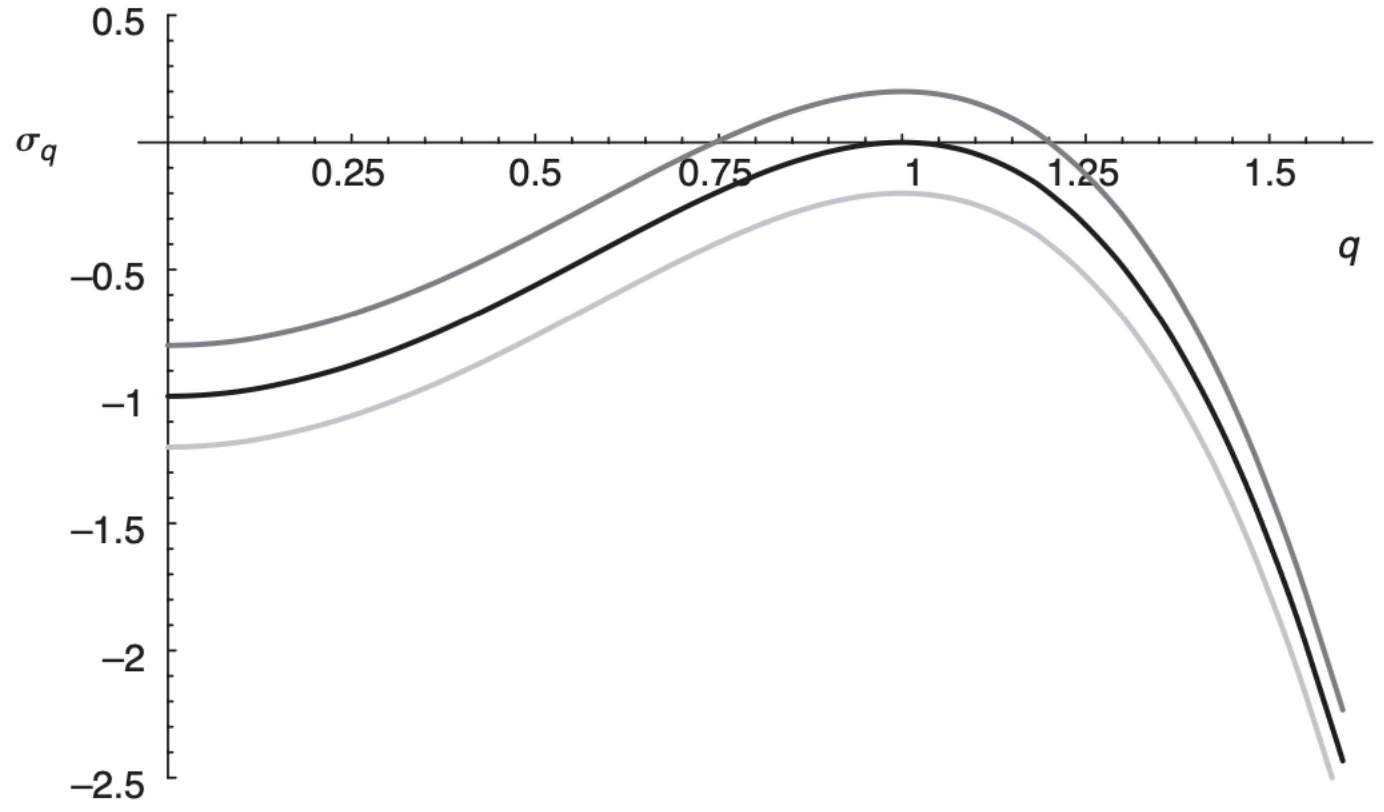

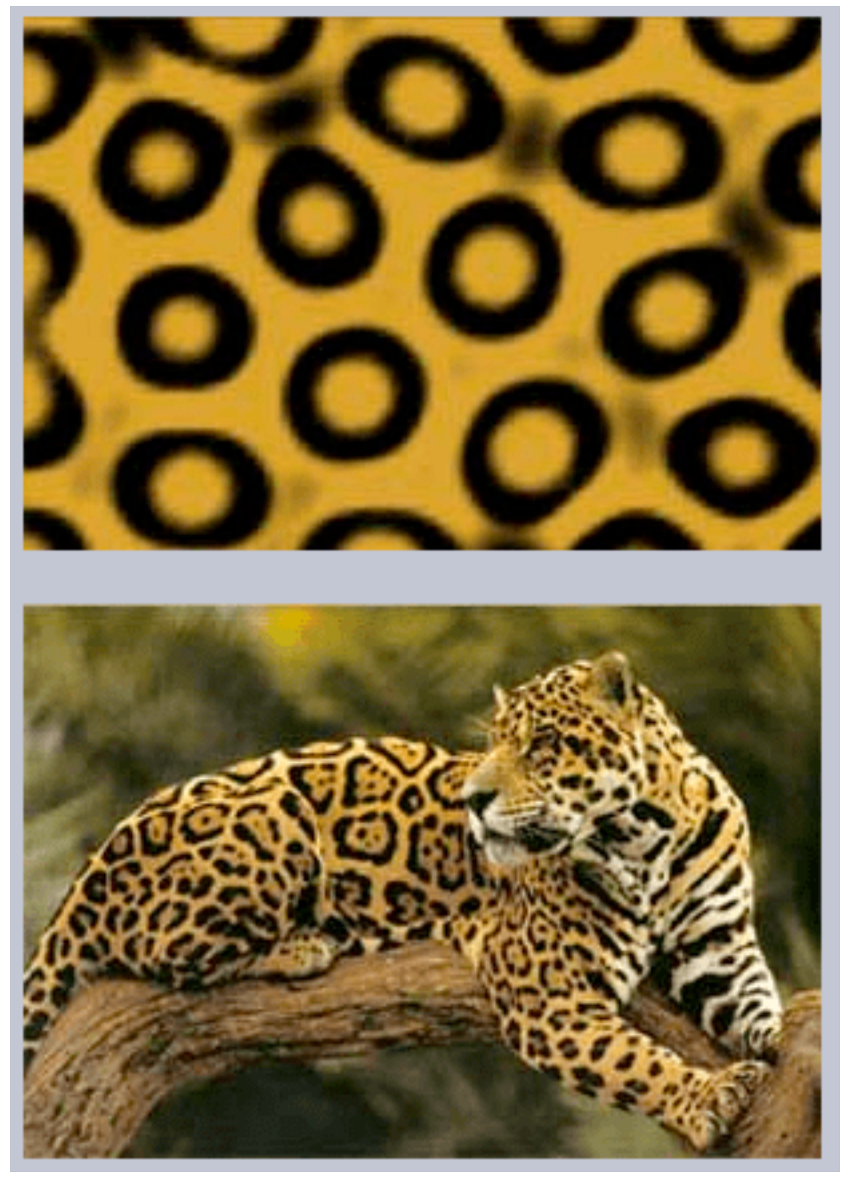

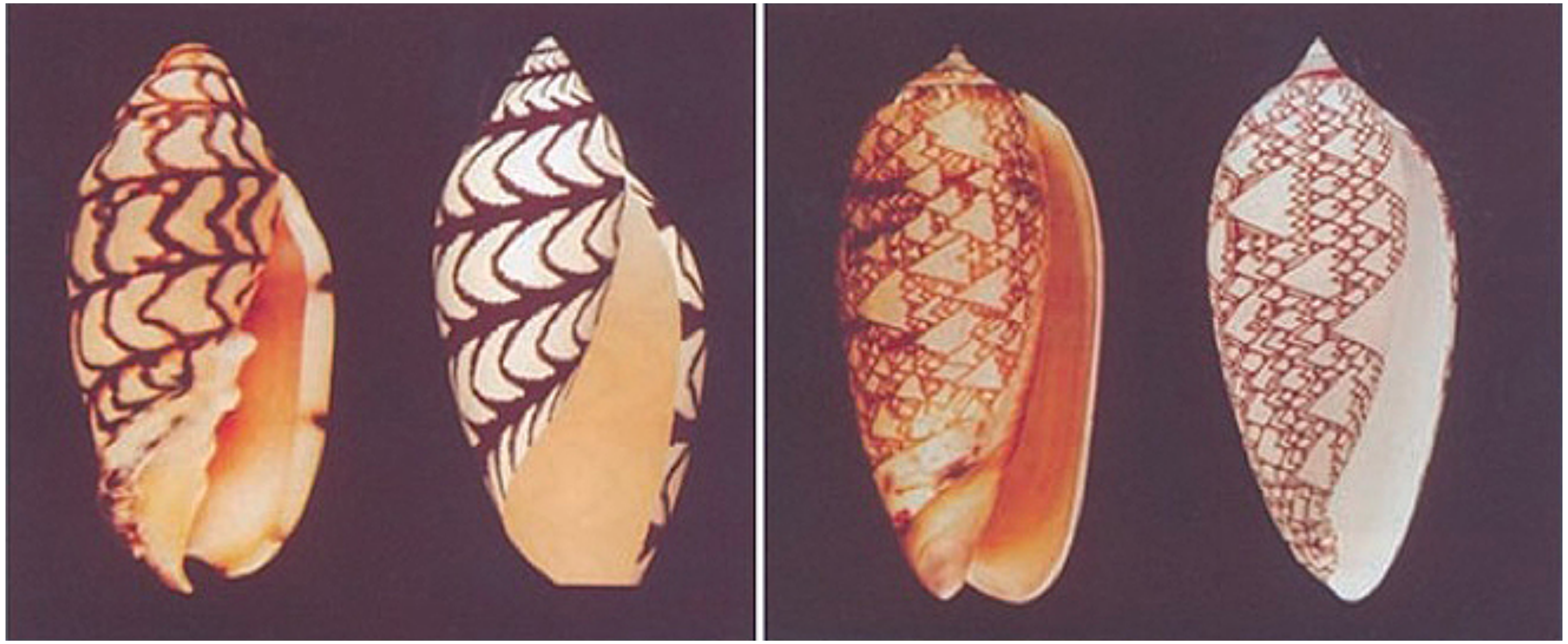

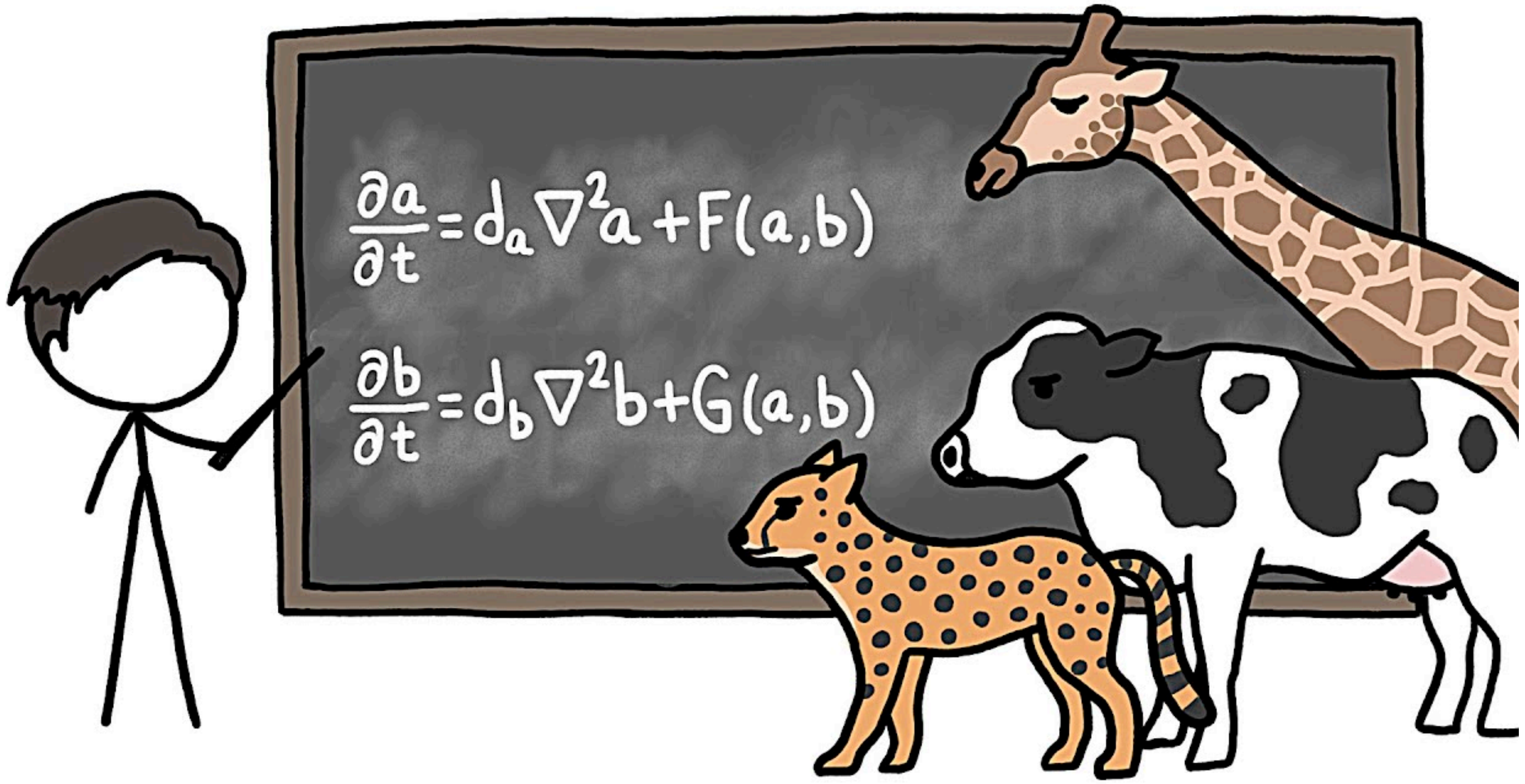
$\frac{\partial a}{\partial t} = d_a \nabla^2 a + F(a,b)$
$\frac{\partial b}{\partial t} = d_b \nabla^2 b + G(a,b)$

(a)

(b)

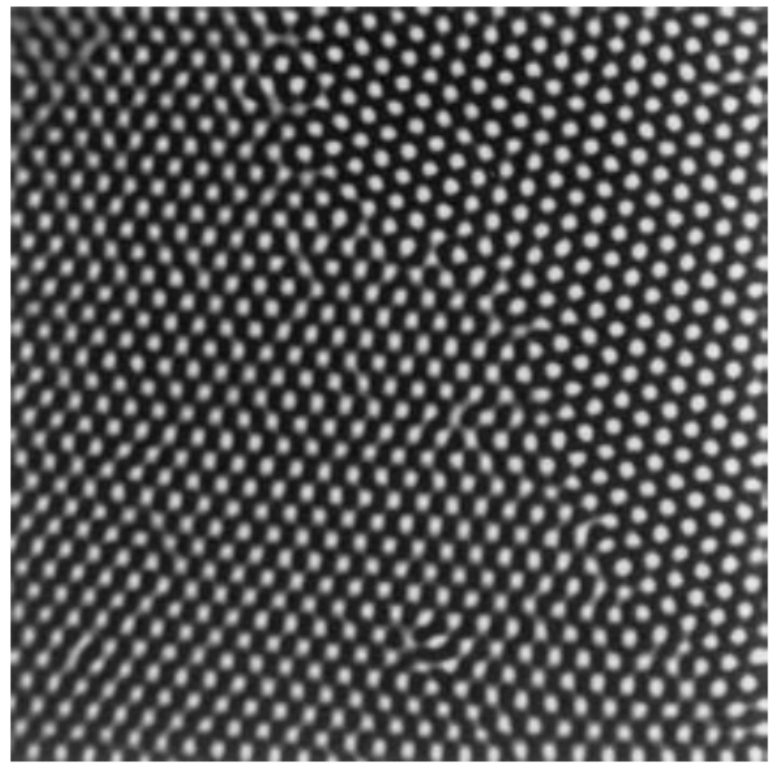

(c)

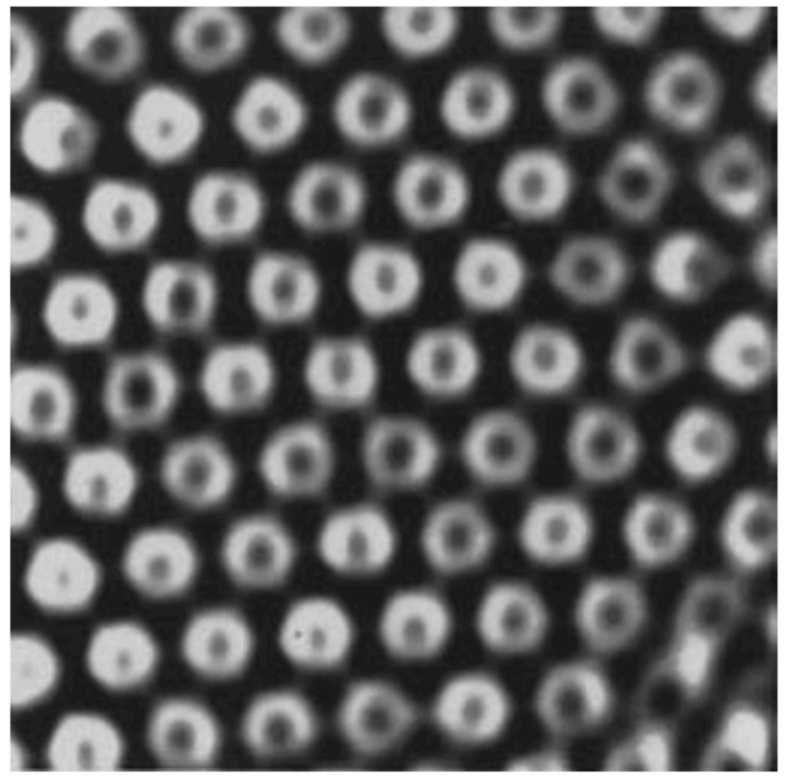

(d)

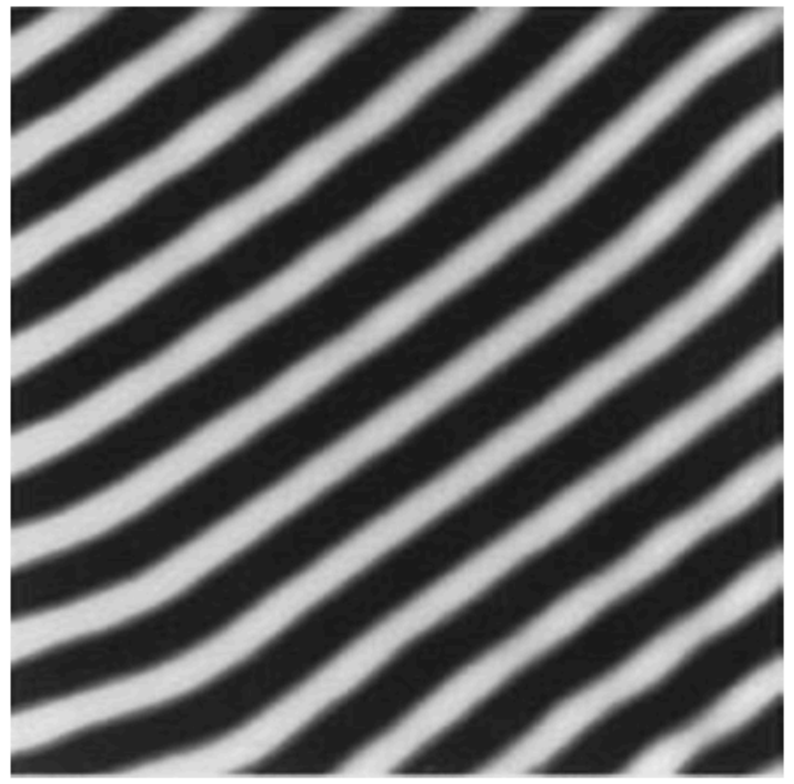

(e)

$$\nabla \cdot \nabla f = \nabla^2 f = \frac{\partial^2 f}{\partial x^2} + \frac{\partial^2 f}{\partial y^2}$$

Reaction-Diffusion (2D)

$$u_t = \gamma f(u, v) + \nabla^2 u, \quad v_t = \gamma g(u, v) + d\nabla^2 v,$$

$$(\mathbf{n} \cdot \nabla) \begin{pmatrix} u \\ v \end{pmatrix} = 0, \quad \mathbf{r} \text{ on } \partial B; \quad u(\mathbf{r}, 0), \ v(\mathbf{r}, 0) \text{ given},$$

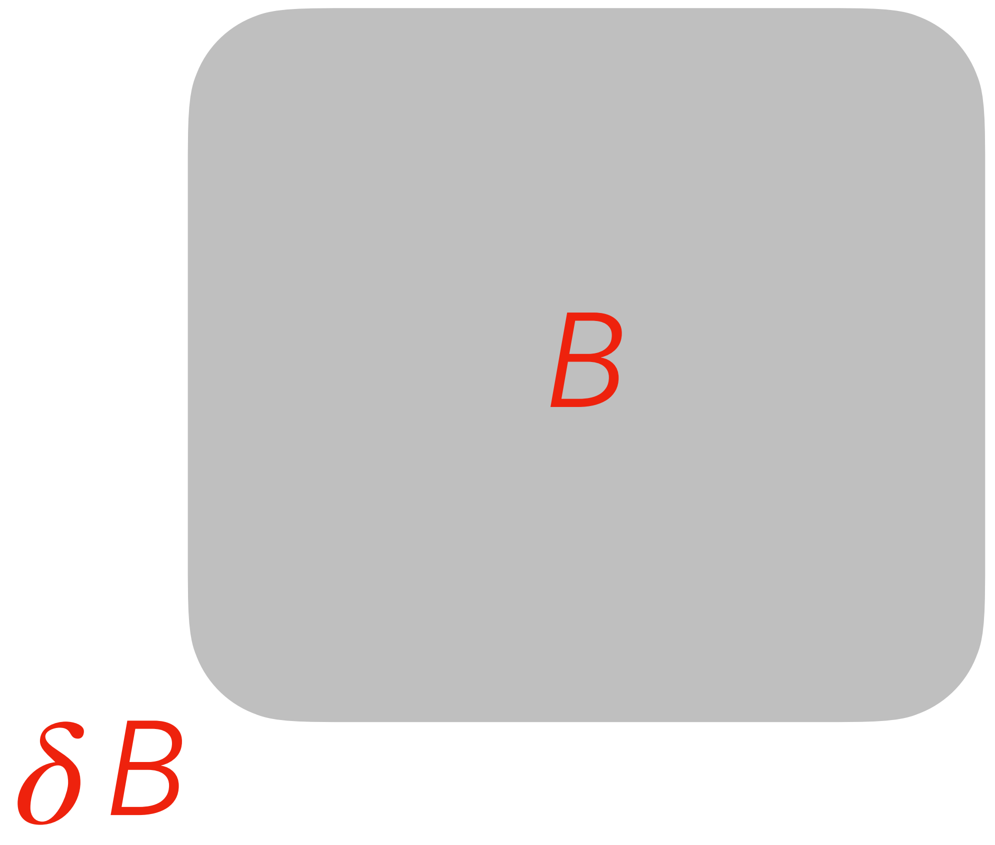

Reaction-Diffusion (2D)

$$u_t = \gamma f(u, v) + \nabla^2 u, \quad v_t = \gamma g(u, v) + d\nabla^2 v,$$

$$(\mathbf{n} \cdot \nabla) \begin{pmatrix} u \\ v \end{pmatrix} = 0, \quad \mathbf{r} \text{ on } \partial B; \quad u(\mathbf{r}, 0), \; v(\mathbf{r}, 0) \text{ given},$$

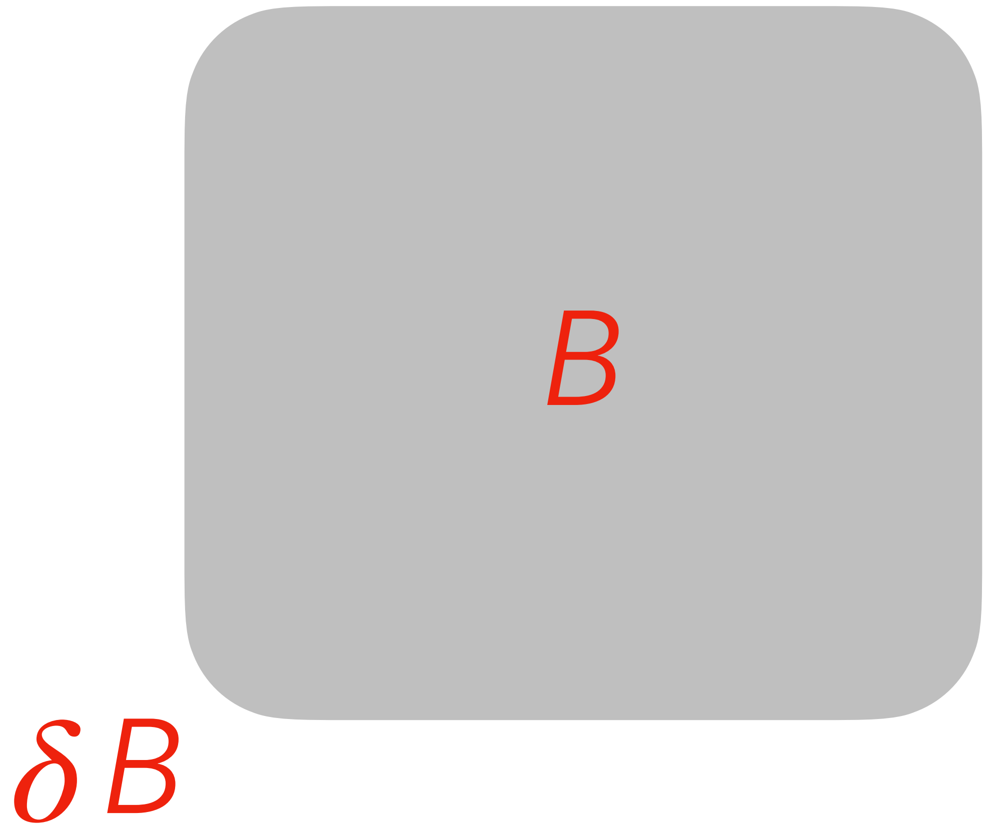

$$\mathbf{w}_t = \gamma A \mathbf{w} + D \nabla^2 \mathbf{w}, \quad D = \begin{pmatrix} 1 & 0 \\ 0 & d \end{pmatrix}$$

Reaction-Diffusion (2D)

$$u_t = \gamma f(u, v) + \nabla^2 u, \quad v_t = \gamma g(u, v) + d\nabla^2 v,$$

$$(\mathbf{n} \cdot \nabla) \begin{pmatrix} u \\ v \end{pmatrix} = 0, \quad \mathbf{r} \text{ on } \partial B; \quad u(\mathbf{r}, 0),\ v(\mathbf{r}, 0) \text{ given},$$

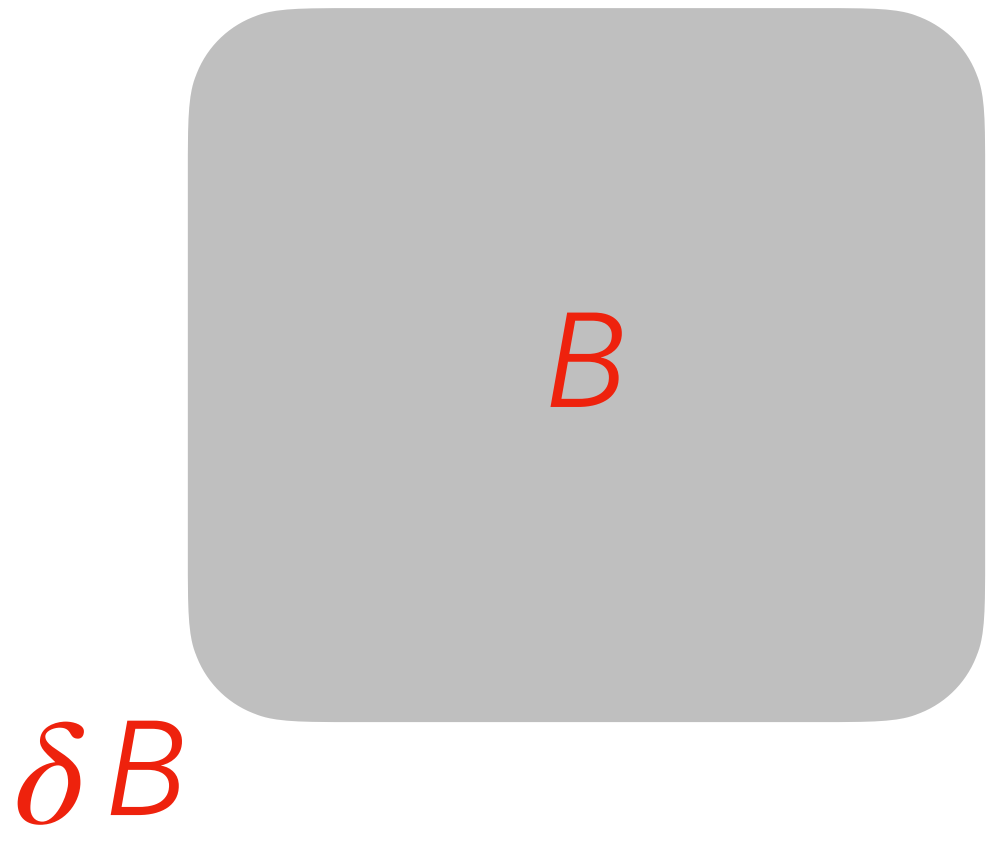

$$\mathbf{w}_t = \gamma A\mathbf{w} + D\nabla^2 \mathbf{w}, \quad D = \begin{pmatrix} 1 & 0 \\ 0 & d \end{pmatrix}$$

$$\nabla^2 \mathbf{W} + k^2 \mathbf{W} = 0, \quad (\mathbf{n} \cdot \nabla)\mathbf{W} = 0 \quad \text{for} \quad \mathbf{r} \text{ on } \partial B$$

Fourier basis (generalized)

Reaction-Diffusion (2D)

$$u_t = \gamma f(u, v) + \nabla^2 u, \quad v_t = \gamma g(u, v) + d\nabla^2 v,$$

$$(\mathbf{n} \cdot \nabla)\begin{pmatrix} u \\ v \end{pmatrix} = 0, \quad \mathbf{r} \text{ on } \partial B; \quad u(\mathbf{r}, 0),\ v(\mathbf{r}, 0) \text{ given},$$

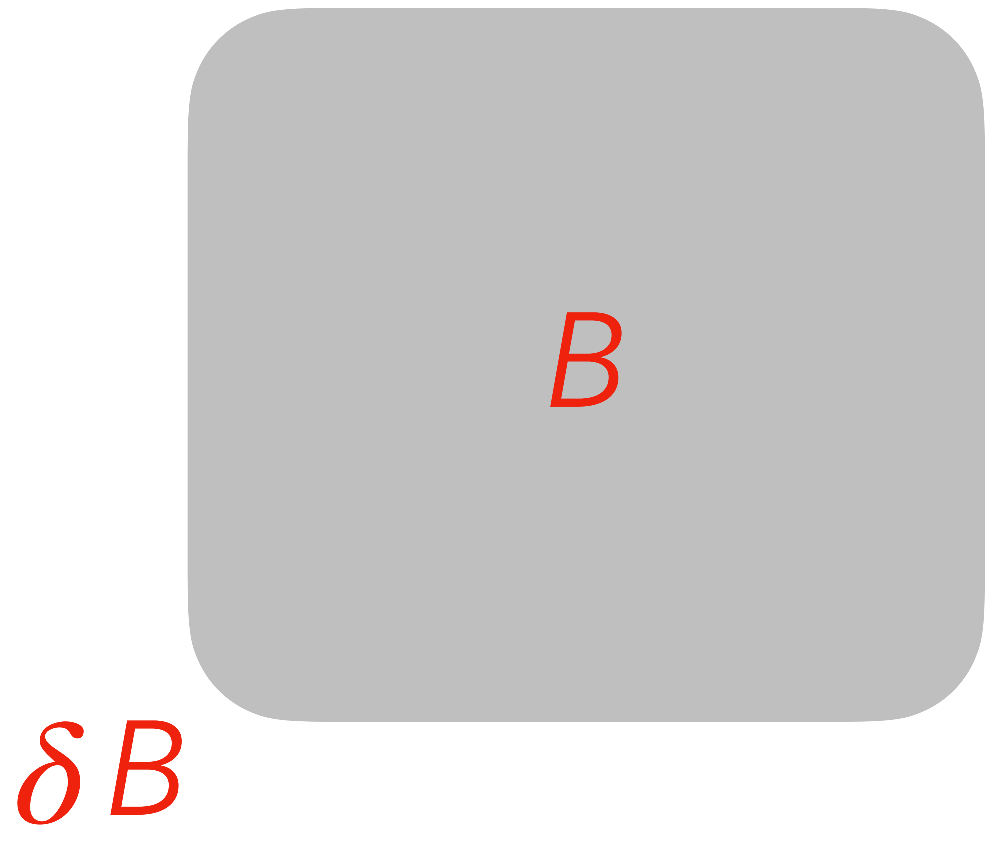

$$\mathbf{w}_t = \gamma A\mathbf{w} + D\nabla^2\mathbf{w}, \quad D = \begin{pmatrix} 1 & 0 \\ 0 & d \end{pmatrix}$$

$$\mathbf{w}(\mathbf{r}, t) = \sum_k c_k e^{\lambda t}\mathbf{W}_k(\mathbf{r})$$

$$\nabla^2\mathbf{W} + k^2\mathbf{W} = 0, \quad (\mathbf{n} \cdot \nabla)\mathbf{W} = 0 \quad \text{for} \quad \mathbf{r} \text{ on } \partial B$$

Fourier basis (generalized)

Reaction-Diffusion

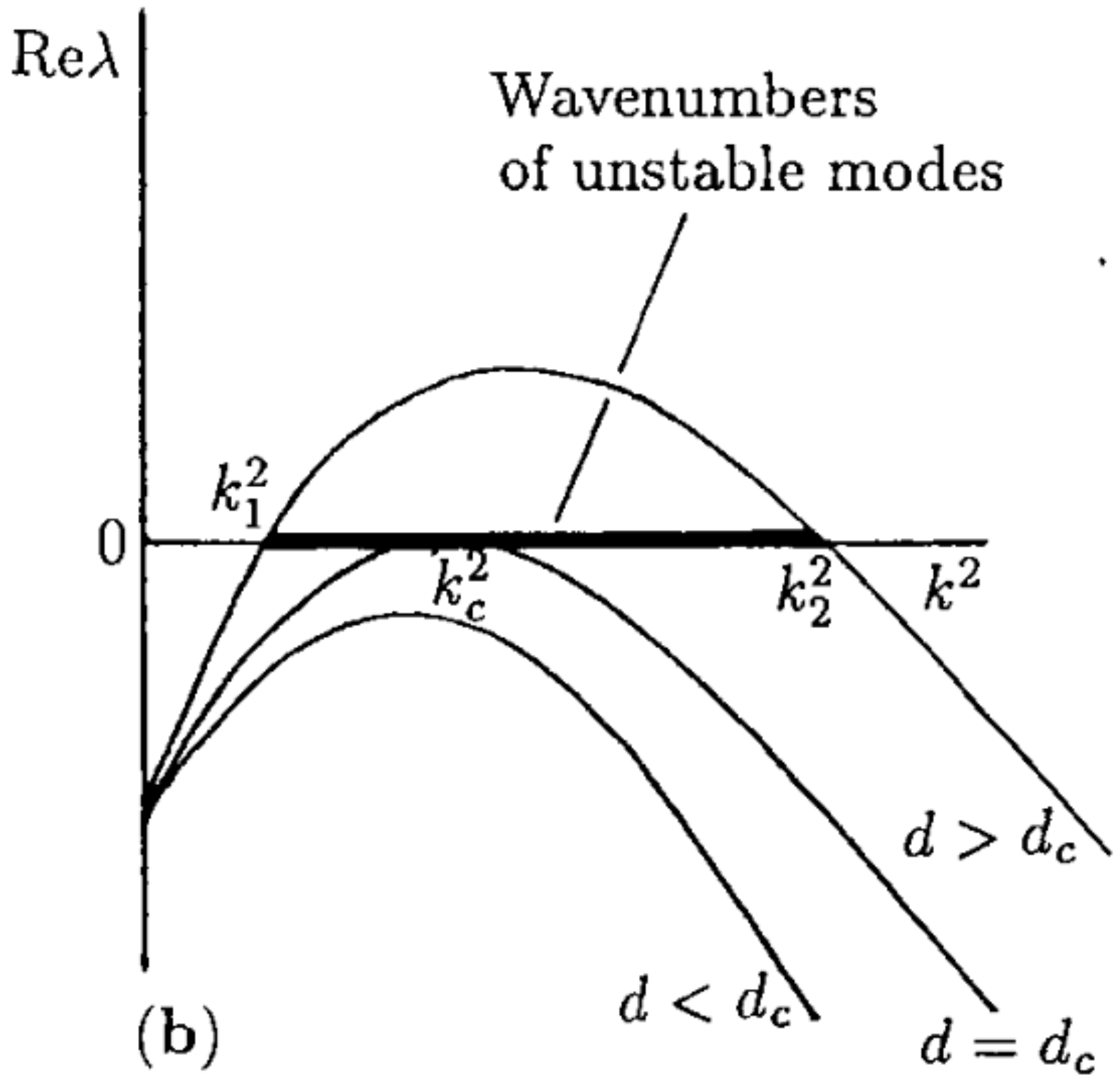

Reaction-Diffusion

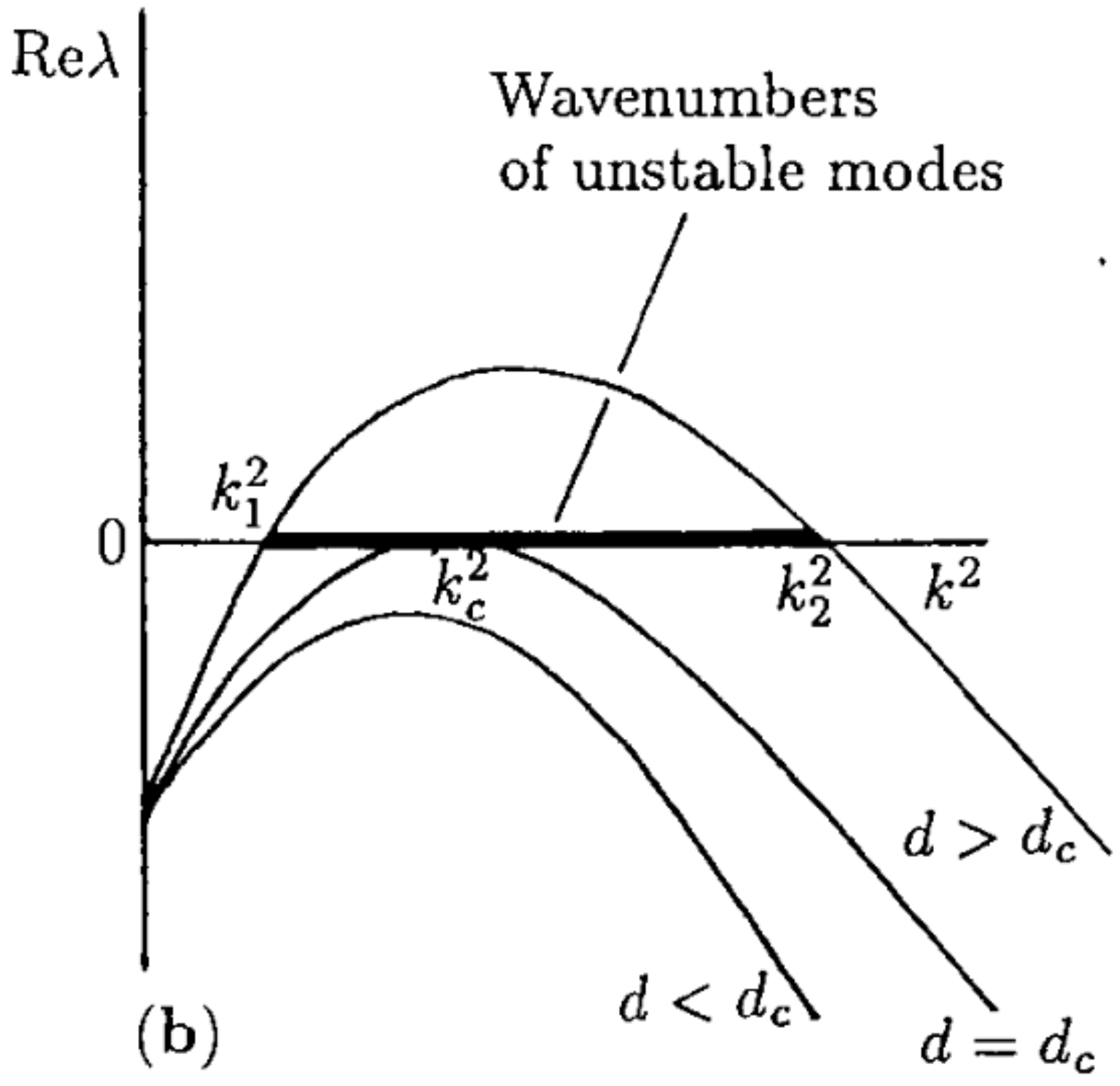

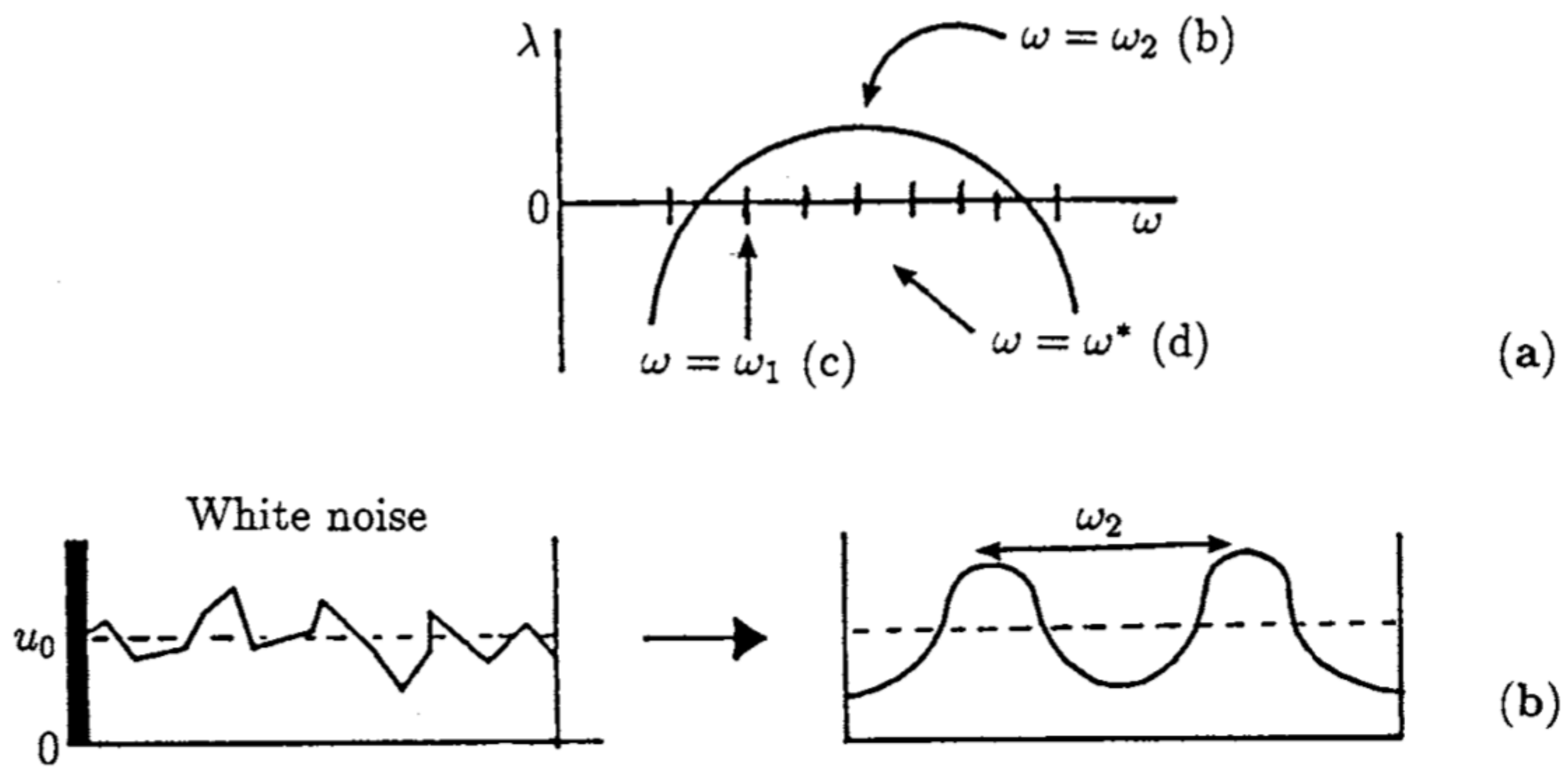

Reaction-Diffusion

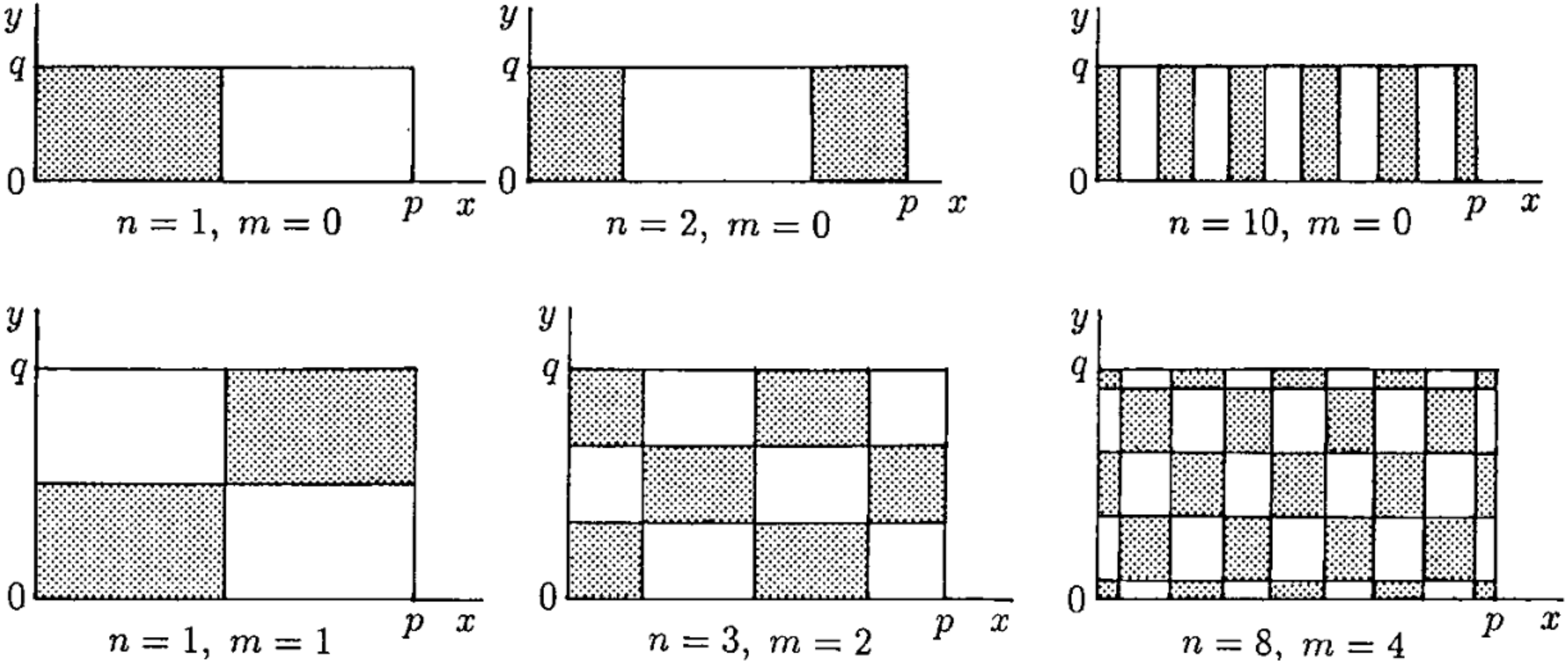

Lattice Patterns

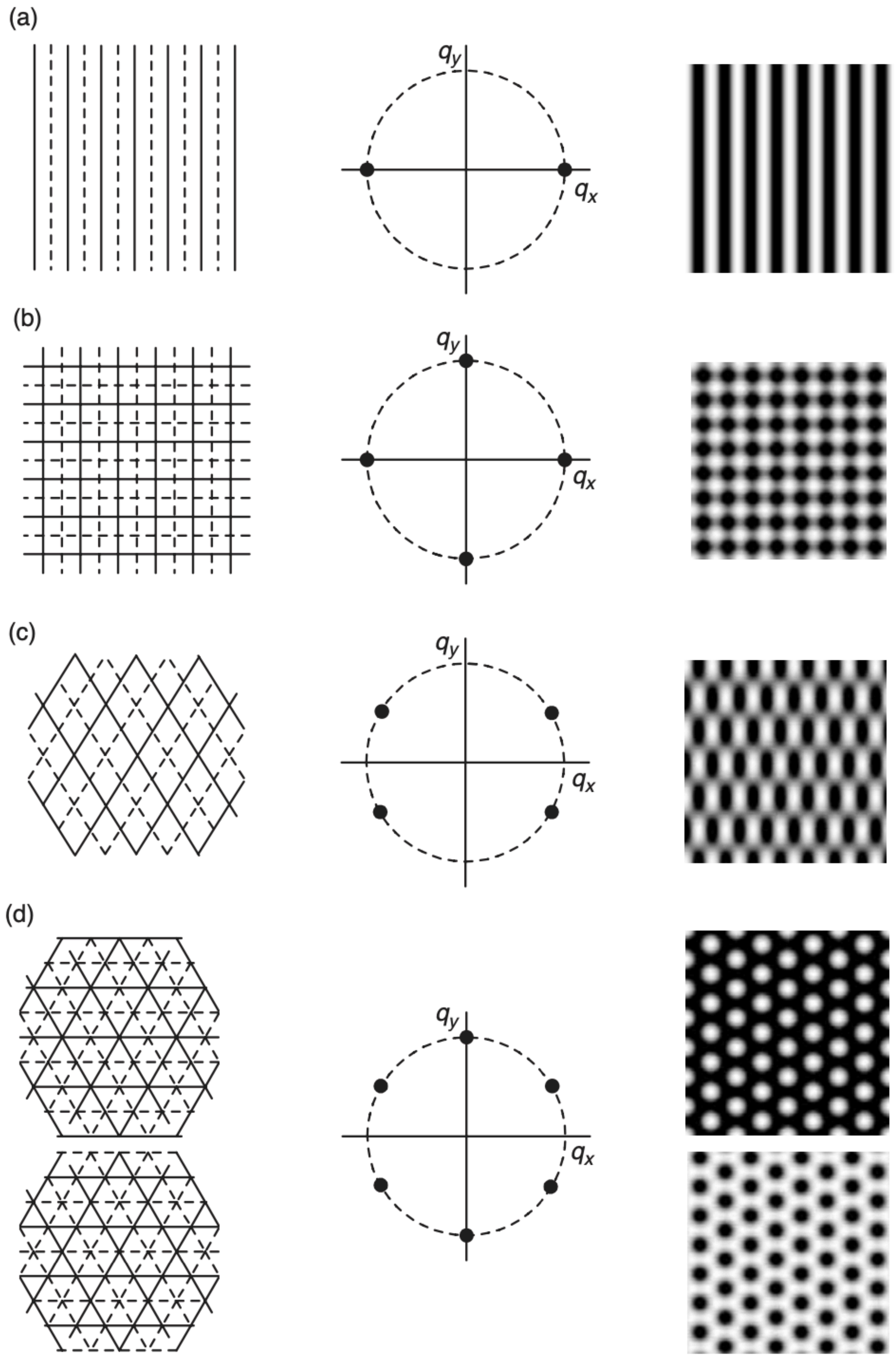

Lattice Patterns

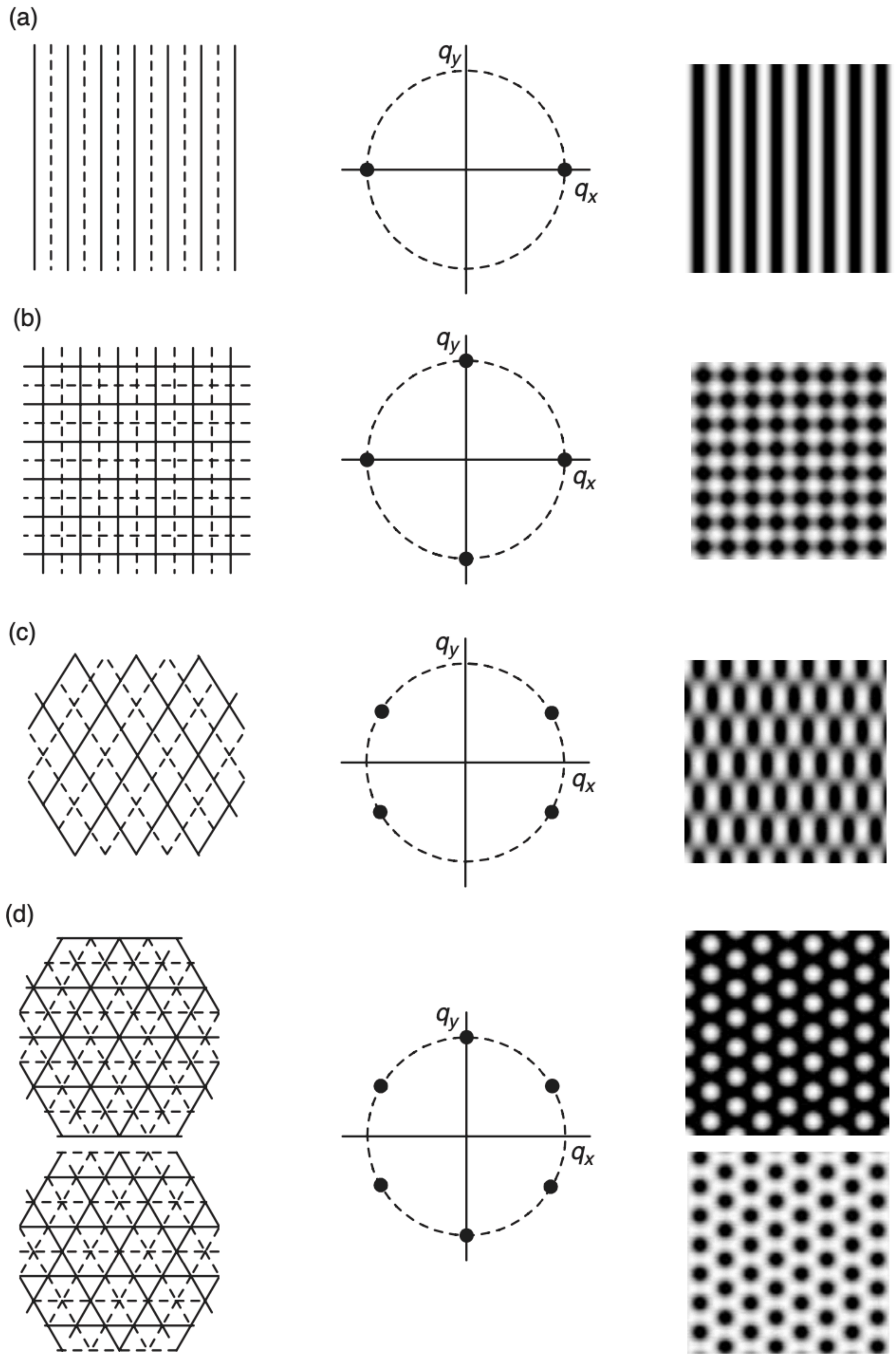

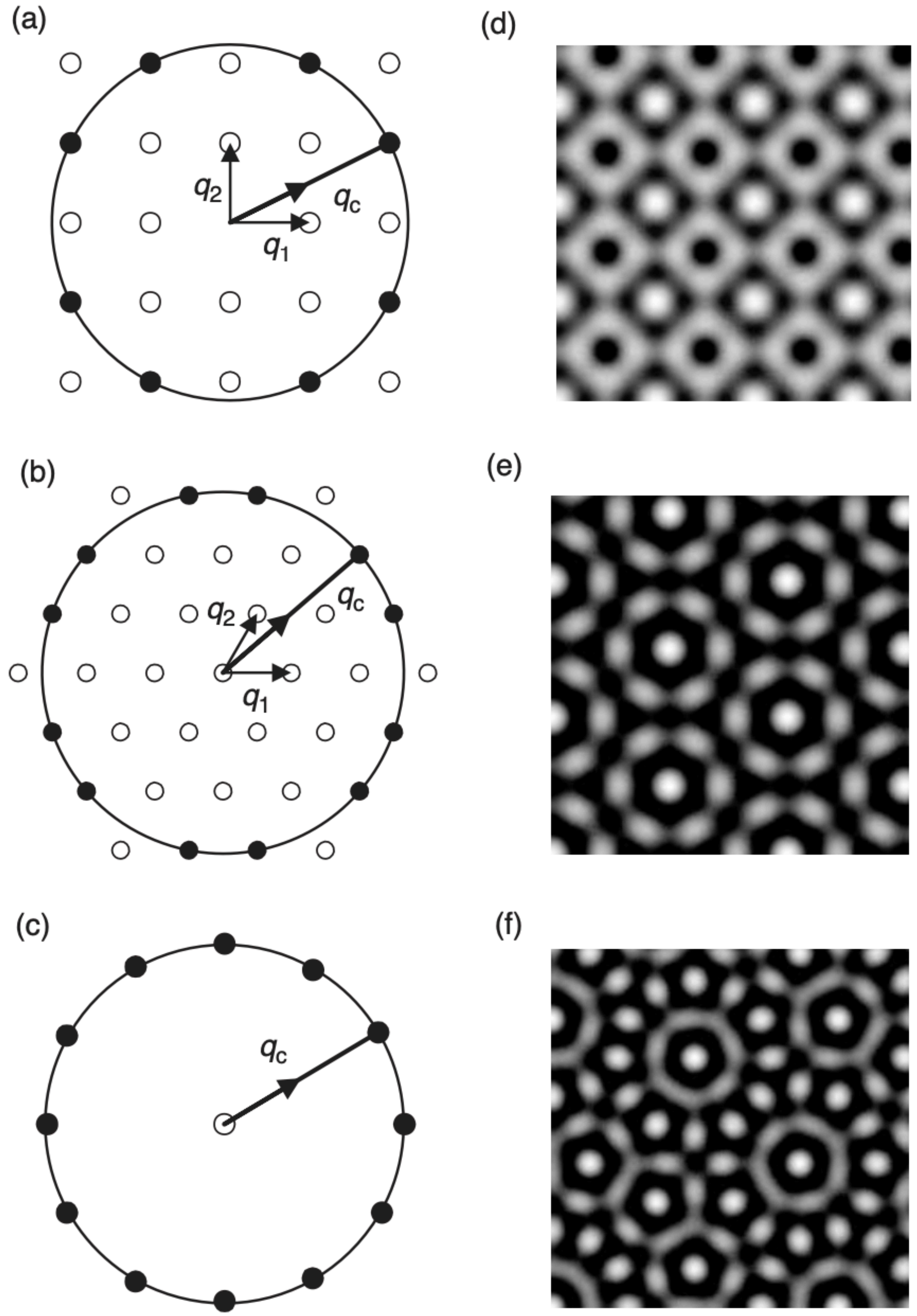

Grid **pattern** -> Superposition of Fourier modes (**Eigenfunctions** of Laplacian)

Grid **scale** -> **Eigenvalue** associated to contributing eigenfunctions

Neural models

1-population Neural field model

$$\frac{dn}{dt} = f(n)$$

1-population Neural field model

$$\frac{dn}{dt} = f(n)$$

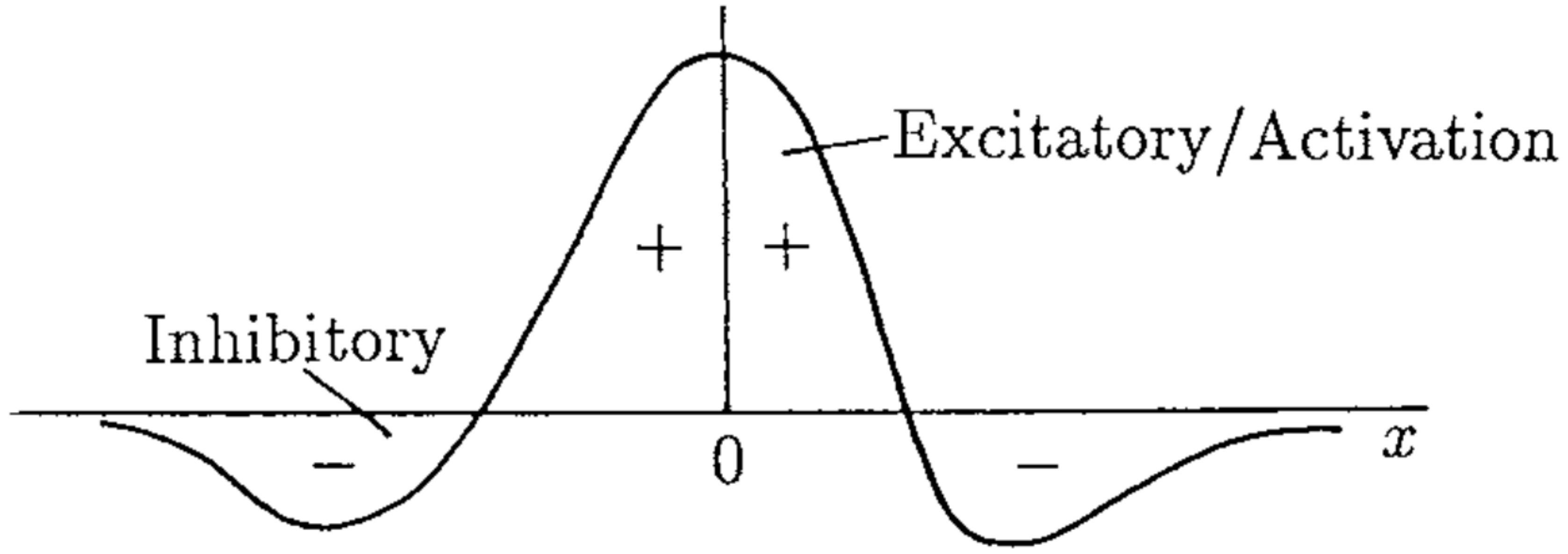

1-population Neural field model

$$\frac{dn}{dt} = f(n)$$

$$\frac{\partial n}{\partial t} = f(n) + \int_{-\infty}^{\infty} w(x - x')n(x', t)\, dx'$$

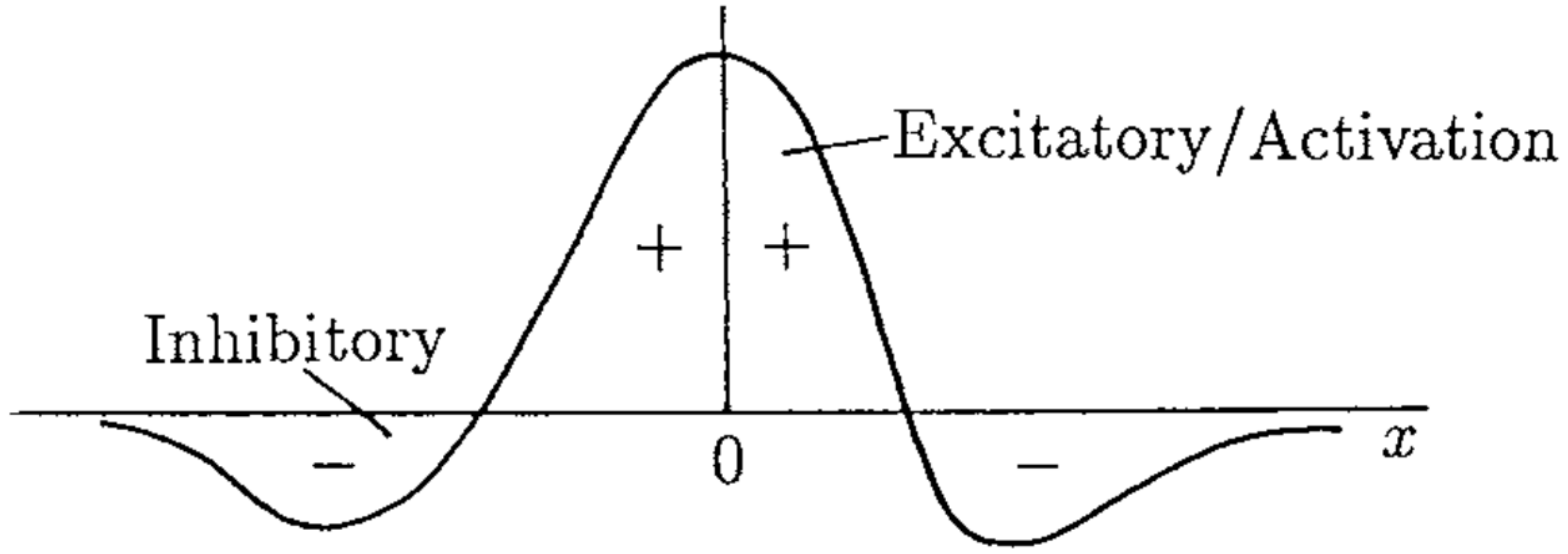

1-population Neural field model

$$\frac{dn}{dt} = f(n)$$

$$\frac{\partial n}{\partial t} = f(n) + \int_{-\infty}^{\infty} w(x - x')n(x', t)\, dx'$$

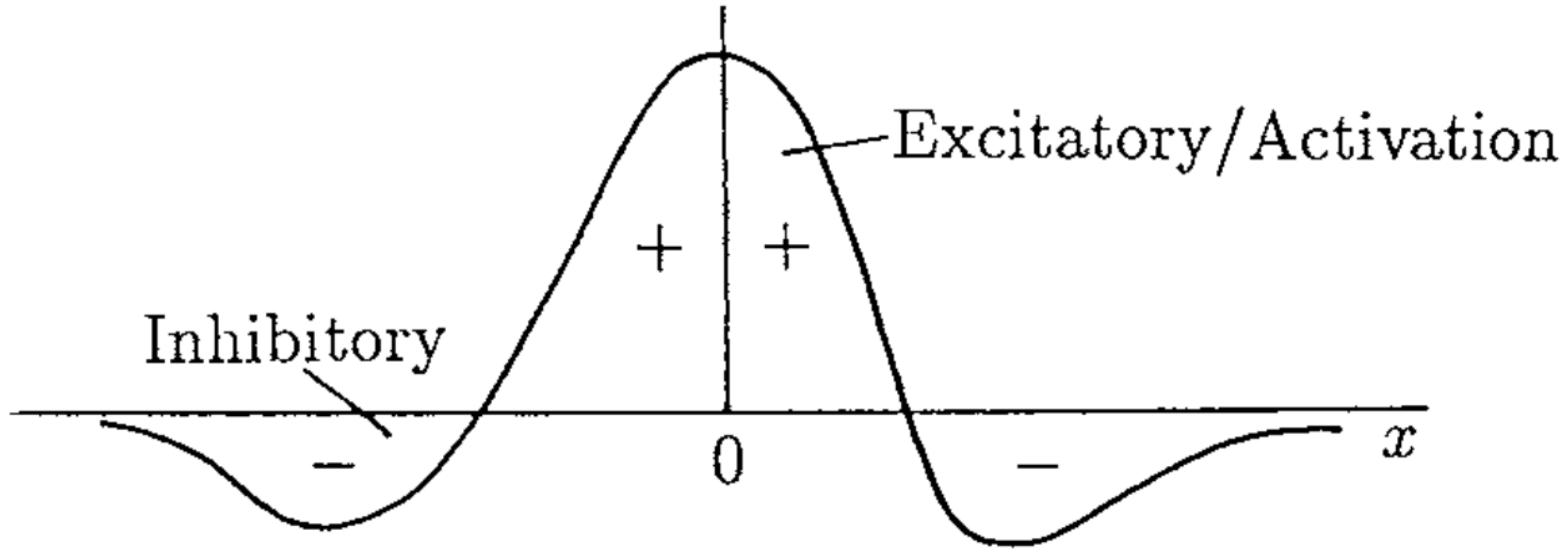

$$\frac{\partial n}{\partial t} = f(n) + w_0 n + w_2 \frac{\partial^2 n}{\partial x^2} + w_4 \frac{\partial^4 n}{\partial x^4} + \cdots$$

$$w_{2m} = \frac{1}{(2m)!} \int_{-\infty}^{\infty} y^{2m} w(y)\, dy$$

2-population Neural field model

$$\frac{\partial E}{\partial t} = -E + S_E(\alpha_{EE} w_{EE} * E - \alpha_{IE} w_{IE} * I),$$
$$\frac{\partial I}{\partial t} = -I + S_I(\alpha_{EI} w_{EI} * E - \alpha_{II} w_{II} * I),$$

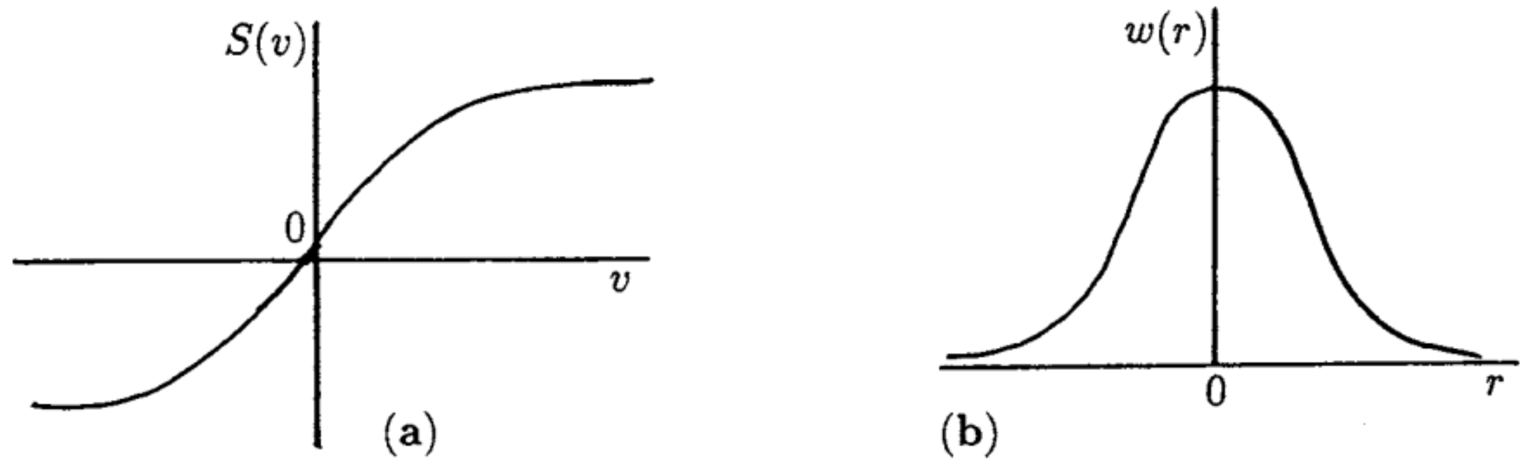

2-population Neural field model

$$\frac{\partial E}{\partial t} = -E + S_E(\alpha_{EE} w_{EE} * E - \alpha_{IE} w_{IE} * I),$$

$$\frac{\partial I}{\partial t} = -I + S_I(\alpha_{EI} w_{EI} * E - \alpha_{II} w_{II} * I),$$

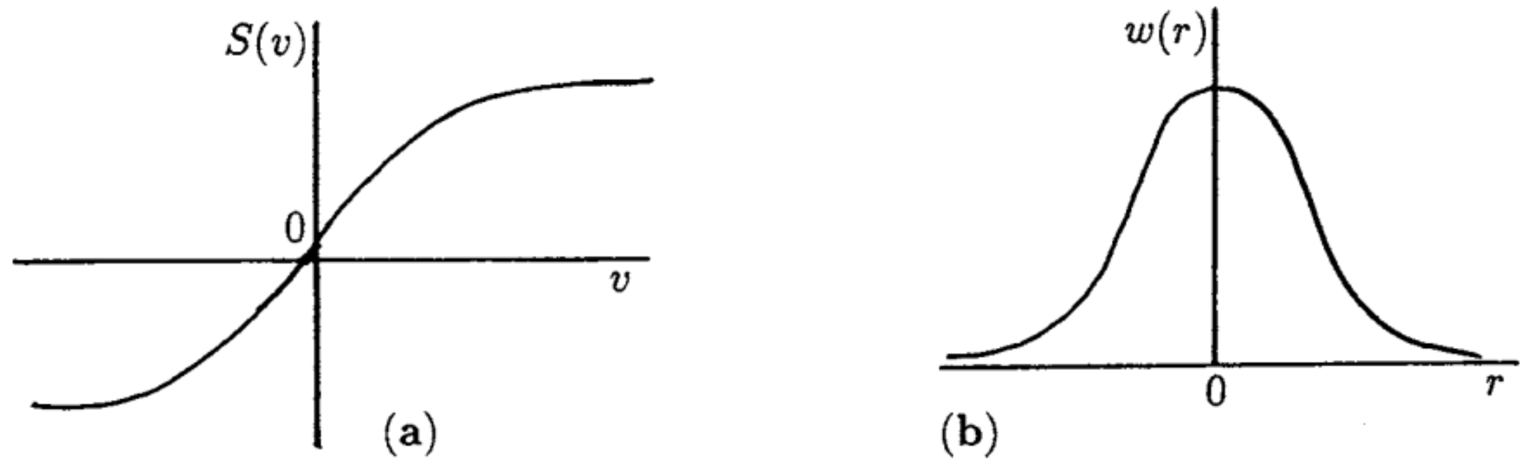

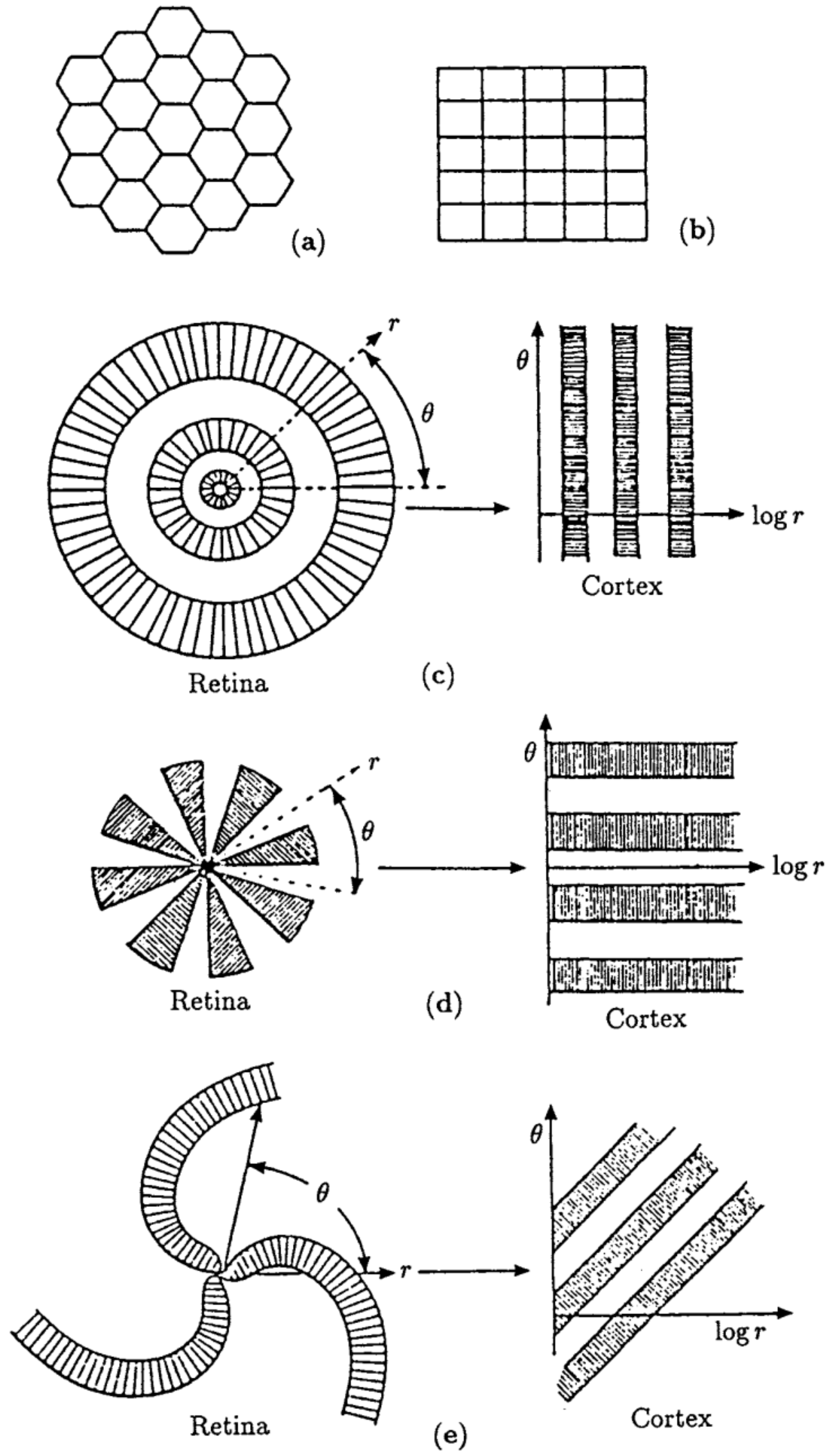

Panoramic view

Panoramic view

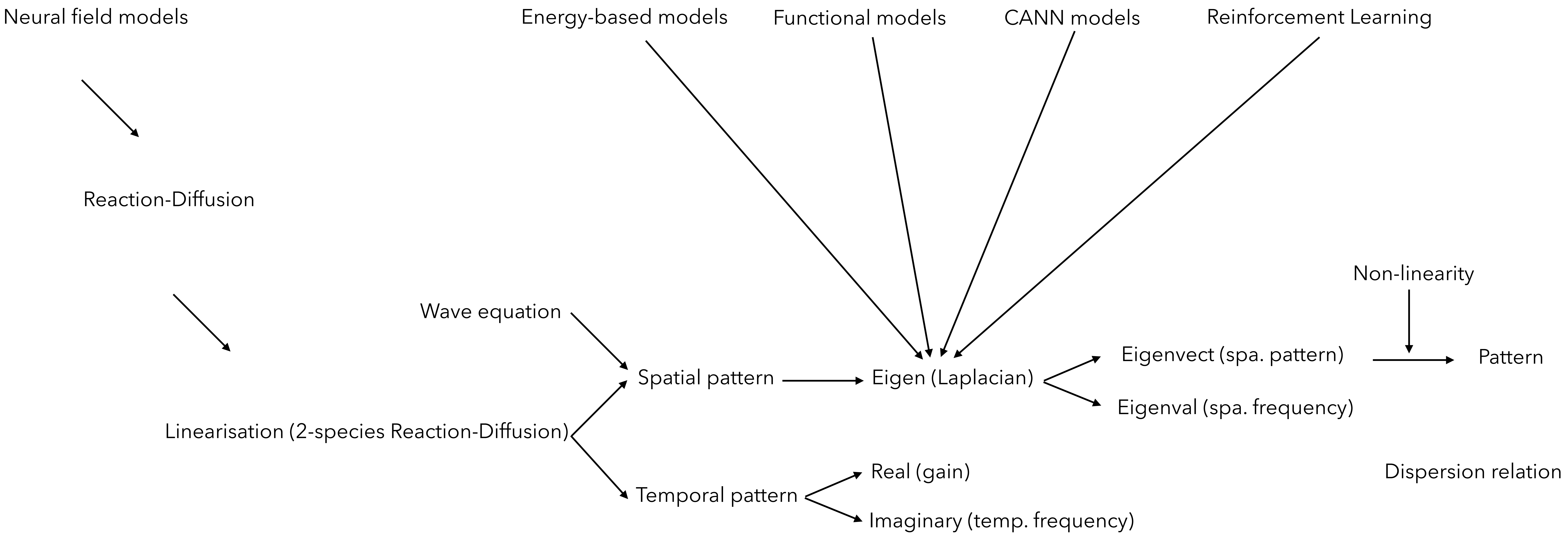

Panoramic view

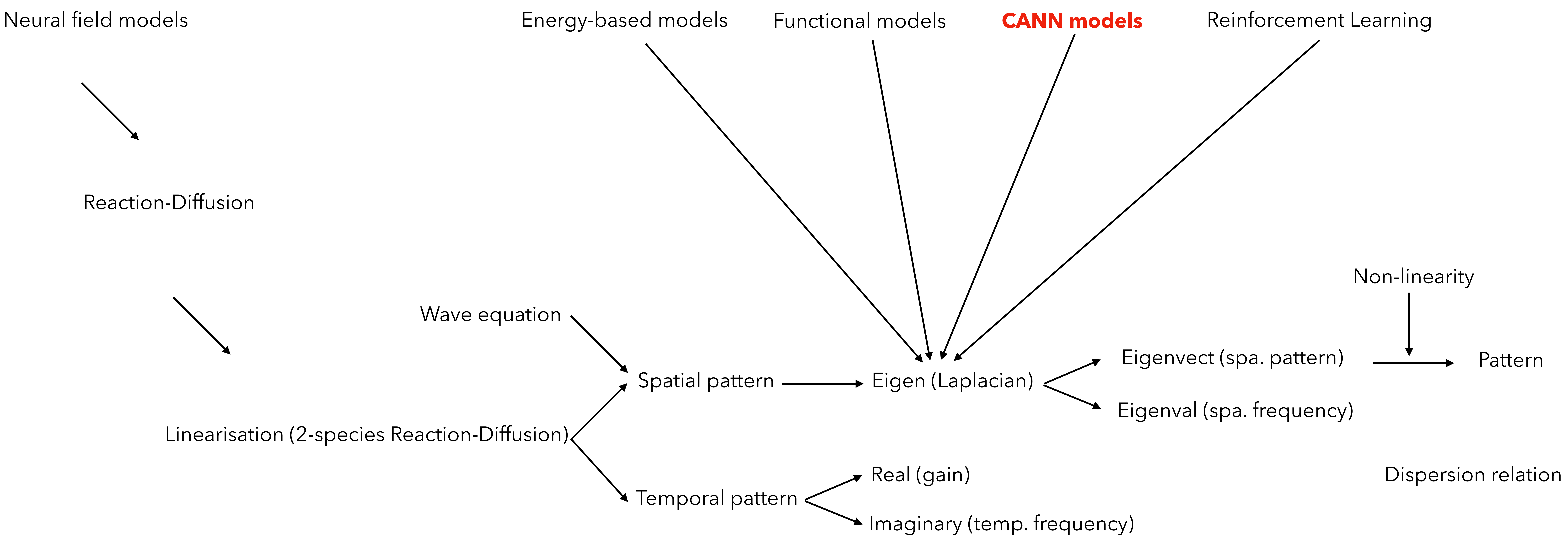

Panoramic view

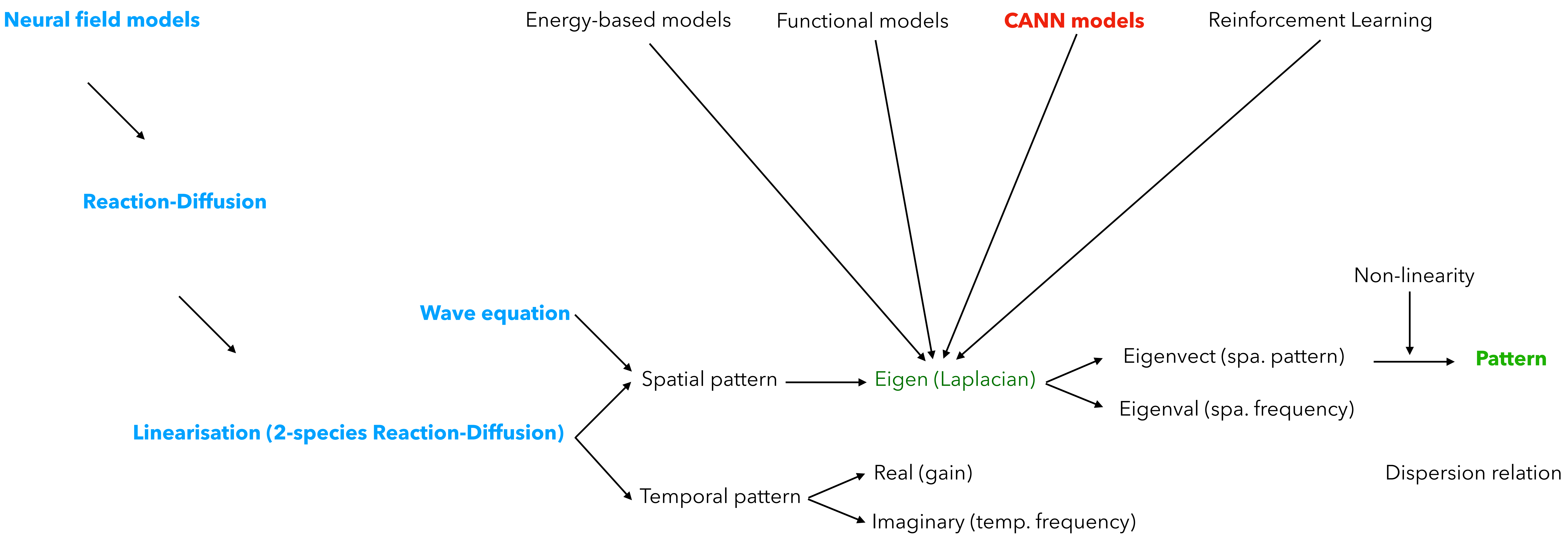

Panoramic view

Neural field models

Energy-based models

Functional models

CANN models

Reinforcement Learning

Reaction-Diffusion

Non-linearity

Wave equation

Eigenvect (spa. pattern)

Pattern

Spatial pattern

Eigen (Laplacian)

Eigenval (spa. frequency)

Linearisation (2-species Reaction-Diffusion)

Real (gain)

Dispersion relation

Temporal pattern

Imaginary (temp. frequency)

Boundary conditions!

Grid **pattern** -> Superposition of Fourier modes (**Eigenfunctions** of Laplacian **on the domain**)

Grid **scale** -> **Eigenvalue** associated to contributing eigenfunctions

Boundary conditions

- Developmentally: Border cells -> Place cells -> Grid cells

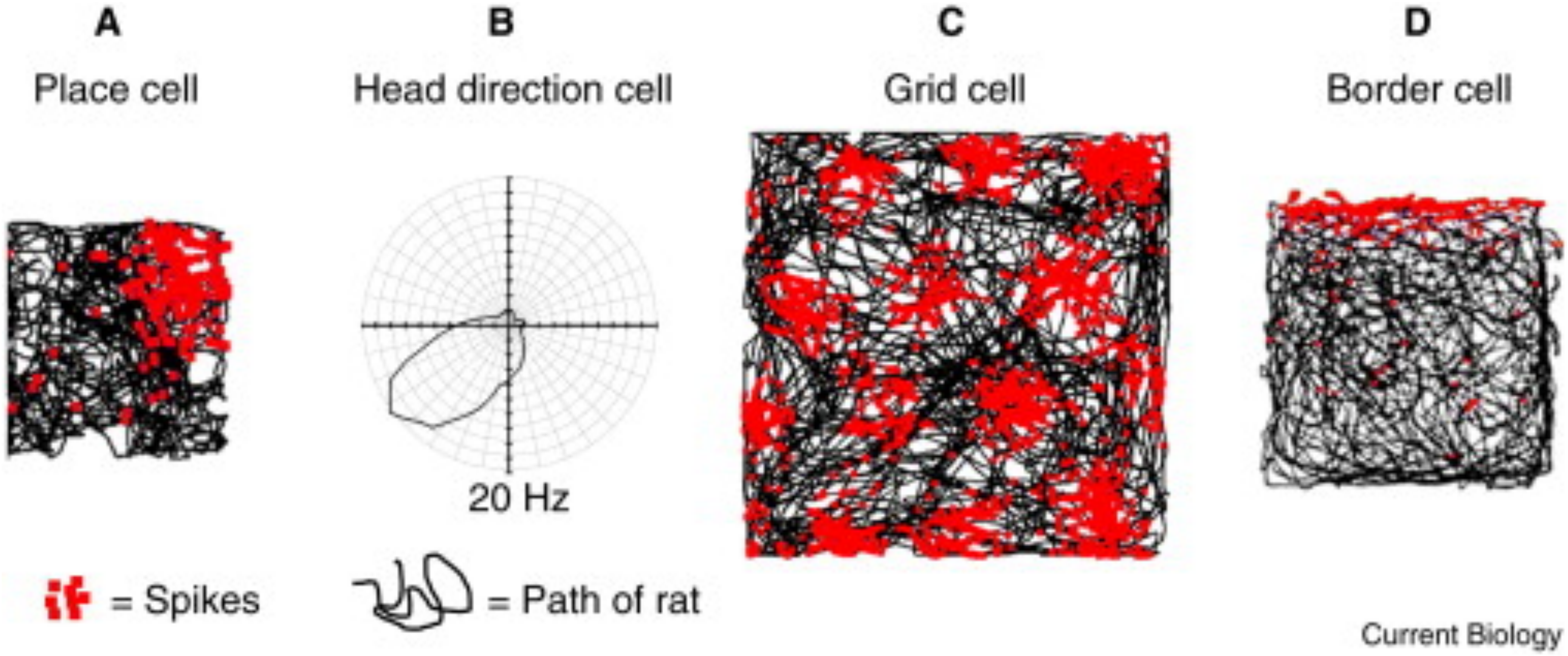

Generalisation of Fourier Analysis

Research hypothesis

Grid cells = Fourier basis for the 2D environments

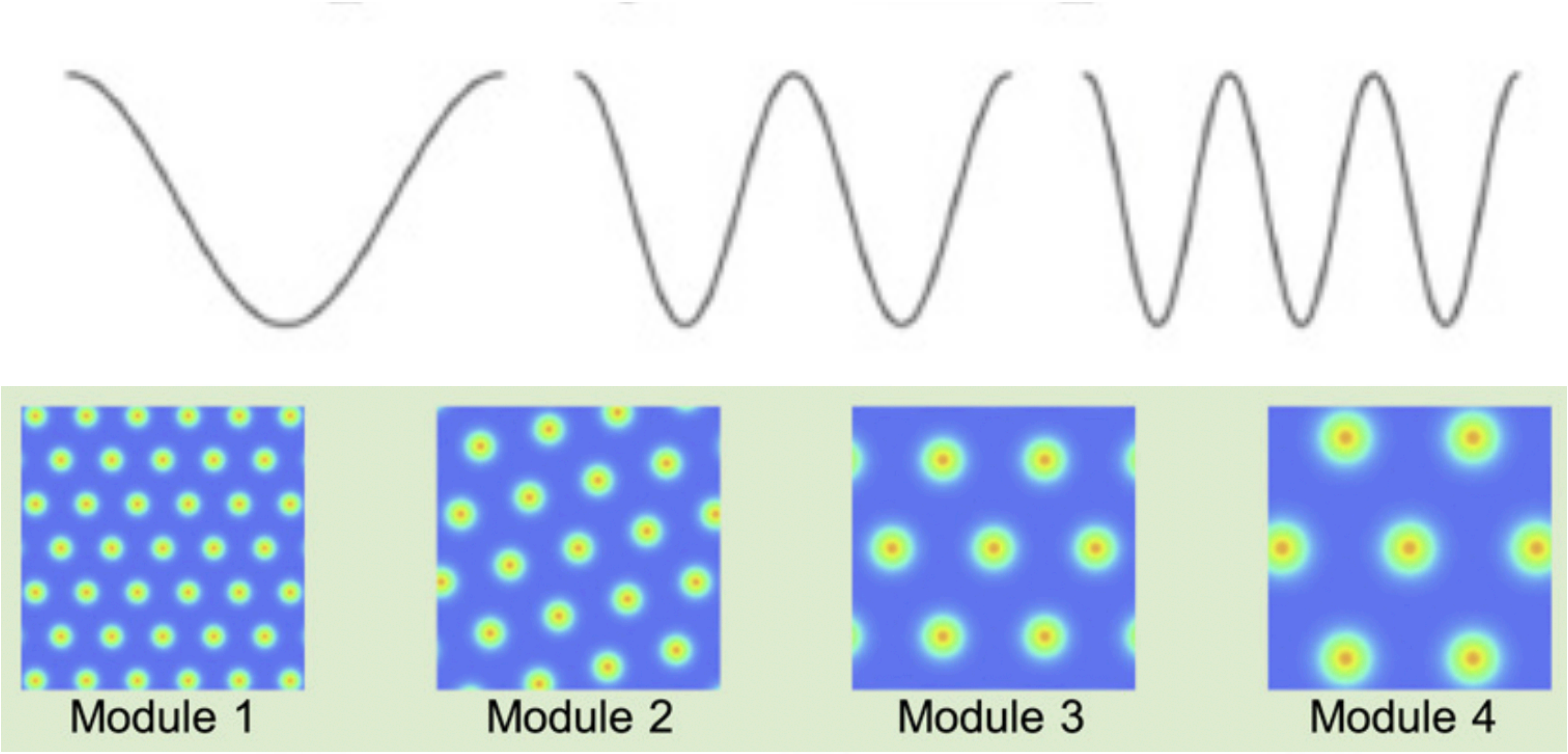

Fourier generalization to manifolds

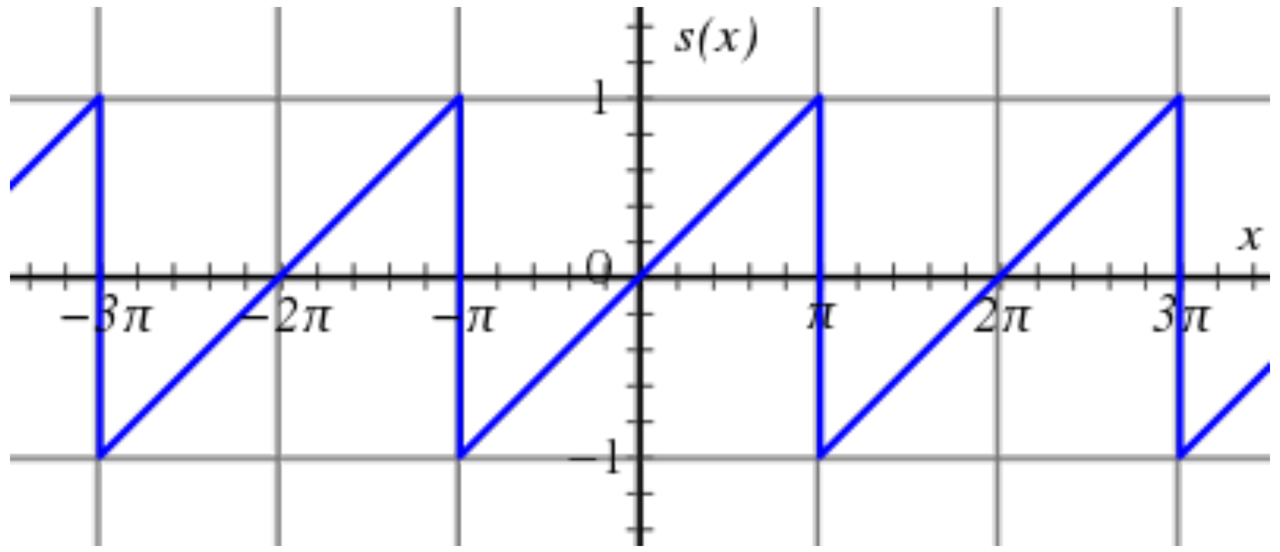

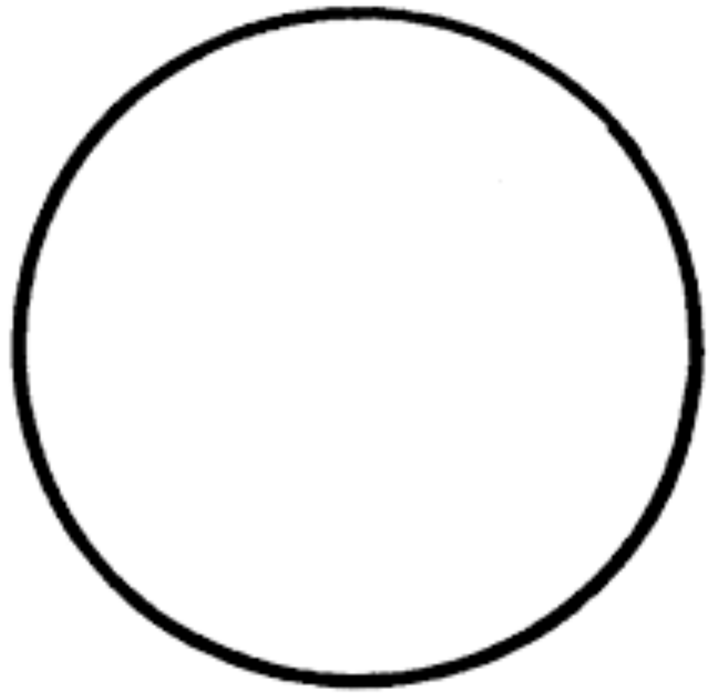

$$\frac{d^2}{dx^2}\sin(wx) = -w^2 \sin(wx)$$

$$\frac{d^2}{dx^2}\cos(wx) = -w^2 \cos(wx)$$

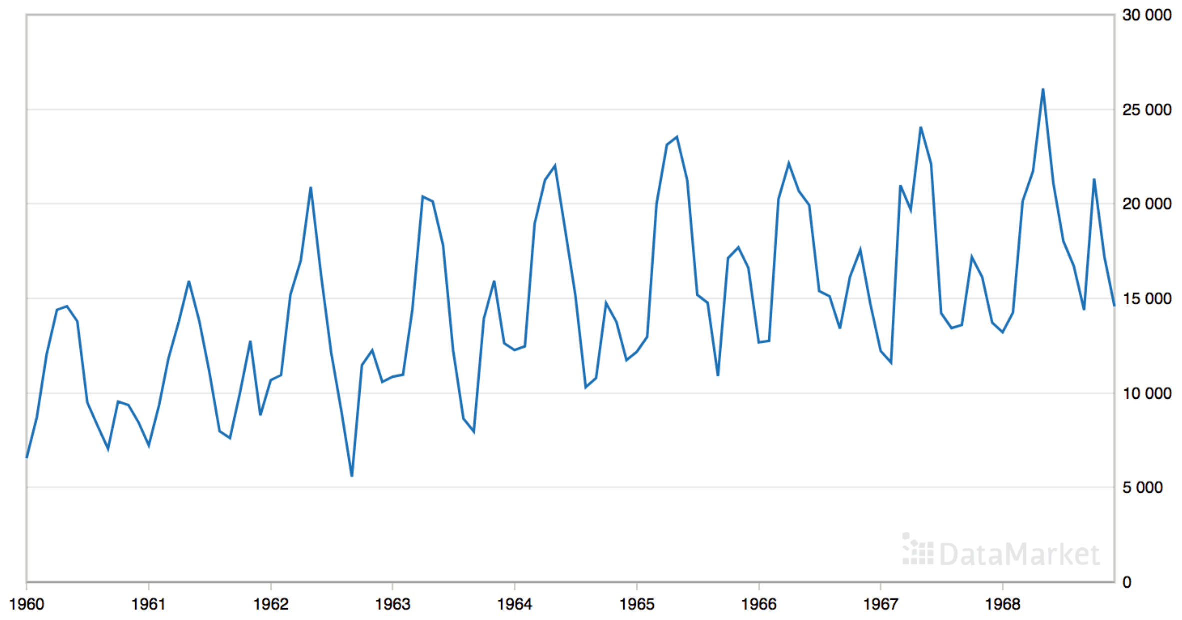

$$\frac{d^2}{dx^2}\sin(wx) = -w^2 \sin(wx)$$

$$\frac{d^2}{dx^2}\cos(wx) = -w^2 \cos(wx)$$

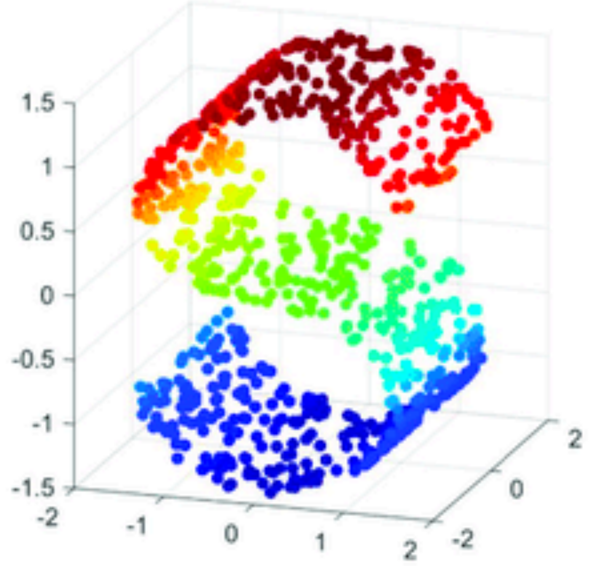

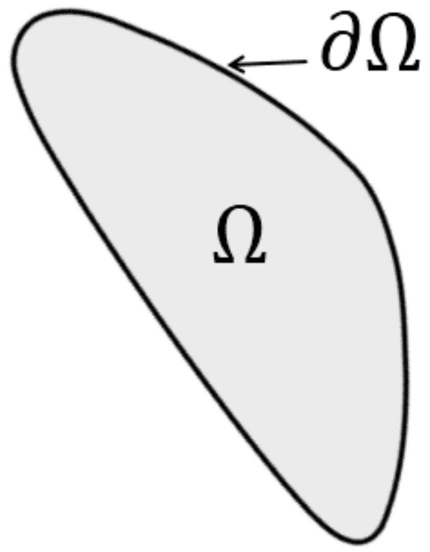

Generalised Fourier

2D Sphere

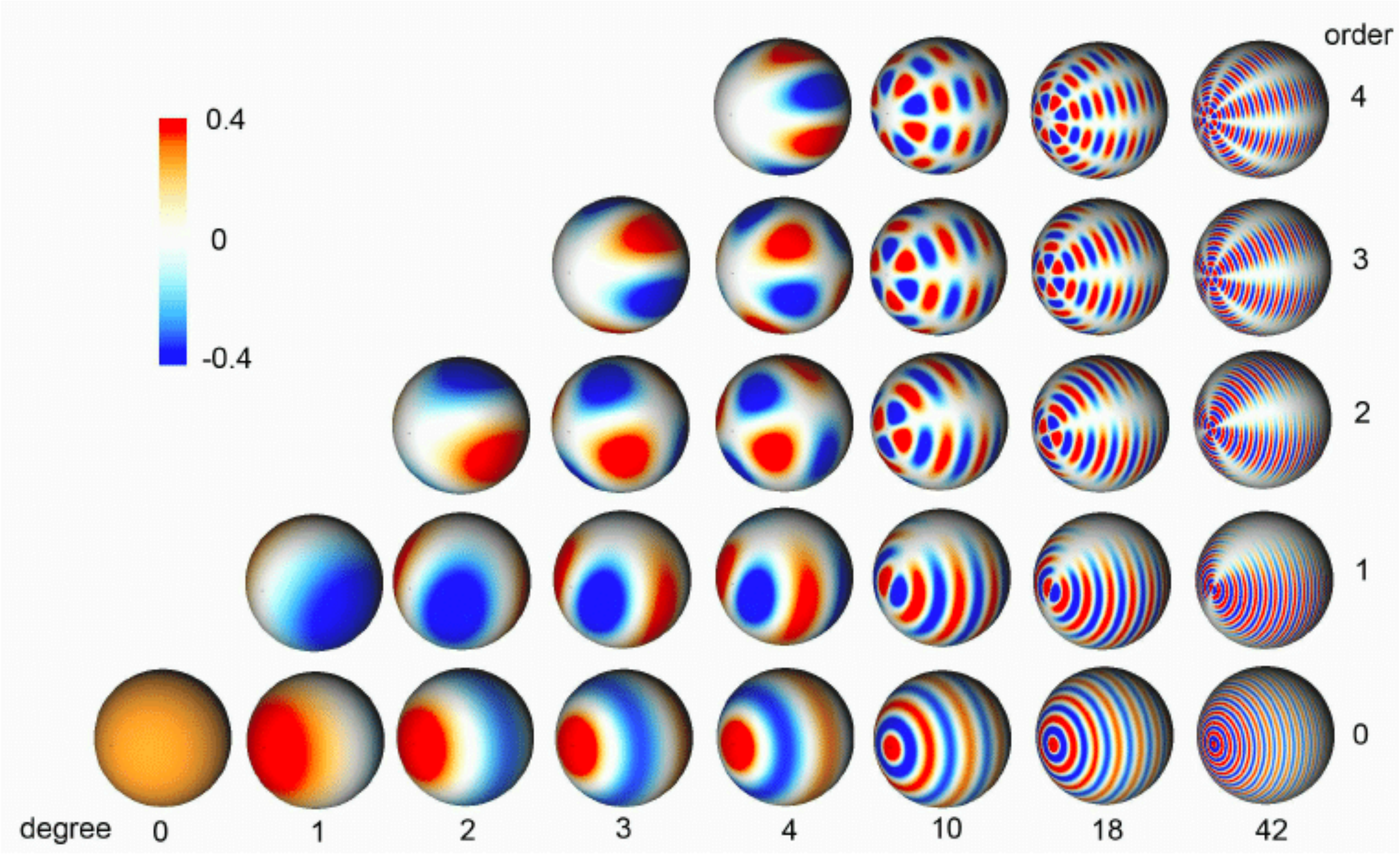

2D Torus

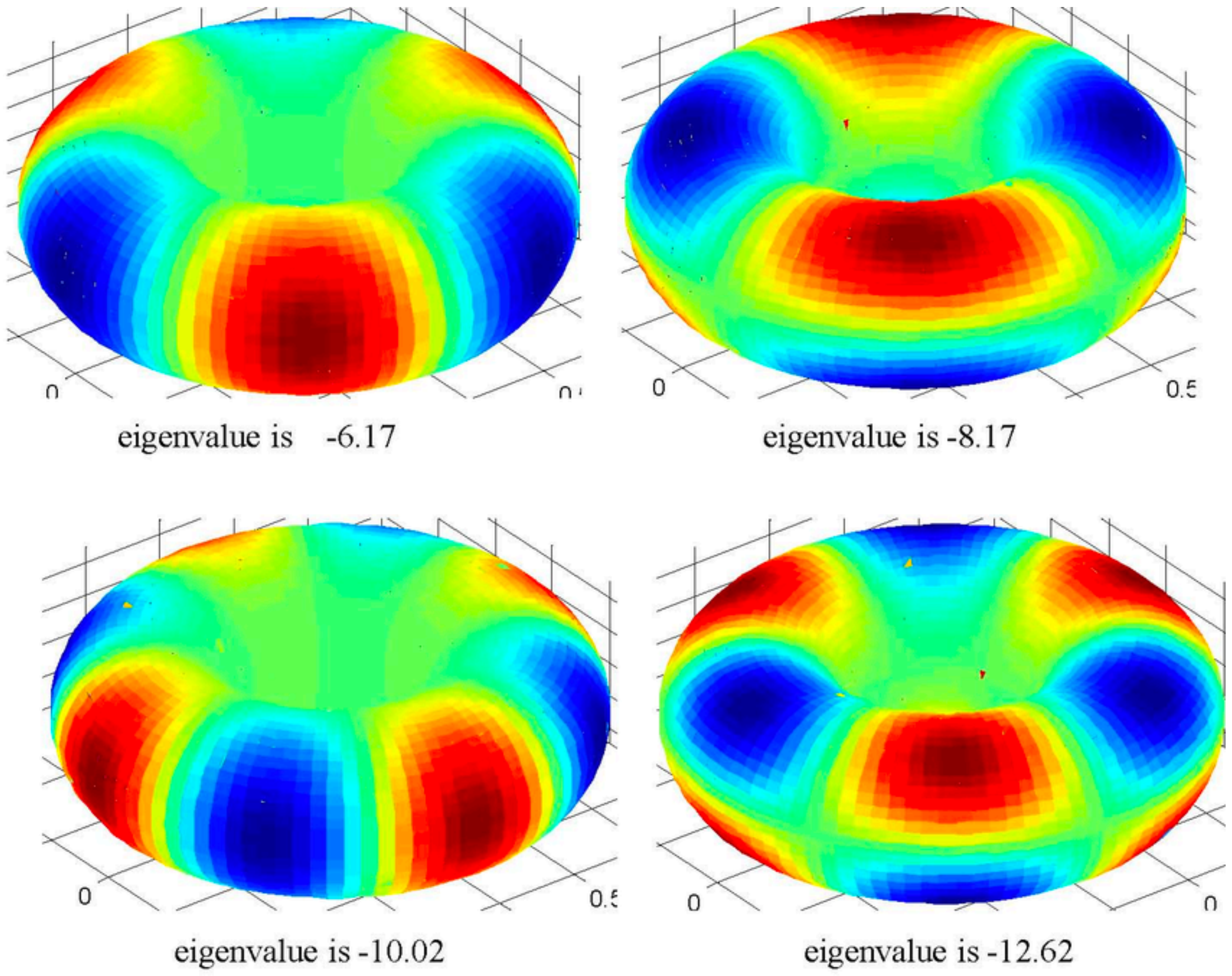

Generalised Fourier

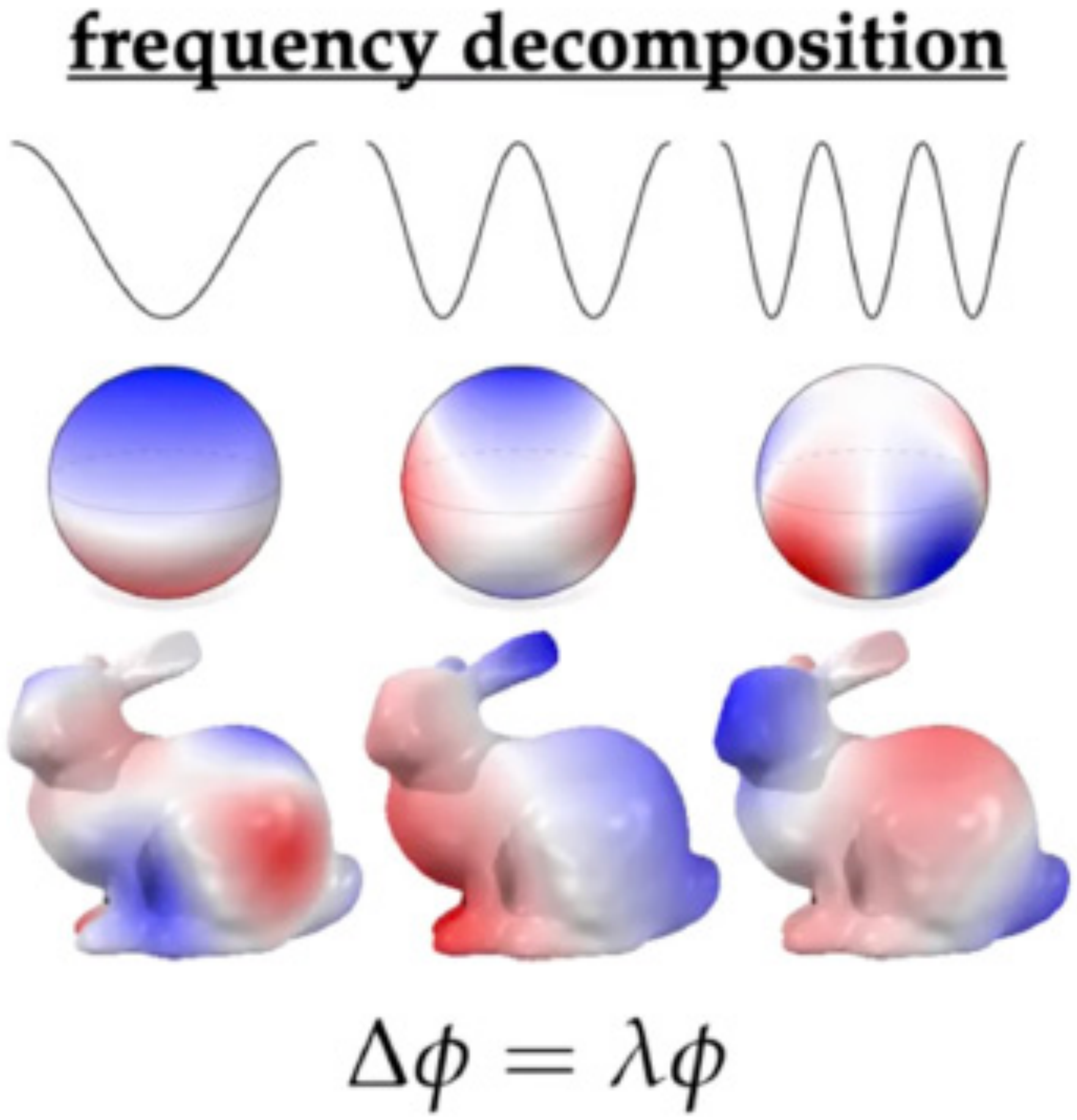

- Basis set to represent functions
- Filtering of scales
- Smoothing and interpolation
- Spectral coordinates
- ...

Spectral coordinates

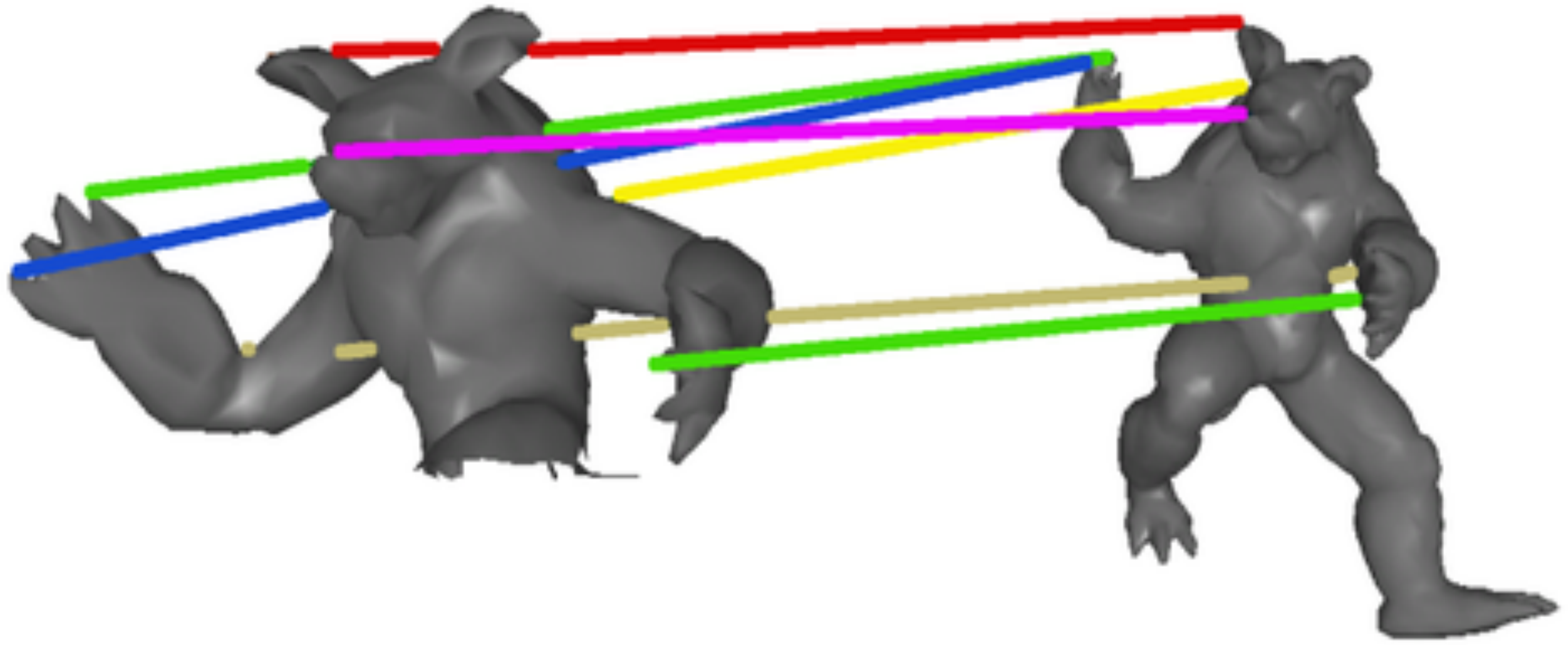

Spectral coordinates

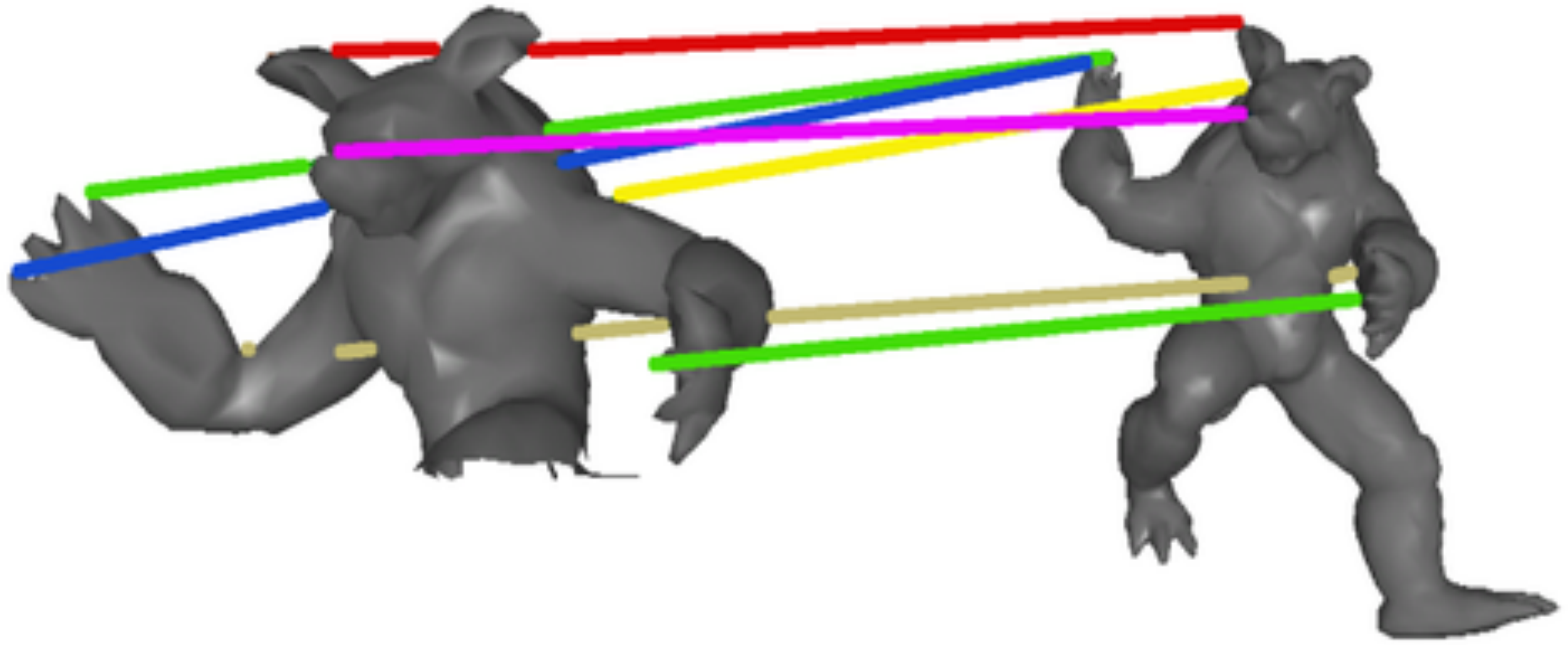

$$M_{i,j}^t = \sum_l \lambda_l^t \psi_l(x_i)\phi_l(x_j)$$

M is related to graph Laplacian

Spectral coordinates

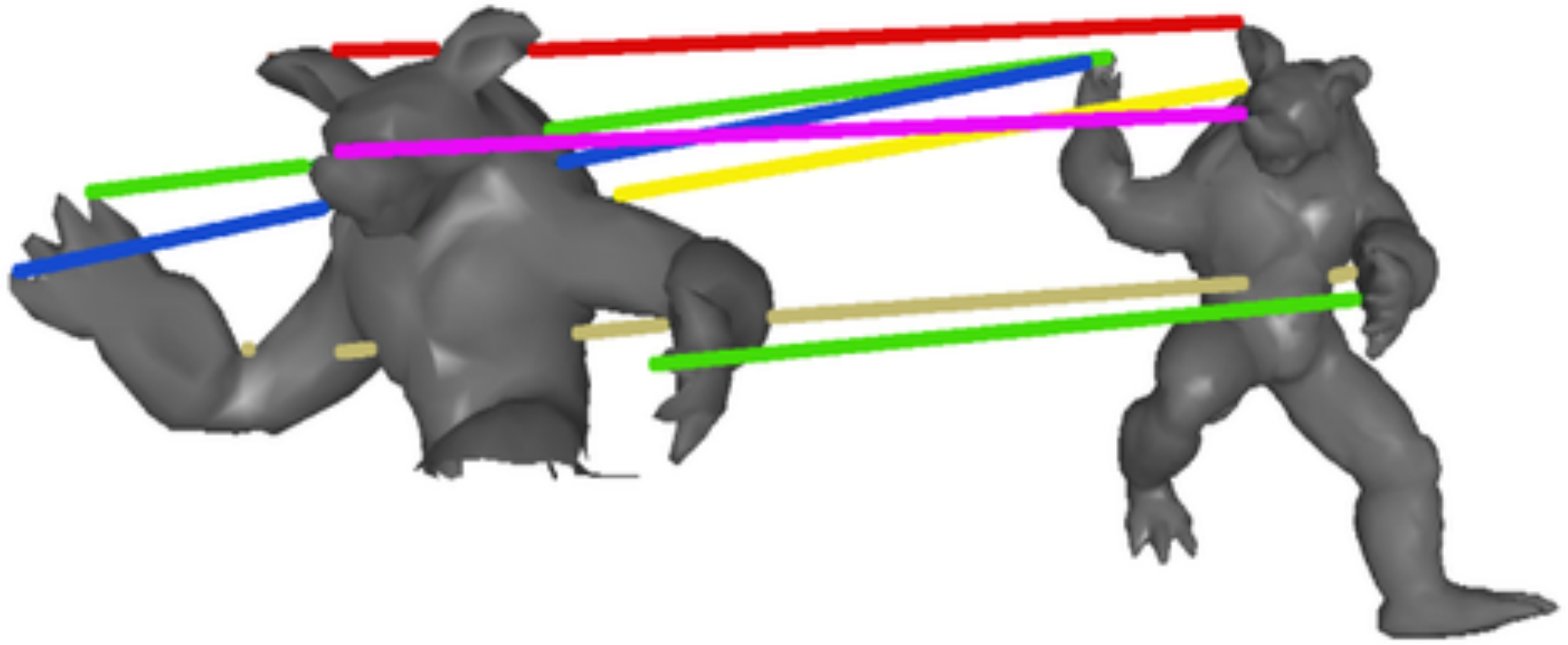

$$M_{i,j}^t = \sum_l \lambda_l^t \psi_l(x_i)\phi_l(x_j)$$

M is related to graph Laplacian

$$\Psi_t(x) = (\lambda_1^t \psi_1(x), \lambda_2^t \psi_2(x), \ldots, \lambda_k^t \psi_k(x))$$

Spectral coordinates

Spectral coordinates

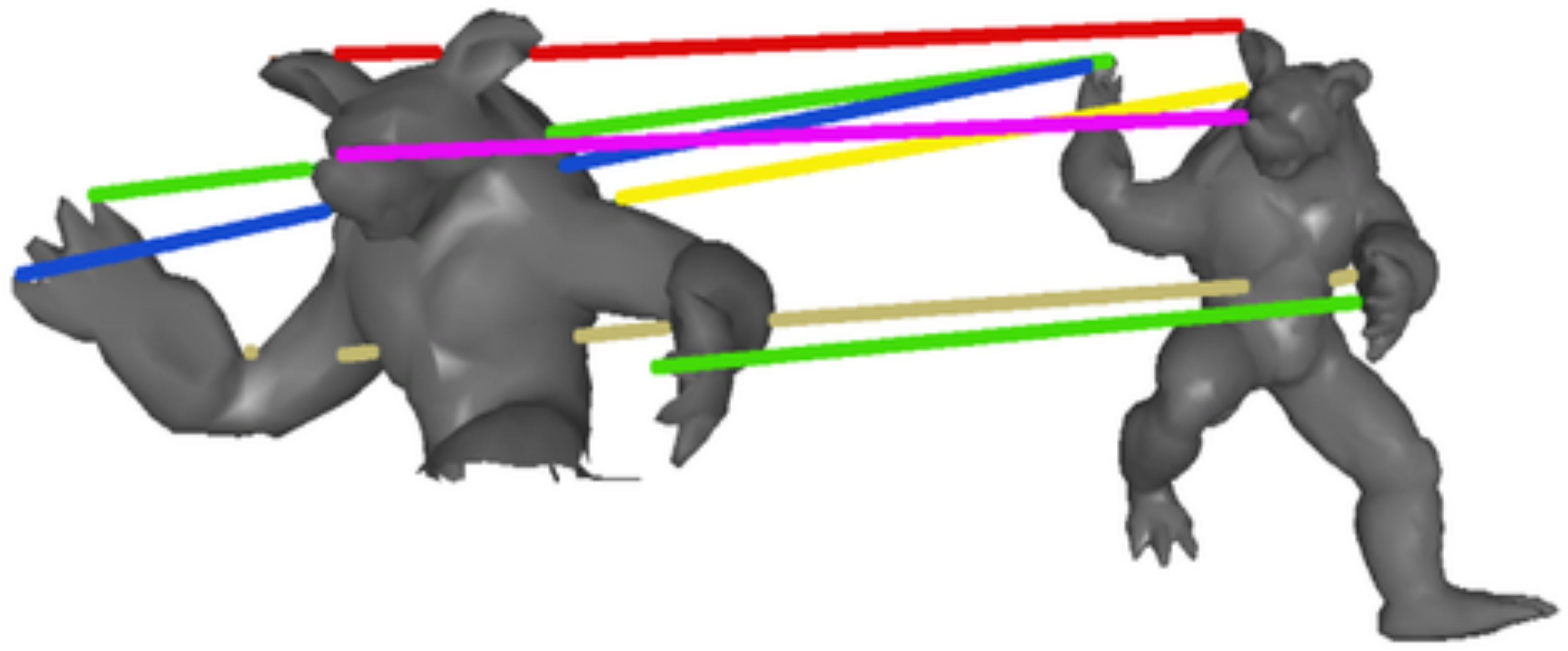

$$M_{i,j}^t = \sum_l \lambda_l^t \psi_l(x_i)\phi_l(x_j)$$

M is related to graph Laplacian

$$\Psi_t(x) = (\lambda_1^t \psi_1(x), \lambda_2^t \psi_2(x), \ldots, \lambda_k^t \psi_k(x))$$

Spectral coordinates

$$D_t(x_i, x_j)^2 \approx ||\Psi_t(x_i) - \Psi_t(x_j)||^2$$

Diffusion distance

Spectral geometry

Relation between geometry/topology and
eigenvalues and eigenfunctions of the Laplacian operator

Spectral Geometry

Relation between geometry/topology and
eigenvalues and eigenfunctions of the Laplacian operator (Quantum mechanics)

Graphs

Relations between graph properties and spectra of the graph Laplacian

Hypercube

Fourier decomposition of Boolean functions: eigenvectors of Graph Laplacian are the characters of $\mathbb{Z}_2^n$

$$f : \{-1,1\}^n \to \mathbb{R}$$

$$f(x) = \sum_{S \subseteq [n]} \hat{f}(S)\chi_S(x), \quad \chi_S(x) = \prod_{i \in S} x_i$$

$$\hat{f}(S) = \langle f, \chi_S \rangle$$

Manifolds

$$(M, g) \to Spec(M, g)$$

Eigenfunctions as minimizers of Dirichlet form

Flat torus (Lattices) $\mathbb{R}^n/\Delta$

Poisson type formula relating the norms of lattice points (lengths of closed geodesics) to frequencies (eigenvalues)

$$\frac{1}{(4\pi t)^{d/2}} Vol(\Delta) \sum_{\lambda \in \Delta} e^{-|\lambda|^2/4t} = \sum_{\lambda \in \Delta^*} e^{-4\pi|\iota|^2 t}$$

Geodesic Flows

Relation between geometry/topology a
and periodic geodesics (Classical mechanics)

Manifolds with boundary

Billiard dynamics

Representation Theory

Non-Abelian groups

Elements of the group are represented by invertible matrices and the group operation by matrix multiplication

Pontryagin Duality

Functions on locally compact Abelian groups $(\mathbb{Z}_2^n)$

Extension of Fourier for functions on groups based on Pontryagin duality (group characters generalize complex exponentials as basis functions)

$$\hat{G} := \mathrm{Hom}(G, \mathbb{R}/\mathbb{Z})$$

$$\chi : G \to U(1) \mid \chi(g_1 g_2) = \chi(g_1)\chi(g_2)$$

$$\hat{f}(\chi) = \int_G f(x)\bar{\chi}(x) d\mu(x)$$

Classical Fourier Analysis

Functions on $\mathbb{R}$ $\mathbb{R}/\mathbb{Z}$ $\mathbb{Z}$ $\mathbb{Z}_n$

Representing functions as sum of trigonometric functions

$$\hat{f}(\xi) = \int_{-\infty}^{\infty} f(x) e^{-i2\pi\xi x} dx$$

9.3.3 Facts

The Laplacian on any compact Riemannian manifold provides us with all the tools of Fourier analysis on our Riemannian manifold. Let us call a function ϕ an *eigenfunction* with *eigenvalue* the number λ if

$$\Delta f = \lambda f \ .$$

The set of all eigenvalues of Δ is an infinite discrete subset of $\mathbb{R}^+$ called the *spectrum* of Δ

$$\operatorname{Spec}(M) = \{\lambda_k\} = \{0 < \lambda_1 < \lambda_2 < \dots\} \tag{9.5}$$

with λ_k tending to infinity with k.

For each eigenvalue λ_i, the vector space of eigenfunctions ϕ satisfying

$$\Delta f = \lambda_i f$$

is always finite dimensional and its dimension is called the *multiplicity* of λ_i. Once we have a basis of the eigenfunctions with this eigenvalue written out, it is trivial to find an orthonormal basis

$$\{\phi_k\}$$

(where k runs from 1 to the multiplicity) of eigenfunctions. Here the orthonormalcy is to be understood for the global scalar product

$$\langle f, g \rangle_{L^2(M)} = \int_M fg \ .$$

As for classical Fourier series, any reasonable function

$$f : M \to \mathbb{R}$$

has Fourier coefficients

$$a_i = \int_M f\phi_i$$

and f is recovered from these coefficients by the converging series

$$f = \sum_i a_i\phi_i \ .$$

In the same spirit, the scalar product of two functions is the sum of products of their coefficients:

$$\int_M fg = \sum_i a_i b_i$$

where

$$f = \sum_i a_i\phi_i$$

$$g = \sum_i b_i\phi_i \ .$$

9.3.4 Heat, Wave and Schrödinger Equations

We will follow the same steps that we did in §1.8: defining heat, wave and Schrödinger equations on Riemannian manifolds. The heat equation for the heat $f(m,t)$ at time t at a point m of the Riemannian manifold M is

$$\Delta f = -\frac{\partial f}{\partial t} . \tag{9.6}$$

The wave equation for the height $f(m,t)$ of the "water" after time t at a point m is

$$\Delta f = -\frac{\partial^2 f}{\partial t^2} . \tag{9.7}$$

where if M were a surface, you would consider M covered in a thin sheet of water, or for M of three dimensions, M is a place through which sound is propagating. The wave equation can also be considered as describing the manifold M as a vibrating membrane object. Finally the Schrödinger equation uses complex valued functions and is written

$$\hbar^2 \Delta f = i\hbar \frac{\partial f}{\partial t} \tag{9.8}$$

where $i = \sqrt{-1}$ and $\hbar$ is Planck's constant.

To solve these equations, at least formally, one uses the same trick as in §§1.8.1. To solve such an equation depending both on time t and a point $m \in M$, the initial idea is to use the fact that, roughly by the Stone–Weierstraß approximation theorem, we need only to consider product functions

$$f(m,t) = g(m)h(t)\ .$$

One will subsequently consider series of them (as in the theory of Fourier series). Look for example at the heat equation. The function $f = gh$ satisfies the heat equation precisely when the functions g and h satisfy

$$\frac{\Delta g}{g} = -\frac{h'}{h} \tag{9.9}$$

where

$$h'(t) = \frac{dh}{dt}$$

is the usual derivative.

Since the first fraction depends only on the point $m \in M$ and the second only on the time t their common value has to be a constant, call it λ. Then the function

$$g : M \to \mathbb{R}$$

is an eigenfunction of Δ with eigenvalue λ, while h is an exponential decay at rate λ. If all eigenfunctions and eigenvalues of Δ are known, we can then solve the heat equation explicitly. Note that the time dependence $h(t)$ is

$$h(t) = \begin{cases} e^{-\lambda t} & \text{for the heat equation} \\ e^{i\lambda t} & \text{for the Schrödinger equation} \\ e^{i\sqrt{\lambda}t} & \text{for the wave equation.} \end{cases}$$

Another way to write the solution $f(m,t)$ with initial temperature $f(m,0)$ is to compute the Riemannian Fourier series

$$f(m,0) = \sum_{k=1}^{\infty} a_k \phi_k$$

and then

$$f(m,t) = \sum_{k=1}^{\infty} a_k \phi_k(m) e^{-\lambda_k t} \ .$$

For the wave equation, the fundamental solution similar to equation 9.10 requires imaginary terms, i.e.

$$e^{i\sqrt{\lambda_k} t}$$

which are linear combinations of

$$\cos\left(\sqrt{\lambda_k} t\right) \ \text{and} \ \sin\left(\sqrt{\lambda_k} t\right) \ .$$

But the dramatic difference between the heat equation and the wave equation is that waves demand not converging series, but distributions. Heat spreads out uniformly with time, while waves bounce up and down forever. This ma-

There are very few examples where the spectrum or the eigenfunctions can be determined explicitly. Two old standards are rectangles and disks. In both cases, separation of variables disentangles the eigenfunctions. Using again the Stone–Weierstraß theorem, and because the boundary condition agrees with the separation, on a rectangle one need only look for product functions $f(x, y) = g(x)h(y)$, and there will be no other eigenfunctions. If the rectangle has side lengths a and b respectively, then the eigenfunctions are

$$\sin \frac{\pi m x}{a} \sin \frac{\pi n y}{b} \tag{1.21}$$

where m and n are any integers, yielding the set of eigenvalues

$$\lambda = \pi^2 \left(\frac{m^2}{a^2} + \frac{n^2}{b^2} \right).$$

i.e. to obtain an eigenvalue at most λ we need m and n to be integer points inside a certain ellipse. We will see below that a simple expression yields an easy first order approximation of $N(\lambda)$ when $\lambda \to \infty$, but the second order term in λ is related to deep number theory and is still not completely understood today. It is believed that the number of integers m, n with

$$m^2 + n^2 \leq \lambda^2$$

is asymptotic to $\pi^2\lambda^2 + O\left(\lambda^{\varepsilon+1/2}\right)$ as $\lambda \to \infty$, for any $\varepsilon > 0$, but there is still no proof. This is called the Gauß circle problem; see §§1.8.5. However, it is known that $\pi^2\lambda^2 + O\left(\lambda^{1/2}\right)$ is too small.

How about a second order approximation? In 1954, Pleijel got the next order approximation. In his paper Kac 1966 [775], Kac works quite hard to get the third term, guessing that the right formula should be:

$$\sum_{i=1}^{\infty} e^{-\lambda_i t} \sim \frac{\mathrm{Area}(D)}{2\pi t} - \frac{\mathrm{length}(\partial D)}{\sqrt{2\pi t}} + \frac{1}{6}(1-r)$$

where r is the number of holes inside D. The second term is Pleijel's. Note that can one hear the area and the perimeter of D, hence the isoperimetric inequality yields again the fact that disks are characterized by their spectrum.

Kac could only prove the third term for polygons. It was proven the next year, 1967, in the very general context of Riemannian manifolds with boundary by McKean and Singer in their fundamental paper of 1967 [910]. You will read much more about it in chapter 9.

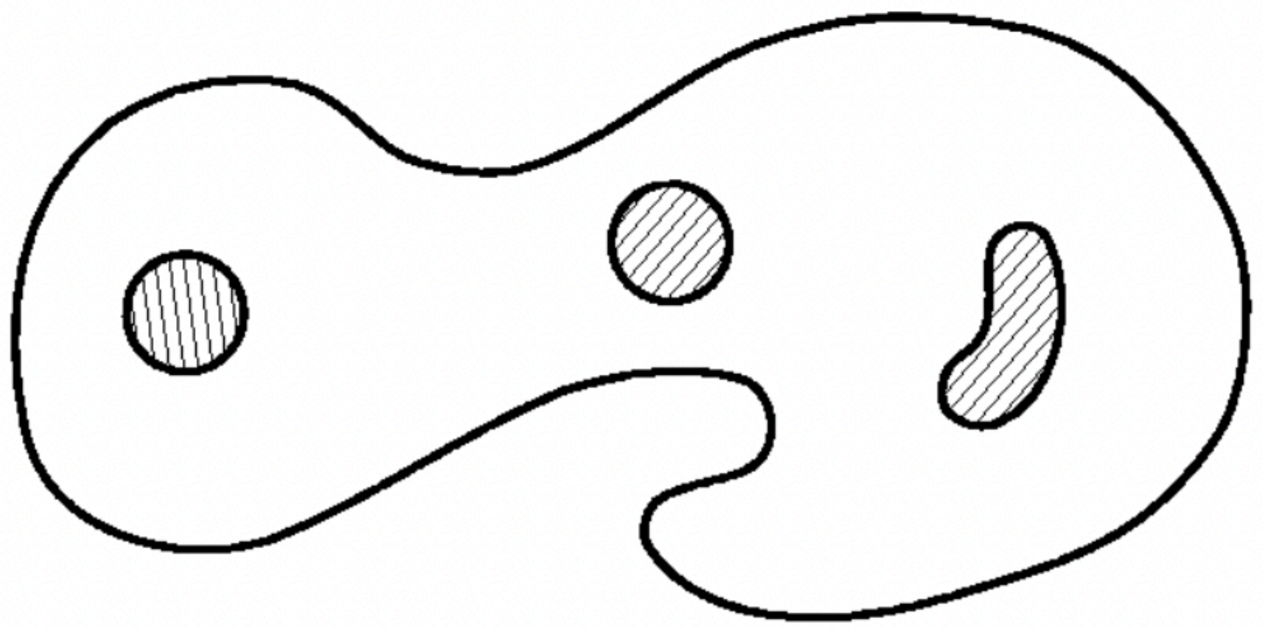

Fig. 1.97. One can hear the number of holes

The Tauberian theorem above shows that the first terms of $N(\lambda)$ and $\sum_{i=1}^{\infty} \exp(-\lambda_i t)$, can each be acquired from the other. But this does not

CAN ONE HEAR THE SHAPE OF A DRUM?

MARK KAC, The Rockefeller University, New York

To George Eugene Uhlenbeck on the occasion of his sixty-fifth birthday

"La Physique ne nous donne pas seulement l'occasion de résoudre des problèmes . . . , elle nous fait presentir la solution." H. POINCARÉ.

Before I explain the title and introduce the theme of the lecture I should like to state that my presentation will be more in the nature of a leisurely excursion than of an organized tour. It will not be my purpose to reach a specified destination at a scheduled time. Rather I should like to allow myself on many occasions the luxury of stopping and looking around. So much effort is being spent on streamlining mathematics and in rendering it more efficient, that a solitary transgression against the trend could perhaps be forgiven.

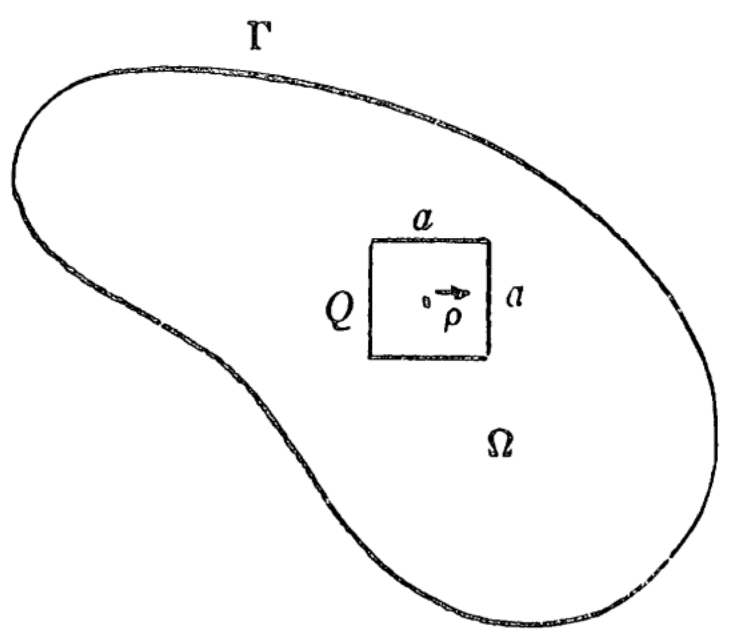

Rayleigh–Faber–Krahn inequality

From Wikipedia, the free encyclopedia

In spectral geometry, the **Rayleigh–Faber–Krahn inequality**, named after its conjecturer, Lord Rayleigh, and two individuals who independently proved the conjecture, G. Faber and Edgar Krahn, is an inequality concerning the lowest Dirichlet eigenvalue of the Laplace operator on a bounded domain in $\mathbb{R}^n$, $n \geq 2$.[1] It states that the first Dirichlet eigenvalue is no less than the corresponding Dirichlet eigenvalue of a Euclidean ball having the same volume. Furthermore, the inequality is rigid in the sense that if the first Dirichlet eigenvalue is equal to that of the corresponding ball, then the domain must actually be a ball. In the case of $n = 2$, the inequality essentially states that among all drums of equal area, the circular drum (uniquely) has the lowest voice.

Rayleigh–Faber–Krahn inequality

From Wikipedia, the free encyclopedia

In spectral geometry, the **Rayleigh–Faber–Krahn inequality**, named after its conjecturer, Lord Rayleigh, and two individuals who independently proved the conjecture, G. Faber and Edgar Krahn, is an inequality concerning the lowest Dirichlet eigenvalue of the Laplace operator on a bounded domain in $\mathbb{R}^n$, $n \geq 2$.[1] It states that the first Dirichlet eigenvalue is no less than the corresponding Dirichlet eigenvalue of a Euclidean ball having the same volume. Furthermore, the inequality is rigid in the sense that if the first Dirichlet eigenvalue is equal to that of the corresponding ball, then the domain must actually be a ball. In the case of $n = 2$, the inequality essentially states that among all drums of equal area, the circular drum (uniquely) has the lowest voice.

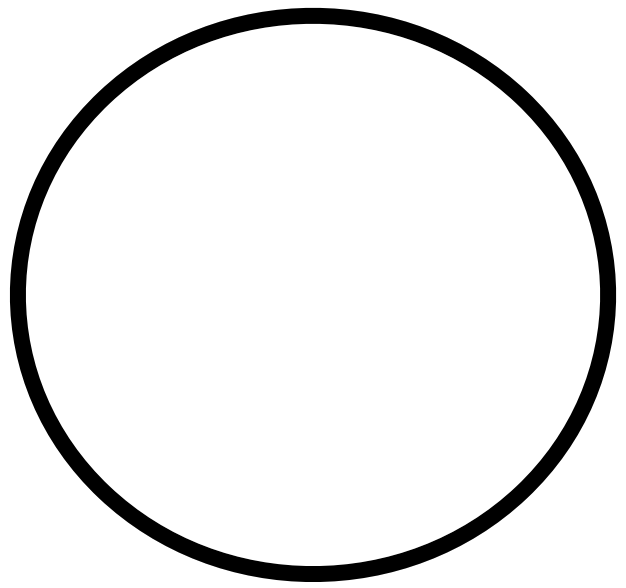

Do grid cells for circular environments have lowest spatial frequency?

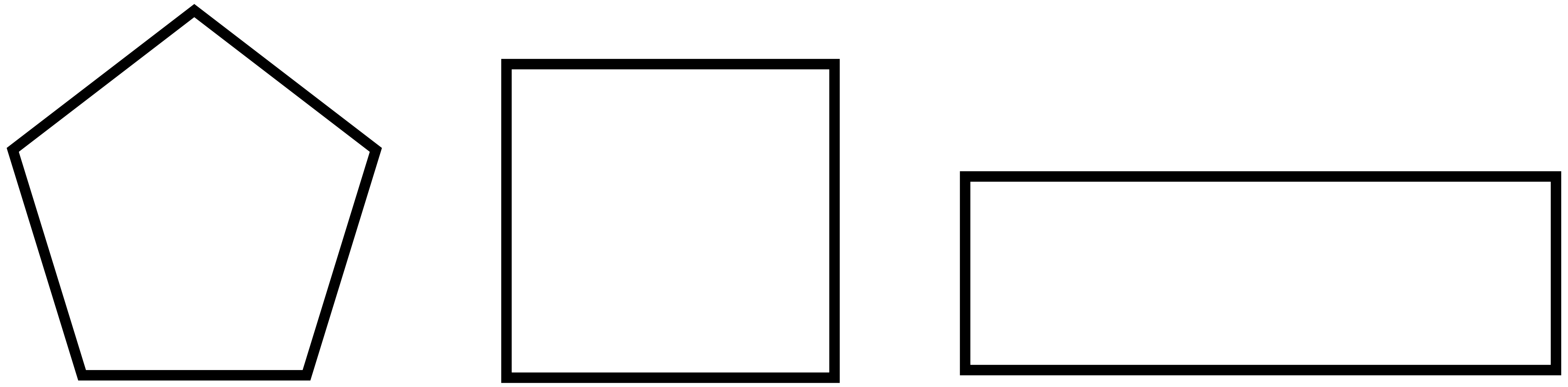

Spectral geometry -> bounds on ratios of eigenvalues

- Dependence on environment shape

- Bounds on grid scale ratios

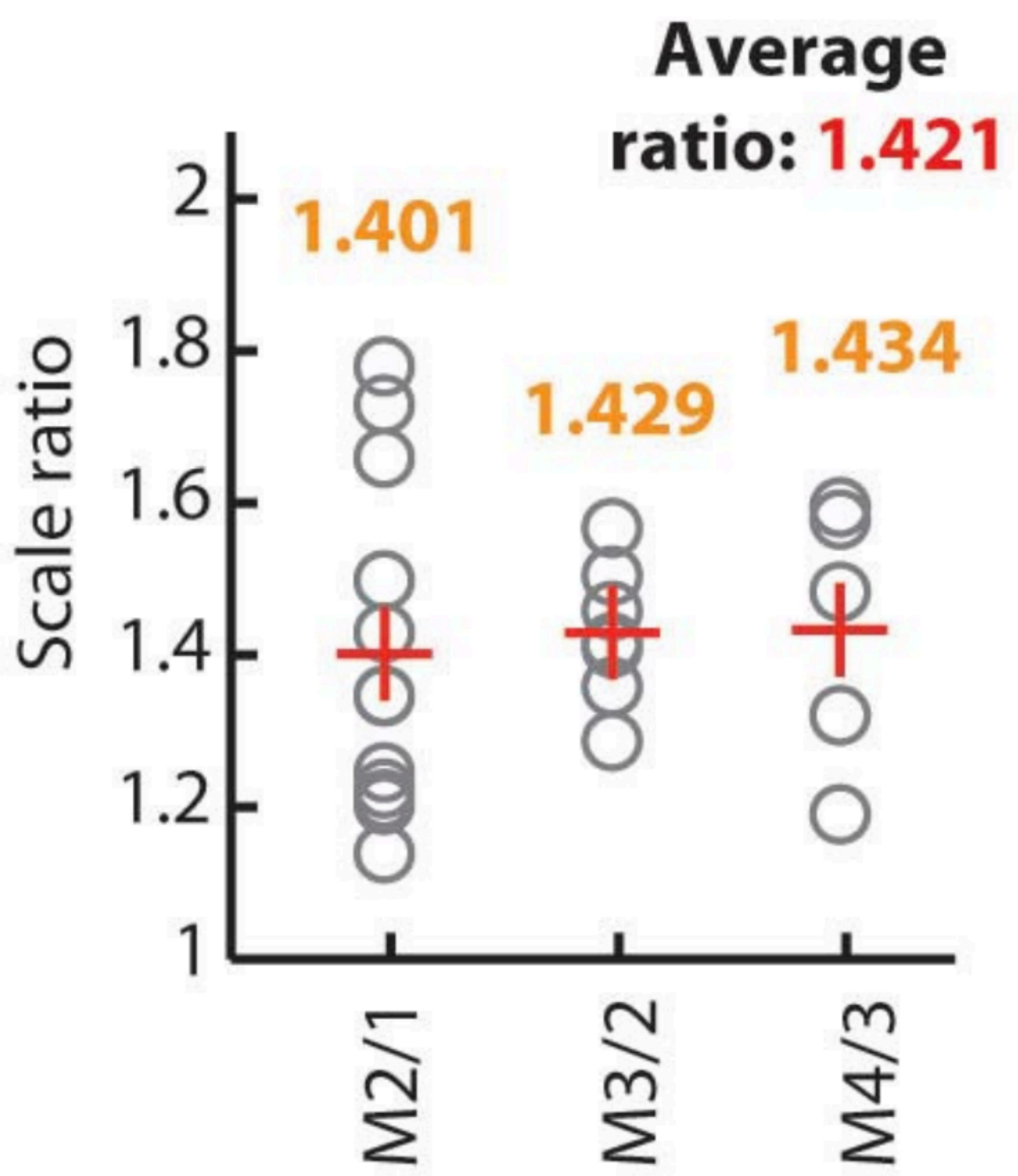

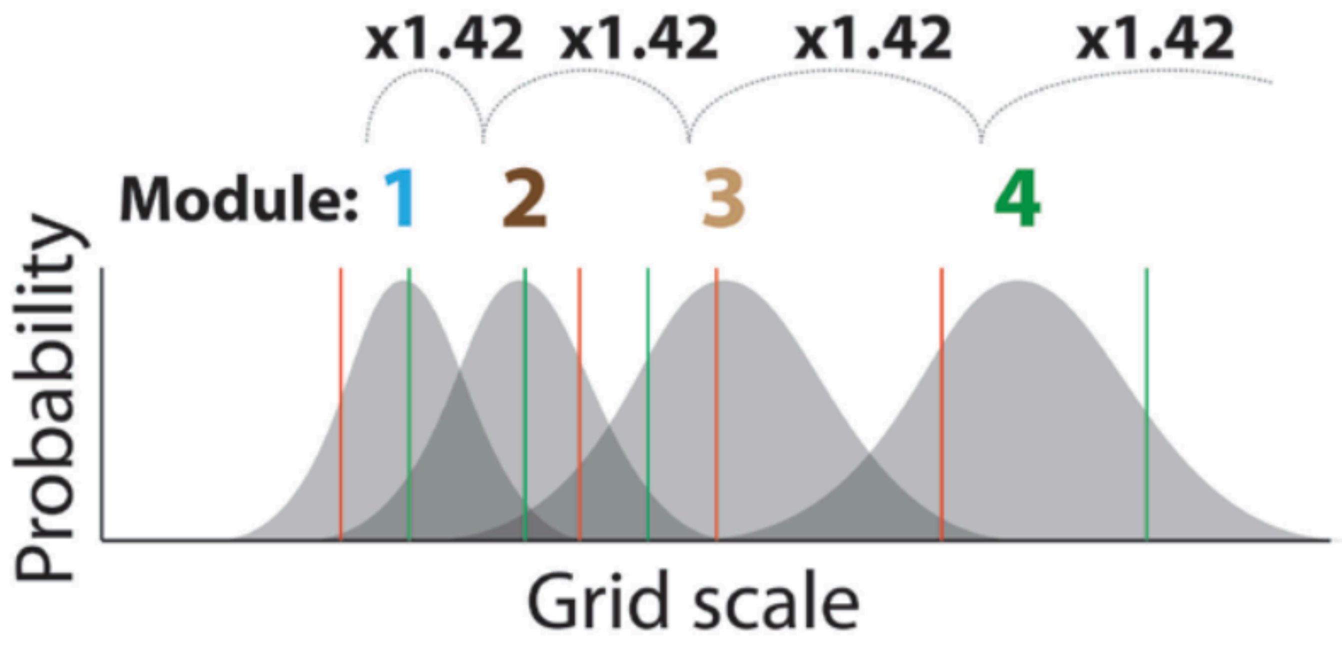

Although the set point is different for different animals, modules scale up, on average, by a factor of ~1.42 (sqrt 2).

Stensola et al. *Nature*, 492, 72-78 (2012)

On tails

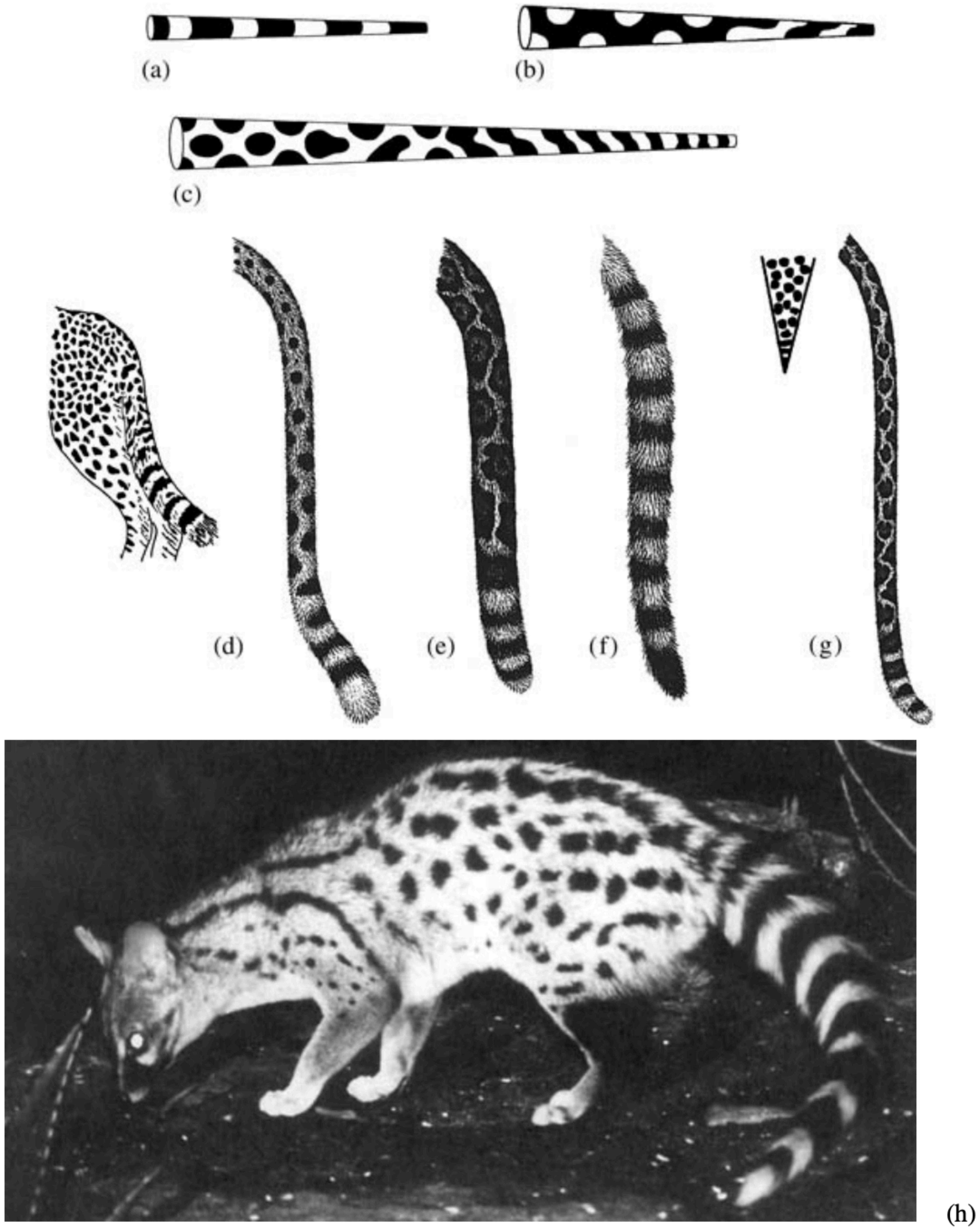
(a)
(b)
(c)
(d)
(e)
(f)
(g)
(h)

k

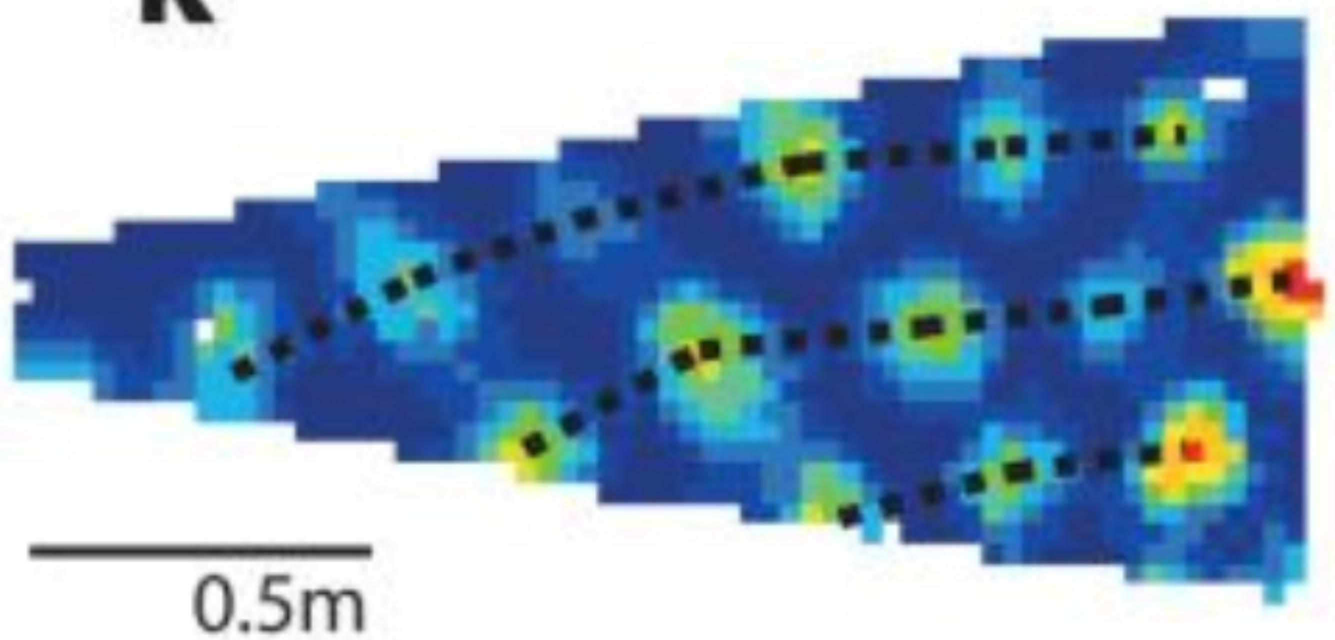

b)

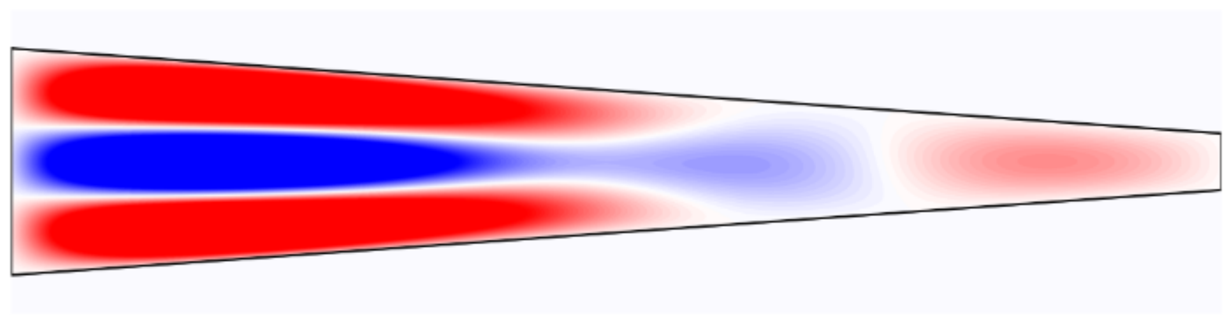

c)

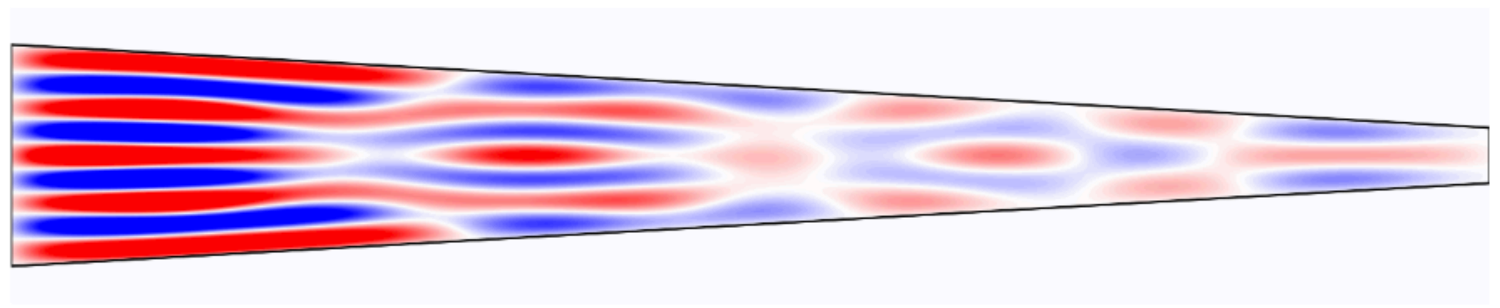

k

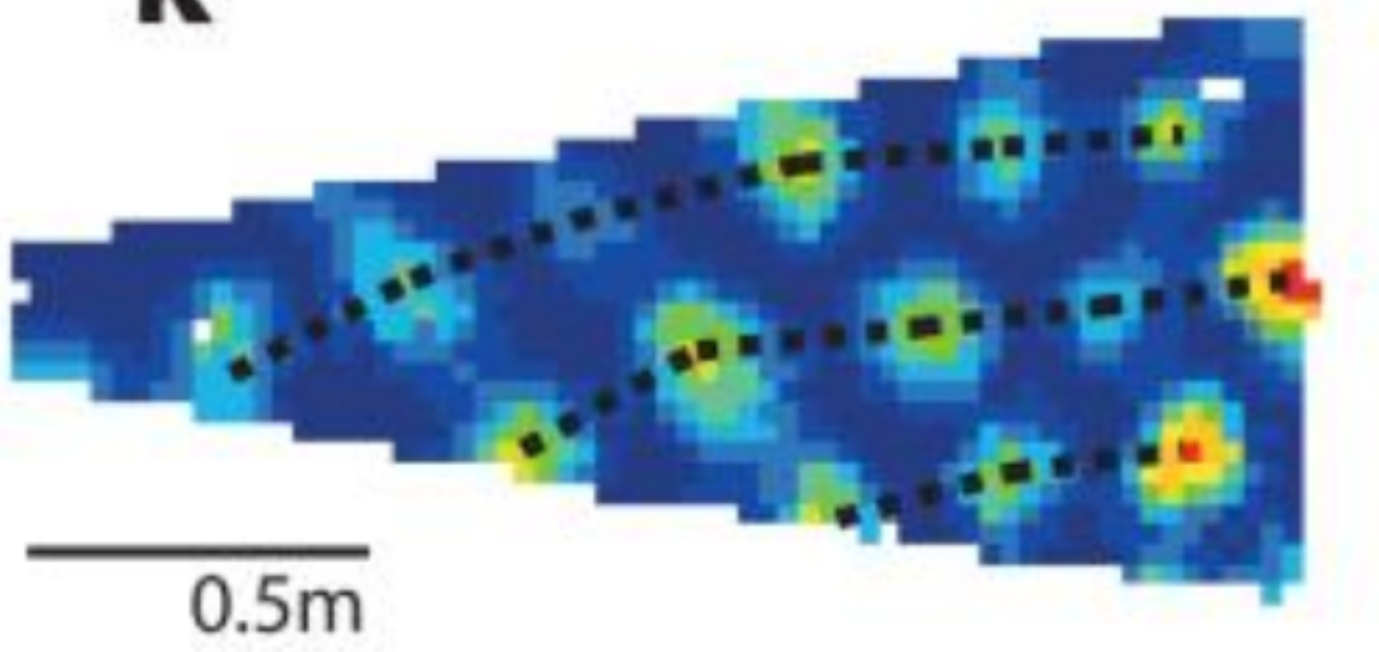

b)

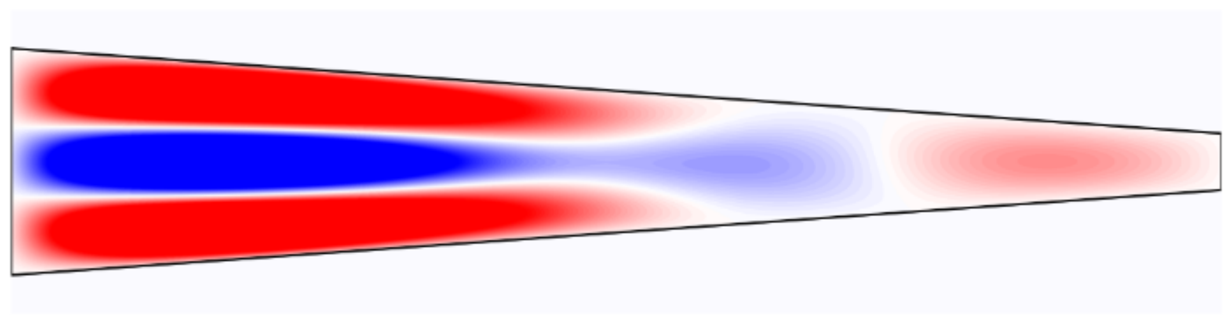

c)

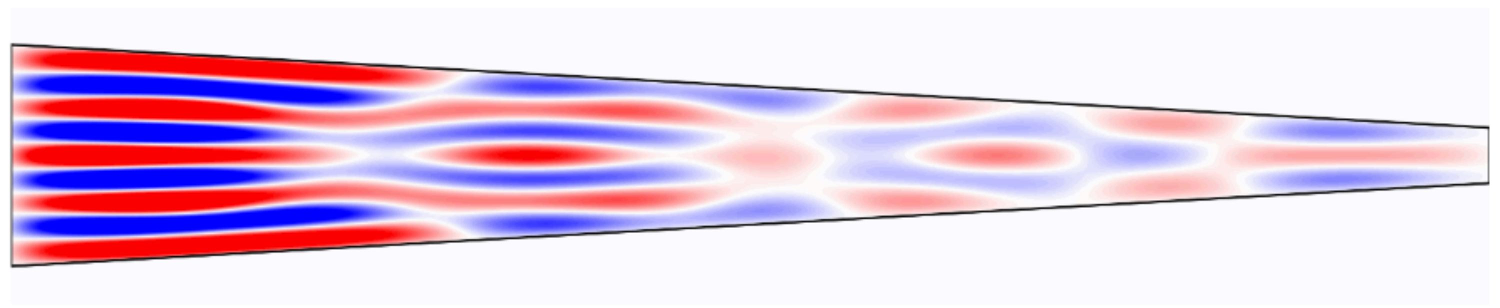

d)

e)


Scapular
stripes
(a)
(b)

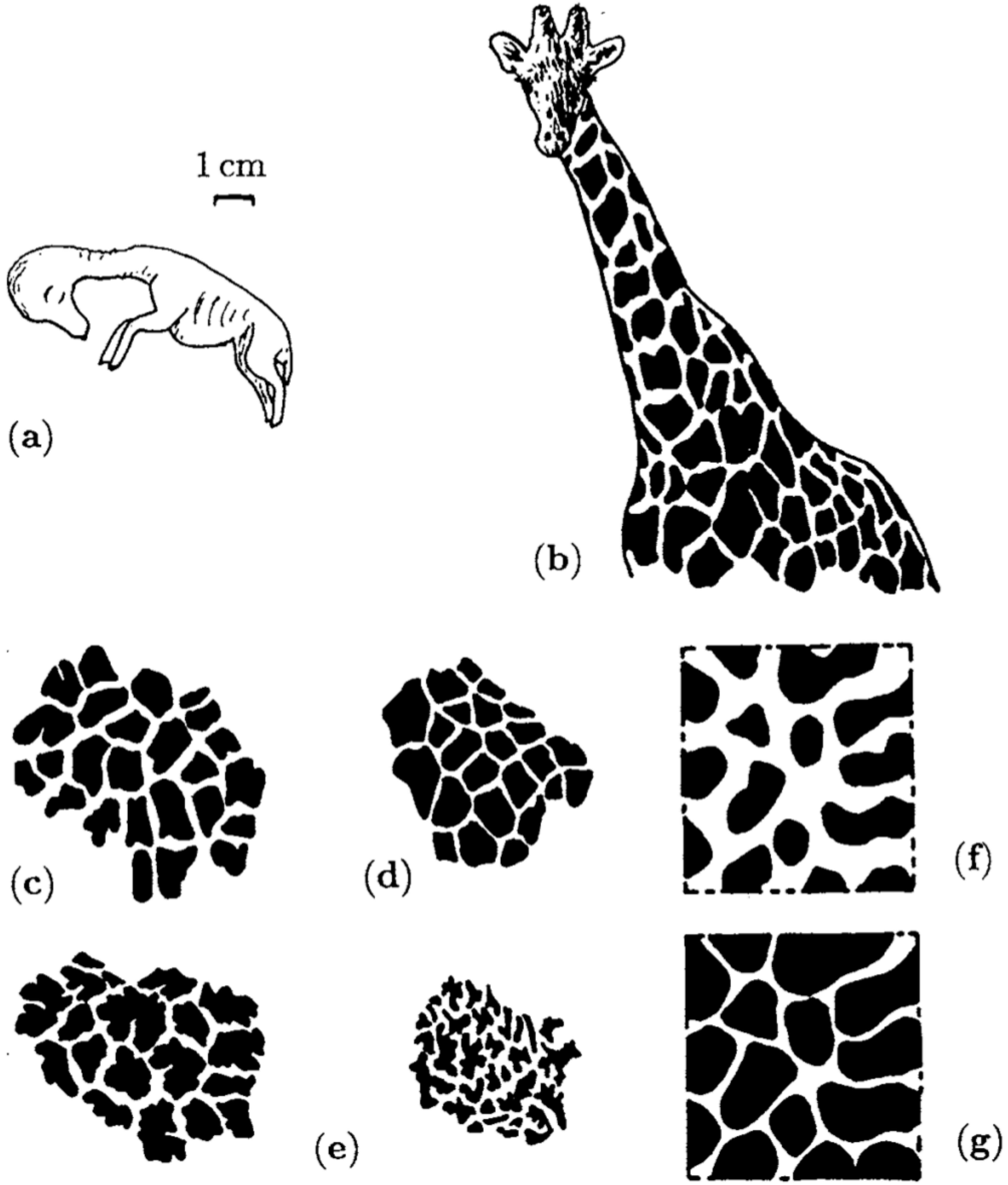
1 cm
(a)
(b)
(c)
(d)
(f)
(e)
(g)

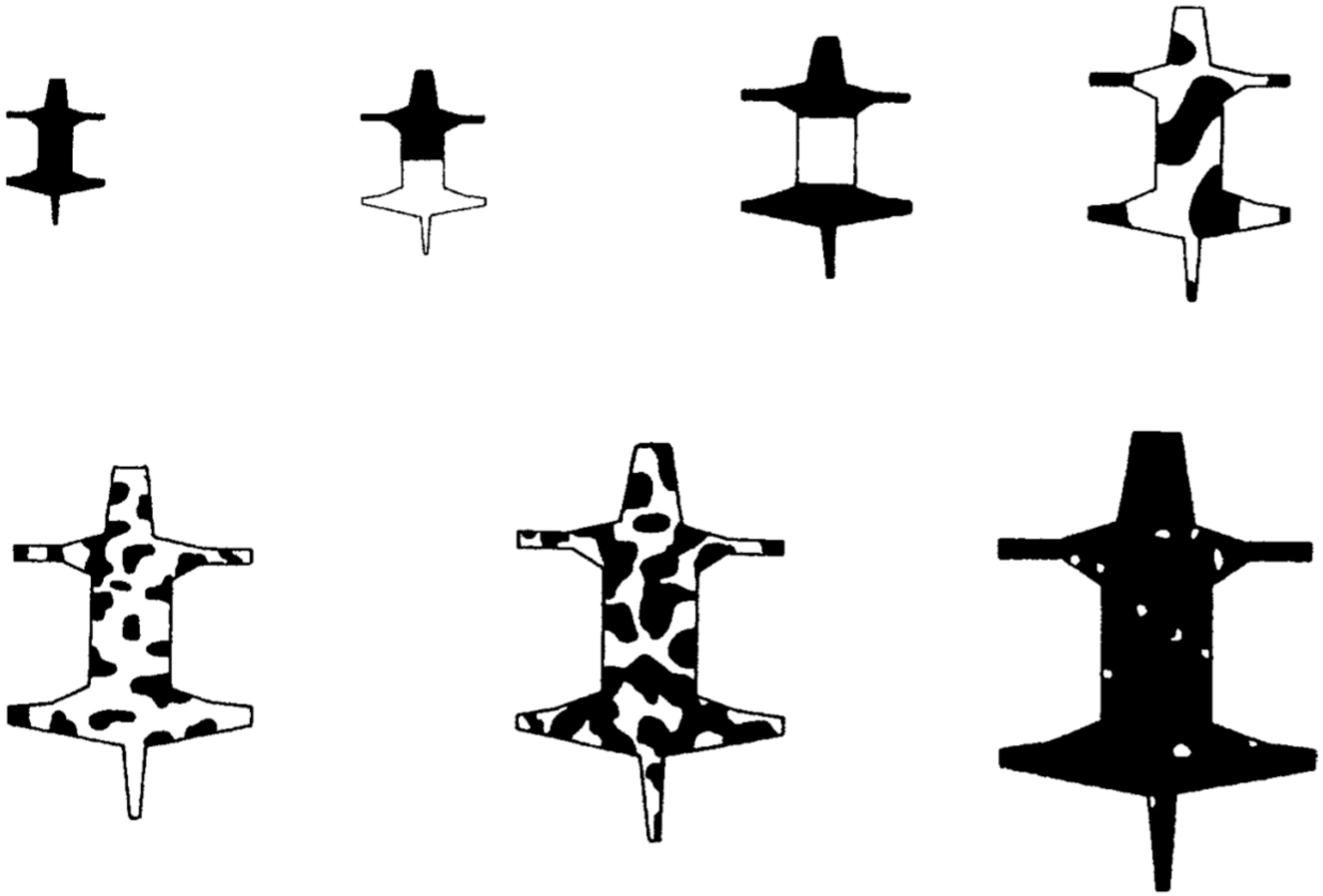

(a)

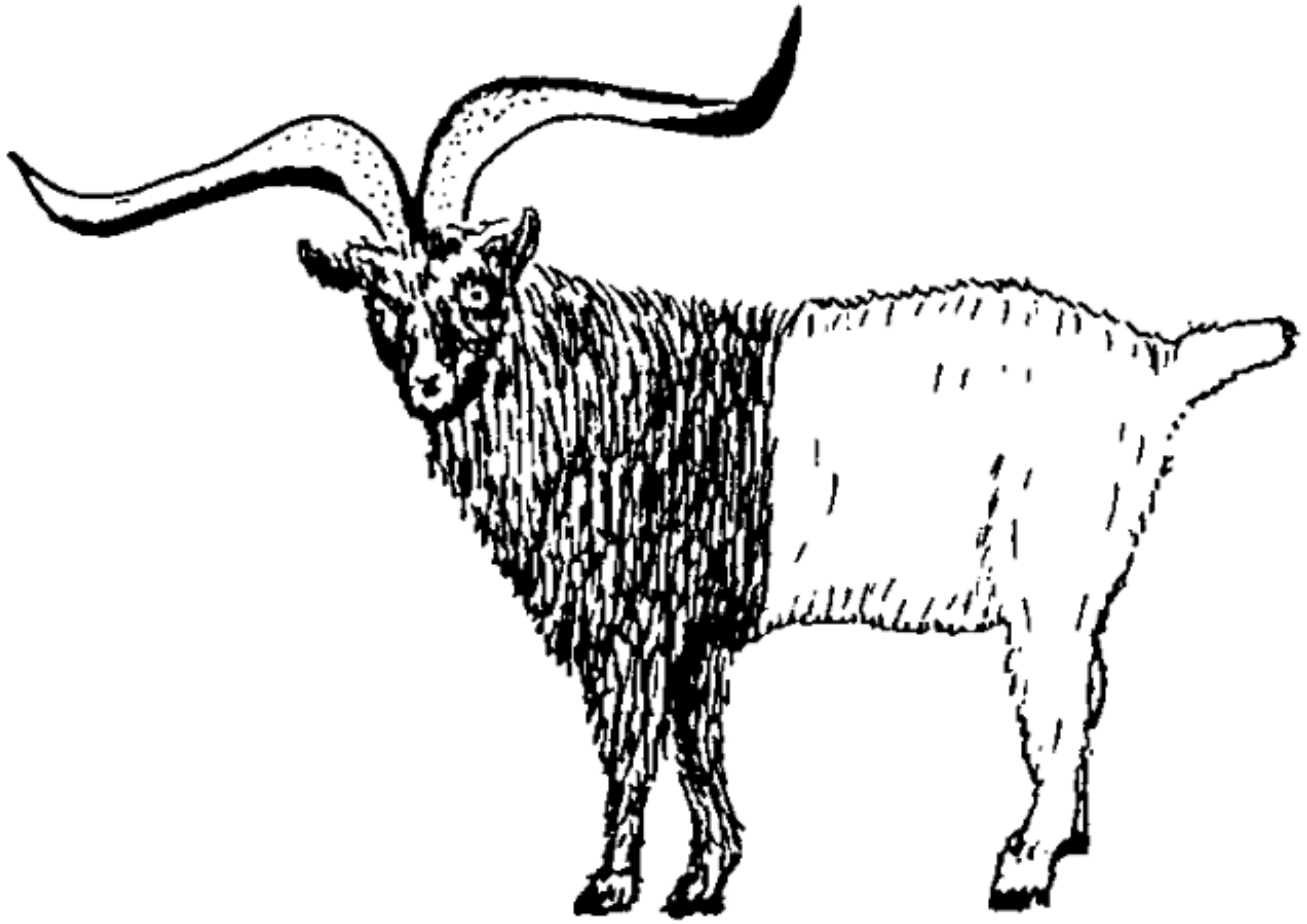

(b)

(c)

(d)

(e)

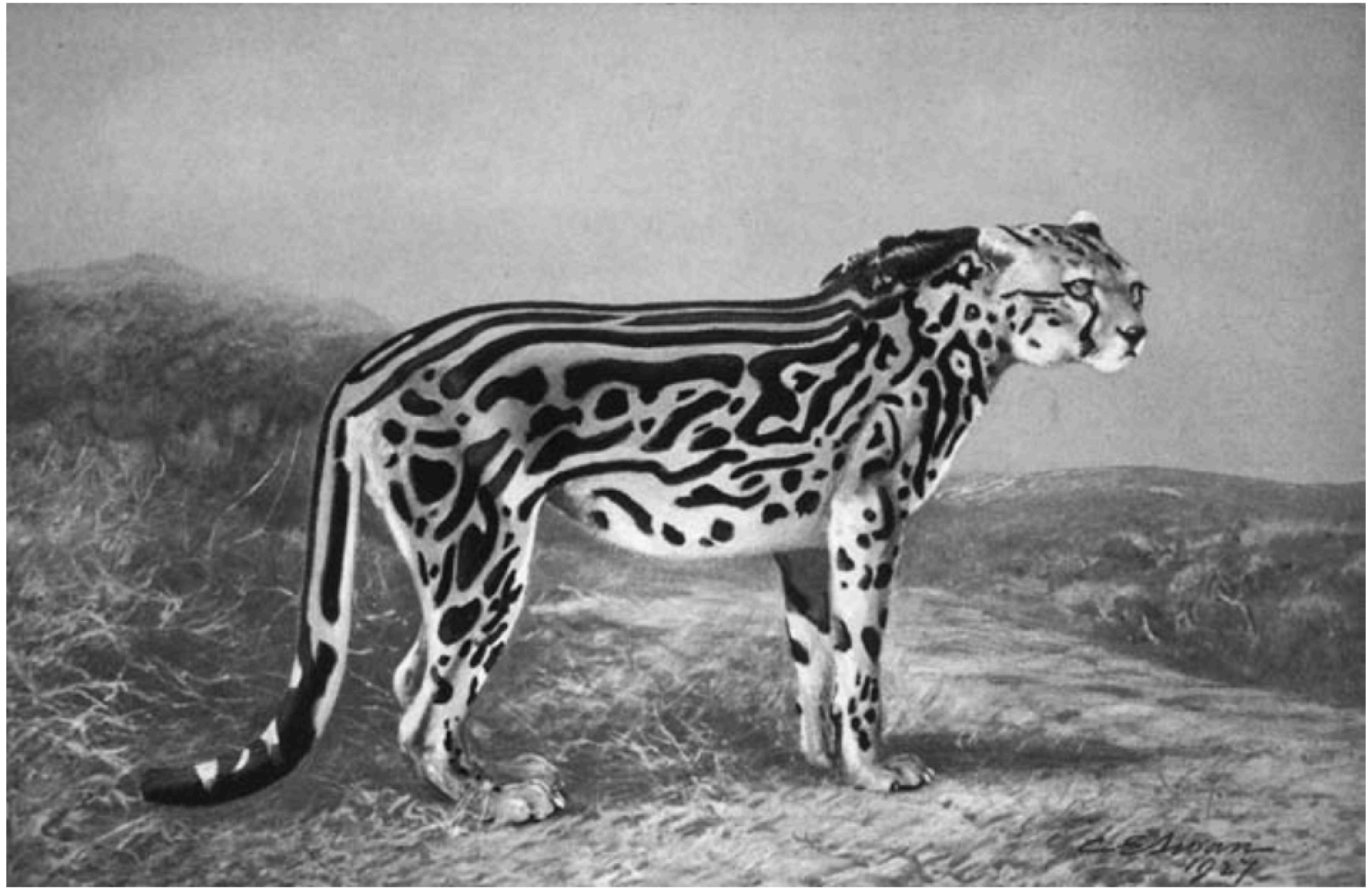

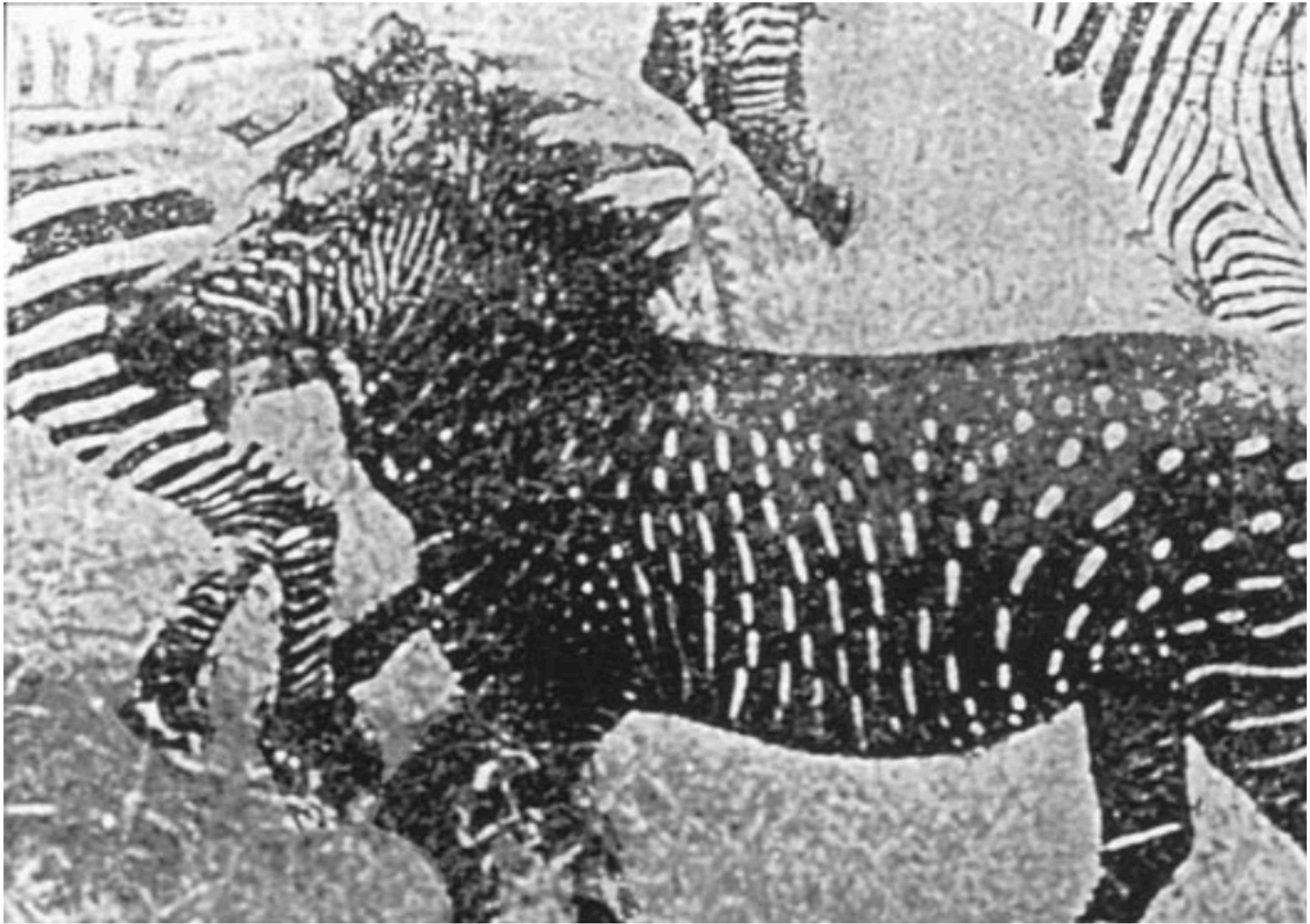


That's all Folks!